MONTREAL REGIONAL MEETING—OCTOBER 23-25, 1956

JULY 1956
No. 1
VOL. 28

JOURNAL
OF THE
AMERICAN CONCRETE INSTITUTE

ACI
PROCEEDINGS
VOL. 53

THIS MONTH

Papers and Reports **1-134**

Structural Design Considerations for Pavement Joints .....
SUBCOMMITTEE III, ACI COMMITTEE 325 **1**

Shearing Strength of Reinforced Concrete Slabs .....RICHARD C. ELSTNER
and EIVIND HOGNESTAD **29**

Prestressed Concrete Pavement for Airfields ....
.....THOMAS CHOLNOKY **59**

Earthquake Resistant Design Based on Dynamic Properties of Earthquakes .....
.....G. W. HOUSNER **85**

Structural Analysis by Dynamic Load Parameters .....JAMES A. CHENEY **99**

Spacing of Reinforcement in Beams .....
.....S. J. CHAMBERLIN **113**

Current Reviews **135-144**

News Letter **1-34**

Breathtaking *isn't too strong a word—*

for this 83-ft.-high, 310-ft.-diameter concrete stadium

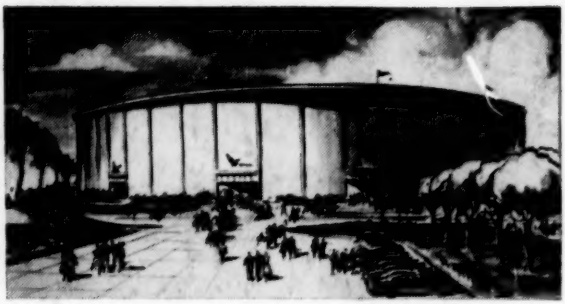

● Montevideo's cylindrical concrete stadium, to seat 20,000, is a masterpiece of simplicity and economy. Wall was built by slip-form method, using 'Incor'* 24-Hour Cement, produced by Lone Star's Uruguayan subsidiary, for speed, economy, equality. Roof, built without forms or falsework, is supported on 256 seven strand cables, strung between a ring 6 ft. 6 in. wide and 1 ft. 5¾ in. thick, concreted around top of wall, and an 18-ft.-diameter steel ring at roof's center.

Working out from center, 9,000 precast concrete slabs, 2 in. thick, with reinforcing rods projecting laterally and shaped into hooks, were fastened to the cables. Roof was then prestressed by overloading 50%, placing concrete in slab joints, and removing overload after concrete had hardened.

Talk about simplicity! Clearly, the designers solved their problems by taking fullest advantage of concrete's flexibility and "doing what comes naturally."

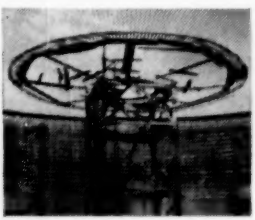

Roof, supported by cables extending from concrete ring atop wall to steel ring at roof's center, consists of 9000 concrete slabs 2" thick, hooked to cables; prestressed by overloading with brick, then concreting joints, later removing overload.

LONE STAR CEMENT CORPORATION

Offices: ABILENE, TEX. · ALBANY, N.Y. · BETHLEHEM, PA. · BIRMINGHAM · BOSTON · CHICAGO · DALLAS · HOUSTON
INDIANAPOLIS · KANSAS CITY, MO. · NEW ORLEANS · NEW YORK · NORFOLK · RICHMOND · WASHINGTON, D.C.

LONE STAR CEMENT, WITH ITS SUBSIDIARIES, IS ONE OF THE WORLD'S LARGEST CEMENT PRODUCERS, 18 MODERN MILLS, 38,000,000 BARRELS ANNUAL CAPACITY

*Reg. U.S. Pat. Off.

JULY 1956
No. 1
Vol. 28

PROCEEDINGS VOL. 53

Cost per copy $1.50. Extra copies to ACI members $1.00.

Papers, committee reports, and other contributions to the **Proceedings** pages of this Journal, as submitted in furtherance of Institute objectives, are, if published, accepted on the sole responsibility of their authors. Institute authority attaches only to standards adopted as provided in the By-laws.

Advertising. See statement under "Alphabetical List of Advertisers" final page **News Letter** section.

Membership dues and Journal subscription rates. Members receive the Journal as one of the considerations of dues payments. Membership grades are: Individual (U. S., its possessions, and North and Central America), $15, Individual (all other foreign countries), $12, Corporation, $50, Contributing, $100, Junior, $7.50, Student, $5. Subscription prices are $12 per year; payable in advance ($15 per year outside North America and U.S. possessions). The Journal is issued monthly, July to June (the volume year being completed by title page, contents, indexes, and closing discussion in Part 2 of the subsequent December issue).

Bound volumes 1 to 51 of PROCEEDINGS of the AMERICAN CONCRETE INSTITUTE (1905 to 1955) are for sale as far as available at prices to be had on inquiry of the Secretary-Treasurer. Special prices apply for members ordering bound volumes in addition to the monthly Journal.

Address: American Concrete Institute, 18263 W. McNichols Road, Detroit 19, Mich. **Copyright, 1956,** American Concrete Institute. Printed in U. S. A. Original entry at the Post Office at Detroit, Mich. Additional entry at Berrien Springs, Mich., as mail of the second class under provisions of the Act of Mar. 3, 1879.

JOURNAL
OF THE
AMERICAN CONCRETE INSTITUTE

Published by the American Concrete Institute under the authority of its Board of Direction

President
FRANK KEREKES

Vice-Presidents
WALTER H. PRICE — DOUGLAS McHENRY

Directors

ROBERT F. BLANKS	J. W. KELLY
CLAYTON L. DAVIS	THOMAS B. KENNEDY
HARRY C. DELZELL	WALTER J. McCOY
PHIL M. FERGUSON	H. C. ROSS
BRUCE E. FOSTER	LEWIS H. TUTHILL
JOSEPH F. JELLEY	GEORGE W. WASHA

Past Presidents
HENRY L. KENNEDY
C. H. SCHOLER — CHARLES S. WHITNEY

Secretary-Treasurer
WILLIAM A. MAPLES

Technical Director
PAUL F. RICE

Managing Editor
ROBERT E. WILDE

Advertising Manager
ANDREW M. SMITH

Manager, Publications Sales
ISABELLE DAVIS

Membership Secretary
EVELYN SCHLITZ

This is to Certify that

John Smith

is a

Member

of this institute and fully entitled to the privileges granted by its Charter and Bylaws

_____
President

_____
Secretary-Treasurer

Date of membership: July 1, 1952

Above is shown the membership certificate now available to all interested members. (Student members become eligible for certificates when they advance to one of the higher membership grades.) The actual certificate is 10 x 12 in. on parchment paper suitable for framing.

Return this order form together with your remittance—to avoid the added expense of billing—and your certificate will be mailed to you. Please allow 60 days for preparation of the certificate.

Please accept my order for a membership certificate at the price of $1.50.

☐ Check ☐ M.O. Enclosed

My name is to appear exactly as follows:

_____
(Print or type)

Signature .....

the ACI JOURNAL

is edited by the Secretary of the Technical Activities Committee under the direction of the Committee

BRYANT MATHER
Chairman

FRANK KEREKES
(ex officio)

WILLIAM A. MAPLES
Secretary

PHIL M. FERGUSON

JAMES A. McCARTHY

W. J. McCOY

MICHAEL V. PREGNOFF

L. H. TUTHILL

I. L. TYLER

WILLIAM A. MAPLES
Editor

ROBERT E. WILDE
Managing Editor

MARY K. HURD
Associate Editor

PORTER HICKS, Jr.
Editorial Assistant

BARBARA SMITH
Editorial Secretary

Contributions to the Journal

The ACI JOURNAL technical pages are a medium for reporting what is of current interest in the concrete field; in research, design, construction, maintenance, or manufacturing. Members and readers are urged to "have their say" as a means of sharing knowledge and experience; time and changing interests demand that new names and new ideas take their places beside the old. Contributions describing new materials and techniques or new applications of familiar practices are welcomed by the Institute.

To guide the flow of material the Board of Direction has assigned to the Technical Activities Committee the selection of papers, committee reports, discussions, and other contributions for JOURNAL publication. To assist in their technical appraisal a corps of experts in various segments of the field volunteer their services. From the technical standpoint, acceptable contributions present original material for improvement of design, manufacturing, or construction; confirm, revise, or upset established ideas or practices; or review, digest, or arrange accumulated experience for more ready use.

General considerations by TAC are whether the contribution will be of interest and service, will fit into a well-balanced publications schedule, and can be published at reasonable expense to the Institute.

To expedite appraisal and publication, if accepted, contributors are requested to furnish glossy prints or inked tracings of illustrations accompanying manuscripts submitted for consideration. Further details of form and physical arrangement of contributions begin on p. 14, 1955 *ACI Directory*. Separate prints of the "publications policy" are available free upon request to the Secretary.

Manuscripts of papers, discussions, and reports should be sent in triplicate to:
Secretary, Technical Activities Committee
AMERICAN CONCRETE INSTITUTE
18263 W. McNichols Rd., Detroit 19, Michigan

In ACI Journal next month

In "Considerations for Construction of Subgrades and Subbases for Rigid Pavement," by SUBCOMMITTEE I, ACI COMMITTEE 325, major problems in the design of rigid pavements are discussed. This approach to the study of subgrades and subbases is motivated by need for economy in solving pavement problems created by the nationwide variation in soil types.

"Some Implications of Recent Diagonal Tension Tests," by PHIL M. FERGUSON, presents a hypothesis of unrestrained failure based on the observed cracking which occurs when a beam fails in diagonal tension without stirrups, and away from complicating loads and reactions. The hypothesis assumes each step in the cracking pattern as a tension failure which can be rationalized in terms of the conventional stress formula.

"Conduction Calorimeter for Measuring Heat of Hydration of Portland Cement at Elevated Temperatures and Pressures," by N. C. LUDWIG and S. A. PENCE, describes an apparatus for measuring continuously the rates and total amounts of heat liberated when cement compositions and water react at temperatures from 80 to 350F with pressures varying from atmospheric to 10,000 psi. Typical test results obtained on portland cement pastes cured at 100F and at various pressures show that the rates and total amounts of heat liberated are increased by pressure at early ages.

India's Bhakra Nangal project for irrigation and power is described in "Bhakra Dam—Design and Construction Features." The dam is a 680 ft high gravity structure; an auxiliary diversion dam, the Nangal-Hydel Canal with its two power plants, and the Bhakra Canals and their distributory systems are part of the same project. General features of Bhakra Dam, including geology of the site, layouts, galleries, outlets and spillway, foundation, and construction are included. The report is by C. L. HANDA and O. P. CHADHA.

"An Expression for Creep and Its Application to Prestressed Concrete," by CEVDET Z. ERZEN, presents a simple expression for total strain (elastic plus creep). The equation for the total strain is used in determining the loss of stress in prestressed beams due to creep of concrete. Resulting analysis indicates that losses in the prestressed beams may be calculated if the variation of modulus of elasticity of concrete with time, and the creep equation of concrete are known.

An empirical method of predicting the strength of concrete based on early test results is presented in MYRON L. GORAL'S paper "Empirical Time-Strength Relations of Concrete." The method uses standard statistical procedures. Two assumptions are made: (1) For a given mix, under given conditions of mixing, placing, and curing, the concrete strength in compression, flexure, and shear is a function of time. (2) At zero time (when concrete is placed), the strength is zero, *i.e.*, the time-strength curve passes through the origin of the coordinate system.

Title No. 53-1

Structural Design Considerations for Pavement Joints*

Reported by Subcommittee III, ACI Committee 325

E. A. FINNEY
Chairman

HENRY AARON
J. A. BISHOP
BENGT F. FRIBERG
J. D. LINDSAY
L. W. TELLER
W. VAN BREEMEN

SYNOPSIS

Considerations are presented for the structural design of joints in concrete pavements for highways and airports. A description, function, and classification of joints; assumptions and materials to be used; and joint design details are included. Special consideration is given to applicable design criteria for tie bars and dowels.

INTRODUCTION

It is recognized that unanimous agreement is not likely on all details of design practice with regard to common types of joints in concrete pavements for both highways and airports. This is due, in part, to variations in conditions, particularly climate and traffic volume, for which provisions must be varied in different areas, and in part to the lack of established theoretical guidance coupled with conflicting observations of the performance of similar designs in different localities. The discussions which follow are applicable in certain cases only to highway pavements and in others only to airport pavements, although some have application to both conditions.

Because of its inherent weakness in tension, concrete is highly susceptible to cracking under tensile stresses induced by volume changes due to temperature fluctuation, autogenous shrinkage of the concrete at early age, and other causes. The nearest approach to obtaining an ideal concrete pavement comparatively free from cracks has been that of dividing the pavement into a series of slabs by introduction of joints of one kind or another, the slabs being as long as possible consistent with practical design requirements and within economic limitations. Depending on their design, the function of joints is to maintain within safe limits the stresses caused by expansion, contraction, and warping of the concrete.

*Received by the Institute May 1, 1956. Title No. 53-1 is a part of copyrighted JOURNAL OF THE AMERICAN CONCRETE INSTITUTE, V. 28, No. 1, July 1956, *Proceedings* V. 53. Separate prints are available at 50 cents each. **Discussion** (copies in **triplicate**) should reach the Institute not later than Nov. 1, 1956. Address 18263 W. McNichols Rd., Detroit 19, Mich.

The report was submitted to the main committee (17 members) with 15 voting affirmatively and none negatively.

Classification and function of joints

All types of joints fall in one of three basic categories, namely, expansion, contraction, and hinge or warping.

Expansion joints—As the term implies, the primary function of an expansion joint is to provide space for the expansion of the pavement and thereby prevent development of compressive stresses of damaging magnitude. When installed between the pavement and a fixed structure, such as a bridge, an expansion joint serves also to prevent the pavement from exerting damaging pressures against the structure. Expansion joints also function as contraction joints.

Contraction joints—The purpose of a contraction joint is to limit tensile stresses to a safe value. Since contraction joints must be free to open, the continuity of the reinforcement, if reinforcement is present, is interrupted at the joints.

Basically, there are three types of contraction joints, namely, "groove joint," "plate joint," and "butt joint."

(1) Groove joint—This joint is created by forming a groove in the upper portion of the pavement. Purpose of the groove is to reduce the pavement cross section and thereby result in higher unit tensile stresses, which will cause a crack to form immediately below the groove, thus forming the joint. Methods employed to form the groove consist of (1) temporary embedment of a suitable mandrel, (2) installation of a thin strip of premolded joint filler material to the required depth, and (3) sawing the pavement after the concrete has hardened.

In addition to the surface groove, a parting strip of wood, metal, or premolded material is sometimes provided at the bottom of the pavement, directly under the groove, to insure formation of a vertical crack and to further encourage early cracking of the concrete at the joint.

(2) Plate joint—This joint is created by erecting a separator or parting strip on the subgrade. The separator, which usually consists of a metal plate or a thin sheet of some other rigid, noncompressible material, serves to interrupt the continuity of the pavement. A groove is usually formed in the concrete immediately above the separator to serve as a reservoir for sealing material.

(3) Butt joint—This joint occurs where fresh concrete is placed against hardened concrete.

Hinge or warping joints—The term "hinge" or "warping joint" applies to any joint which permits hinge action but no appreciable separation of adjacent slabs. Hinge joints are intended primarily to relieve warping stresses. In contrast to contraction or expansion joints, appreciable changes in joint width are prevented by continuation of reinforcing steel through the joint, or by installation of steel tie bars across the joint. In effect, a joint of this type acts simply as a hinge, that is, it merely permits abutting slabs to undergo a certain amount of vertical angular displacement.

Butt joints become hinge joints when adjacent slabs are held together with tie bars or reinforcing steel.

Construction joints—This term applies to the joint necessitated by any prolonged stoppage of concreting operations, such as at the end of the day's work, equip-

ment breakdown, or delay in delivery of materials. It may be any one of the three joints—expansion, contraction, or hinge—depending on the features of the pavement design and prevailing practice.

Longitudinal joints—Because of longitudinal cracking that has occurred extensively in highway pavements constructed with full-width slabs, it has become general practice to divide the pavement into lanes by longitudinal joints.

Primarily, these joints function to relieve temperature warping stresses, and may be constructed in several ways. This joint may be an ordinary butt joint resulting from "lane-at-a-time" construction, or one created during full-width construction by embedding a metal or fiber plate in the concrete along the proposed line of the joint and so shaped as to create mechanical interlocking of slab edges; or it may be created by weakening the pavement with a deeply formed groove, sawing, or with an embedded strip of premolded material. Adjacent lanes are usually prevented from separating and faulting by steel tie bars spaced at proper intervals. Under current practice the joint may or may not be sealed, depending upon the manner of construction or on factors associated with local design and construction policies. However, in accordance with good practice longitudinal joints should be properly sealed.

Mechanical load-transfer devices

Joints constitute points of structural weakness in a pavement. To overcome this weakness some form of load transfer should be provided even though pavement thickness at the corner or edge is designed to carry the load without overstressing the concrete. Loads passing over a joint without load transfer may produce excessive deflections, resulting in permanent damage to the subgrade. This in turn may lead to excessive vertical displacement of slab ends and eventual faulting at joints even though concrete stresses are not serious.

Mechanical load-transfer devices may be divided into two major classifications:

1. Those which develop within themselves resistance to shear but little or no resistance to bending; included are face-interlock types such as deformed plates and some proprietary makes of load-transfer devices.

2. Those which develop within themselves resistance to both shear and a small amount of bending, of which the dowel bar is the most common. Most proprietary load-transfer devices employ this principle in their design.

Mechanical load-transfer devices should possess the following attributes:

1. They should be simple in design so that they may be practical to install and permit positive encasement by the concrete.

2. They should be capable of distributing load stresses throughout the adjacent concrete in a manner such that these stresses will not exceed the allowable design value. In this respect, it is especially important that high localized stresses in the concrete at the joint face be prevented.

3. They should offer no material restraint at any time to the opening of the joints.

4. They should retain their mechanical stability under wheel-load weights and frequencies comparable to those for which the pavement itself has been designed.

5. They should be constructed in a manner such as to meet specified performance requirements relative to load-transfer capacity.

6. They should be resistant to corrosion (see Van Breemen[15]).

The conventional round steel dowel is used to a greater extent than any other mechanical load-transfer device. For any given load and pavement condition, it is recommended that all other mechanical load-transfer devices be equivalent in load-transfer capacity to that of a round dowel of the dimensions determined under "Load-Transfer Devices," pp. 8, 13.

Aggregate interlock

Use of aggregate interlock to transfer loads across joints and to maintain mutual alignment of abutting slabs is generally associated with nonreinforced pavement. Experience indicates that aggregate interlock may be satisfactory as a means of load transfer only under unusually favorable conditions of joint opening and foundation support. It is not satisfactory under a large volume of heavy commercial traffic.

Assumptions

As a prerequisite to the following recommendations on joint design, it is assumed that the concrete will be of first-class quality and that the pavement will be constructed on a subgrade or subbase which, in addition to possessing the required degree of stability, is not susceptible to pumping.

Further, it is assumed that all joints will be sealed with suitable sealing materials under proper workmanship to prevent water and solid foreign materials from entering the joint.

Materials

The following indicate the basis and limitations of specification requirements covering the quality of materials used in joint design and construction.

Dowels—Material for dowel bars should conform to the requirements for intermediate or hard-grade steel of the current specifications for billet-steel bars for concrete reinforcement (ASTM A 15); rail-steel bars for concrete reinforcement (ASTM A 16); or axle-steel bars for concrete reinforcement (ASTM A 160).

Deformed tie bars—Material for tie bars should be structural, intermediate, or hard-grade steel conforming to current specifications for billet-steel bars or axle-steel bars for concrete reinforcement (respectively, ASTM A 15 and A 160), or rail-steel bars (ASTM A 16).

Deformations of tie bars should conform to minimum requirements for deformation of deformed bars for concrete reinforcement (ASTM A 305).

Joint fillers—Expansion joint filler should conform to current specifications for preformed expansion joint fillers for concrete (AASHO M 153-52 or AASHO M 90).

Joint-sealing compound—Sealing materials should conform to requirements of federal specifications for joint sealing: SS-S-164—sealer, hot-poured type; SS-S-00167—sealer, hot-poured, jet-fuel-resistant type; SS-S-156—sealer, cold application, emulsion type; or SS-S-159—sealer, cold application, mastic type; or SS-S-170—sealer, joint, two-component, jet-fuel-resistant, cold applied.

STRUCTURAL DESIGN OF JOINTS IN CONCRETE HIGHWAYS

Expansion joints

The width of expansion space per joint and the total expansion space needed are governed by pavement design details, aggregates used, and local climatic conditions. Current design practice, for practical reasons, limits the maximum width of expansion joint openings to 1 in. The more common opening is ¾ in. To provide more than 1 in. expansion space at any special location, such as bridges and railroad crossings, where it is desirable to limit compressive forces to a safe value, it is recommended that two or three expansion joints of standard width at spacings of approximately 20 ft be installed. This need apply only in cases where expansion joints are omitted as general practice.

Mechanical load-transfer devices are necessary at expansion joints. Methods for determining the size, length, and spacing of dowels are considered under "Load-Transfer Devices," p. 8.

At expansion joints, the sliding ends of the dowels must be enclosed in a close-fitting metal cap or thimble to provide space for movement of the dowel in the concrete during an expansion cycle. The space should be equivalent to the width of the expansion joint, plus ¼ in.

The moving portion of dowel bars in expansion joints must be treated properly to prevent bond and to reduce joint friction. Treatments for this purpose generally

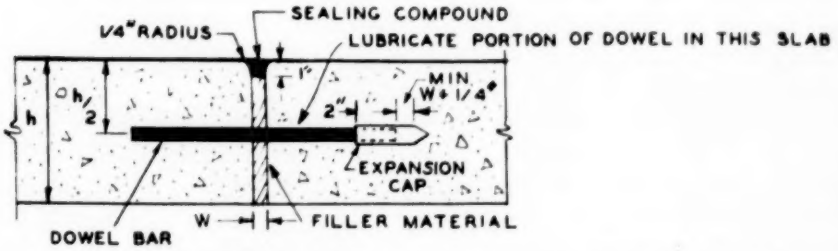

Fig. 1—Recommended design details for highway transverse expansion joint

consist of a paint coat of red or blue lead followed by a coating of lubricating grease of the mineral type; or single coat applications of lubricating grease, asphaltic cut-back materials of grades RC1 or RC2, or asphaltic oils of grade MC2.

The joint filler should be so fabricated as to accommodate the specified load-transfer devices and permit sealing at the top of the joint. To permit adequate sealing, the top of the filler material should be placed ¾ to 1 in. below the pavement surface.

Recommended design details for expansion joints are shown in Fig. 1.

Contraction joints

Contraction joints may be formed in different ways. The type selected is generally determined by construction conditions and local design policy.

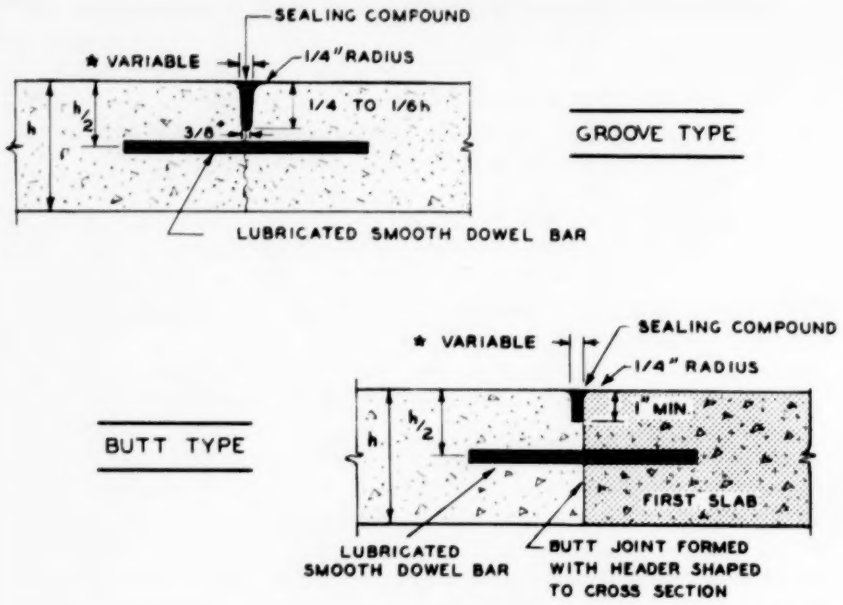

Fig. 2—Recommended design details for highway transverse contraction joints
*Width at least twice annual variation in joint width but not less than 1/8 in.

Groove—The groove contraction joint is more widely used than any other. In general, the depth of the surface groove should be not less than 1/6 nor more than ¼ the thickness of the pavement. Depth of the groove may be decreased to not less than 1½ in. if a groove is also formed at the bottom of the pavement by installing a parting strip of suitable height (1 in.) on the subgrade and in the same vertical plane as the surface groove. Depth of the groove plus the height of the parting strip should not exceed 1/3 the pavement thickness. The width of the groove should be at least twice the annual variation in joint width, but not less than 1/8 in. This recommendation is made to facilitate sealing of the joint and to insure that the joint will remain in a sealed condition; however, it may be waived if test results or experience records indicate that the joint sealer to be used performs adequately with narrower joint openings.

Experience has demonstrated that the groove may be formed successfully by sawing the concrete at a proper age. A groove conforming to above dimensions may be obtained by using two saw blades separated by spacers of proper thickness.

Mechanical load-transfer devices are recommended under all conditions where joint spacing exceeds 20 ft, and at lesser spacings where service conditions are severe. When dowels are used, proper provision must be made to prevent bond and reduce joint friction (see paragraph 4, p. 5).

Flat plate—A thin transverse strip of material is left in place to form the joint. The strip should be capped in a manner such that when the cap is removed it

will form a groove adequate for filling and retaining joint-sealing material. Load-transfer devices are recommended under all conditions of joint spacing.

Deformed plate—Recently, plates with horizontal deformations or corrugations have been used for the dual purpose of forming the joint and providing mechanical interlock. In the absence of conclusive performance data, no design recommendations can be made at this time. However, design features of this joint indicate that it should not be used when slab lengths exceed 20 ft (see "Aggregate Interlock," p. 4).

Butt—This is essentially a construction joint which should be treated in the manner of other types of contraction joints requiring load-transfer devices.

Recommended details for contraction joints are illustrated in Fig. 2.

Hinge or warping joints

There are two types of hinge joints, namely, groove and formed tongue-and-groove. They are used in longitudinal joint construction. At hinge joints, separation of abutting slabs is prevented by bonded steel tie bars or two-piece connectors. Load transfer is accomplished by aggregate or mechanical interlock and to some extent by the tie bars. Determination of size, length, and spacing of tie bars is treated on p. 13.

Groove—Although the formed groove method is more commonly used, formation of the groove by cutting the pavement with a concrete saw is rapidly taking its place and the latter is preferentially recommended.

Tongue-and-groove—The essential elements of this joint are the formed tongue-and-groove, which provide load transfer, and deformed tie bars to hold the slabs in intimate contact. The tongue-and-groove may be formed in full-width construction by a preformed metal plate left in place. In lane-at-a-time construction it is recommended that the desired groove in the slab edge be formed by using deformed metal strips attached to the forms.

Top edges of the butt type of hinged joint should be finished with a groove so that the joint may be sealed effectively.

Recommended design details for hinge joints are illustrated in Fig. 3.

Tie bars

Tie bars hold the faces of abutting slabs in intimate contact, thus insuring adequate load transfer. Tie bars are not designed to act as load-transfer devices. Tie bars are designed to withstand the maximum tensile forces required to overcome friction between pavement and subgrade, from the joint in question to the nearest free edge.

Recommended sizes, lengths, and spacing of tie bars for different pavement conditions are presented in Table 1. The basis for these recommendations is covered on p. 13.

Use of bent tie bars which are later straightened out, as in lane-at-a-time construction, is not recommended. Instead, it is recommended that an approved two-piece connector be used. Tensile strength of such connectors should be at least that of conventional tie bars which would be required for a given pavement design.

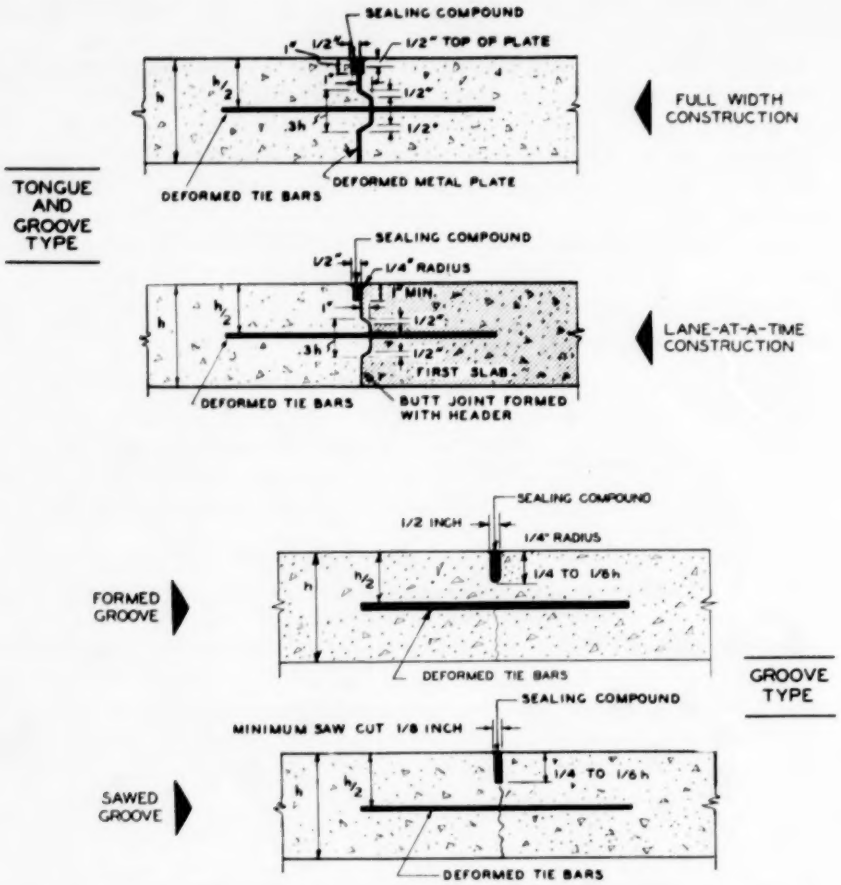

Fig. 3—Recommended design details for highway longitudinal hinge or warping joints

Load-transfer devices

The load-transfer device most generally employed consists of a plain round steel bar, commonly referred to as a dowel bar assembly or doweling system.

Design of the doweling system is, of course, dependent on the loads for which the pavement is designed. Dowels should be of such dimensions as to safely resist the shearing and bending stresses induced in the dowels by loads standing on or moving across the joint in combination with the stresses produced by warping or permanent curling of the concrete, and they should have sufficient bearing area so that the bearing pressure between dowel and concrete will not be excessive.

The required spacing of dowels is dependent on design requirements for the pavement as a whole. Theory, research, and experience indicate that individual

TABLE 1—RECOMMENDED MAXIMUM SPACING FOR ½- AND ⅝-IN. TIE BARS*

Type and grade of steel	Working stress, psi	Pavement thickness, in.	½-in. diameter bars				⅝-in. diameter bars			
			Over-all length, in.	Spacing, in.†			Over-all length, in.	Spacing, in.†		
				Lane width 10 ft	Lane width 11 ft	Lane width 12 ft		Lane width 10 ft	Lane width 11 ft	Lane width 12 ft
Structural grade billet or axle steel	22,000	6	20	46	42	38	24	48	48	48
		7		39	36	33		48	48	48
		8		34	31	28		48	48	45
		9		30	28	25		48	43	40
		10		27	25	23		43	39	36
Intermediate grade billet or axle steel	27,000	6	24	48	48	47	27	48	48	48
		7		48	44	40		48	48	48
		8		42	38	35		48	48	48
		9		37	34	31		48	48	48
		10		34	31	28		48	48	44
Rail steel or hard grade billet or axle steel	33,000	6	27	48	48	48	33	48	48	48
		7		48	48	48		48	48	48
		8		48	47	43		48	48	48
		9		46	42	38		48	48	48
		10		41	37	34		48	48	48

*Deformations of tie bars conforming to ASTM A305. Working stress based on 0.67 of minimum yield point strength of steel. Over-all length includes 3-in. allowance for centering.
†It is recommended that spacing of tie bars should not exceed 48 in.

dowels must be closely spaced for efficient performance. This is equally applicable to proprietary load-transfer devices. In current practice the spacing ranges from 12 to 15 in.

Recommended minimum practical requirements for dowels for various pavement thicknesses are presented in Table 2. These recommendations are based on the procedure for the design of load-transfer devices presented under "Determination of Size and Spacing of Round Dowels," p. 15.

Recommendations for load transfer at joints have been based on the most commonly used type of load-transfer device, the common round steel dowel. If proprietary load-transfer devices are used in lieu of dowels they must have, for the given conditions, a load-transfer capacity equal to or better than that of the recommended dowel.

Dowel supporting assemblies

The general use of dowels has encouraged development of many different assemblies to hold the dowels in place during concreting. However, the fabricated wire frame is perhaps the type most commonly used. Certain proprietary load-transfer devices depend upon the joint filler or a special plate to hold them in position.

Supporting assemblies should be sufficiently rigid to maintain proper horizontal and vertical alignment of the dowels, within a tolerance of ⅛ in. per foot of dowel length, during the entire

TABLE 2—MINIMUM RECOMMENDED DOWEL REQUIREMENTS FOR EXPANSION OR CONTRACTION JOINTS IN HIGHWAY CONSTRUCTION*

Pavement thickness, in.	Dowel diameter, in.	Dowel length, in.	Dowel spacing, in.
6	¾	18	12
7	1	18	12
8	1	18	12
9	1 ⅛	18	12
10	1 ¼	18	12

*For practical reasons adjustments have been made to the theoretical requirements as presented in Table 10.

concreting operations. Spring-type clip devices to hold dowels in place are not recommended. Width of the assemblies should be consistent with dowel length, but should not be less than 15 in. for proper stability.

On subgrades of cohesionless granular materials some means of preventing the assembly from settling during placing of the concrete should be provided. This may be accomplished by attaching metal plates to the lower members of the assembly, or by placing the assembly on a wide, continuous base plate.

STRUCTURAL DESIGN OF JOINTS IN AIRPORT CONCRETE RUNWAYS

The same essential engineering problems encountered in highway pavements are encountered in the construction of airport runways. Airport pavements constructed in accordance with accepted standard practices used in highway construction will have similar joint design characteristics. In airport pavements, however, there are certain additional factors to satisfy aircraft operations. Highway design considers not only the magnitude of wheel loads but also the frequency of their application to certain critical locations on the pavement, whereas in the case of airports, the frequency of load application is important primarily on taxiways, aprons, and runway ends where aircraft traffic is channelized. This channelization does not occur on the main portion of the runway. On the other hand, airport pavements must be designed to accommodate wheel loads considerably heavier than those found in current commercial highway vehicles. Thus, airport requirements necessitate somewhat different procedures resulting in joint design and pavement thicknesses materially different from those required for highway pavement.

Joint design recommendations applicable to both types of pavement construction already covered in the previous text have been omitted to avoid unnecessary duplication.

Expansion joints

In airport work involving large paved areas, certain longitudinal and transverse joints are constructed as expansion joints.

Longitudinal—Recommended longitudinal expansion joint design details are shown in Fig. 4. Dowels should not be used at longitudinal expansion joints, but the edges of the slabs along the joints should be thickened to at least 1.25 times normal slab thickness. Thickness of the joint filler should be ¾ in.

Transverse—It is recommended that the joint filler for transverse expansion joints should be not less than ¾ in. nor more than 1 in. thick (see Fig. 5).

Contraction joints

Groove—The groove contraction joint is recommended. The groove should be of sufficient width and depth to perform its function and to permit proper sealing. When the groove is made by a removable mandrel, the top edges should be care-

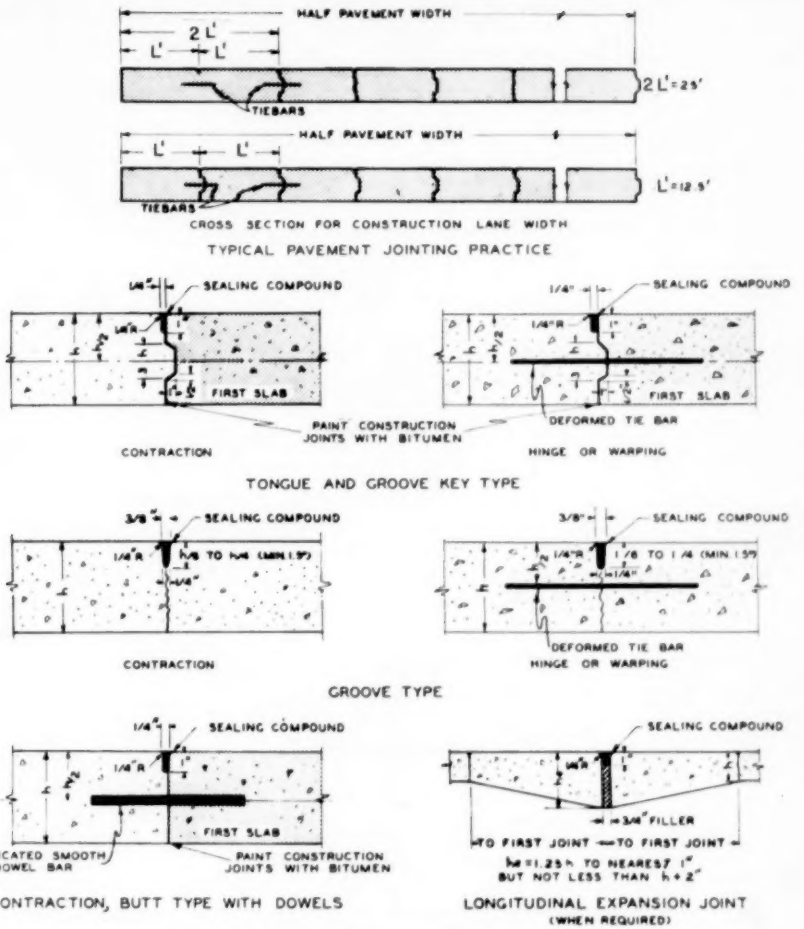

Fig. 4—Recommended design details for airport runway longitudinal joints

1—Deformed tie bars to be installed in groove and keyed joints occurring within span, 25 ft of free edge of pavement
2—Butt construction joints, with dowels spaced as required, may be used in lieu of keyed joints
3—All joints shall be sealed with approved material

fully formed and finished with an edging tool. In general, depth of groove may range from 1/6 to ¼ the thickness of the slab. Within these limits the depth should never be less than 1½ in., nor less than 1/6 the thickness of the slab, nor less than the maximum size of aggregate, whichever is the greater. The groove may be formed by sawing the pavement after the concrete has hardened.

Keyed and butt (construction joints)—These joints naturally result from lane-at-a-time construction operations and may be constructed either with a key (tongue-and-groove interlock), with or without tie bars, or as a plain butt joint

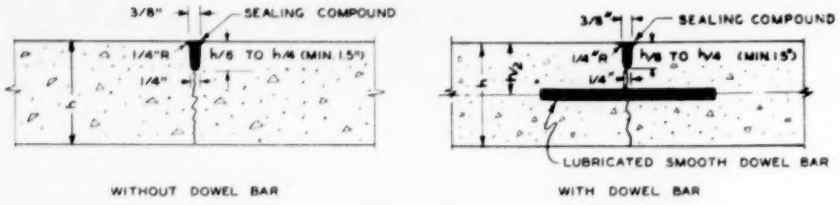

GROOVE TYPE CONTRACTION JOINTS

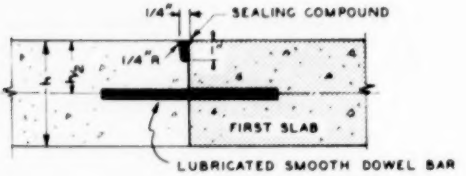

CONTRACTION, BUTT TYPE WITH DOWELS

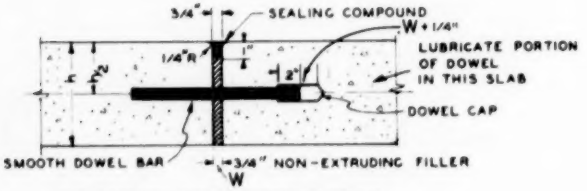

EXPANSION TYPE WITH DOWELS

Fig. 5—Recommended design details for airport runway transverse joints

1—Dowels shall be used in groove joints in aprons, taxiways, and thickened end sections of runways. They may be omitted in other portions of runways
2—Dowel size and spacing shall be as required
3—All joints shall be sealed with approved material

with smooth dowel bars. In either case the edges should be finished with a grooving tool or otherwise constructed so as to form a slot along the joint of such dimensions that it can be sealed with an approved sealing compound. Recommended design details are shown in Fig. 4.

Hinge or warping joints

Depending upon design requirements, hinge or warping joints may be constructed as groove joints, tongue-and-groove joints, or as plain butt joints. In all three cases, tie bars must be employed to hold abutting slabs in intimate contact.

Details for this type of joint construction are shown in Fig. 4.

Tie bars

The diameter, length, and spacing of tie bars for different grades of steel may be determined by the equations or graphs to be found in the following section dealing with the design of tie bars. However, the recommended minimum diameter of tie bars for airport work is ⅝ in. The recommended range of tie bar length is 30 to 36 in. at a spacing of 30 in. on center.

TABLE 3—RECOMMENDED DOWEL REQUIREMENTS FOR LONGITUDINAL BUTT JOINTS, TRANSVERSE EXPANSION, CONSTRUCTION, AND CONTRACTION JOINTS IN AIRPORT CONSTRUCTION

Pavement thickness, in.	Dowel diameter, in.	Dowel length, in.	Dowel spacing, in.
6	¾	18	12
7	¾	18	12
8	1	18	12
9	1	18	12
10	1	18	12
11	1 ¼	20	15
12	1 ¼	20	15
13	1 ¼	20	15
14	1 ¼	20	15
15	1 ¼	20	15
16	1 ½	24	15
17	1 ½	24	15
18	1 ½	24	15
19	1 ½	24	15
20	1 ½	24	15

Load-transfer devices

Some form of mechanical load transfer is recommended at all transverse expansion and construction joints as well as at butt longitudinal construction joints. Recommended size, length, and spacing of dowels for load transfer are shown in Table 3.

Dowel bars must be properly treated to prevent bond and reduce joint friction. Treatments for this purpose generally consist of a paint coat of red or blue lead followed by a coating of lubricating grease of the mineral type; or single coat applications of lubricating grease, asphaltic cut-back materials of grades RC1 or RC2, or asphaltic oils of grade MC2.

DETERMINATION OF SIZE, SPACING, AND LENGTH OF TIE BARS

The function of tie bars is to resist tensile forces which tend to separate the slabs on each side of a joint. Tie bars are not designed and are not intended to serve as load-transfer devices. However, in holding the slab faces together at a joint they do permit interlocking action across the joint face, which effects load transfer across the joint. The tensile force which tie bars resist is the force of subgrade resistance between pavement and subgrade from the joint designed to the nearest free edge.

Size and spacing

The recommended cross-sectional area of tie-bar steel per foot-length of joint may be obtained from Eq. (1).

$$A_s = L'Fw/f_s \quad \ldots\ldots (1)$$

A_s = area of steel, sq in., required per foot of joint
L' = distance in ft between the joint in question and the nearest free joint or edge

F = coefficient of subgrade resistance between pavement and subgrade (usually taken at 1.5)
w = weight per sq ft of slab in lb = (12.5 × average thickness of slab in in.)
f_s = allowable working stress of steel, psi. A value of 0.67 of the yield point is recommended.

Table 4 gives the recommended allowable working stresses for various grades of billet steel.

TABLE 4—RECOMMENDED ALLOWABLE WORKING STRESSES FOR BILLET, AXLE, OR RAIL STEEL FOR TIE BARS

ASTM Designation: A 15-52T, A 160-52T, and A 16-52T

Type and grade of steel	Yield point (minimum), psi	Recommended working stresses,* psi
Billet and axle steel, structural grade	33,000	22,000
Billet and axle steel, intermediate grade	40,000	27,000
Rail steel or billet and axle steel, hard grade	50,000	33,000

*Based on 0.67 of the minimum yield point.

The selected size and spacing of tie bars should be such that the cross-sectional area of steel in square inches, per foot of joint, is at least equal to the amount given by the above formula. Fig. 6, 7, and 8 may be used for selecting the size and spacing of tie bars for different types and grades of steel.

Length

A tie bar should be long enough to provide sufficient anchorage on each side of the joint to develop the allowable working strength of the tie bar. In addition, an allowance should be made for inaccurate centering of the tie bar. A 3-in. allowance is recommended. Expressed as a formula, this becomes:

$$L_T = \frac{2f_sA_s}{uQ} + 3 \text{ in.} \quad \ldots\ldots (2)$$

L_T = length of tie bar, in.
f_s = allowable working stress of steel, psi [use same value employed in solving Eq. (1)]
A_s = cross-sectional area of one tie bar, sq in.
Q = perimeter of tie bar, in.
u = allowable bond stress. The maximum working stress for bond in deformed bars (deformations meeting ASTM A 305) is generally taken as 0.10 of the compressive strength of the concrete, up to a maximum of 350 psi. It is permissible to use this maximum value in the design of tie bars, since paving concrete should have a compressive strength in excess of 3500 psi. For plain bars or bars not meeting the requirements of ASTM A 305, the allowable bond stress should be limited to 0.045 of the compressive strength of the concrete or 158 psi for 3500-psi concrete.

The lengths of the tie bars given in Fig. 6, 7, and 8 agree with Eq. (2).

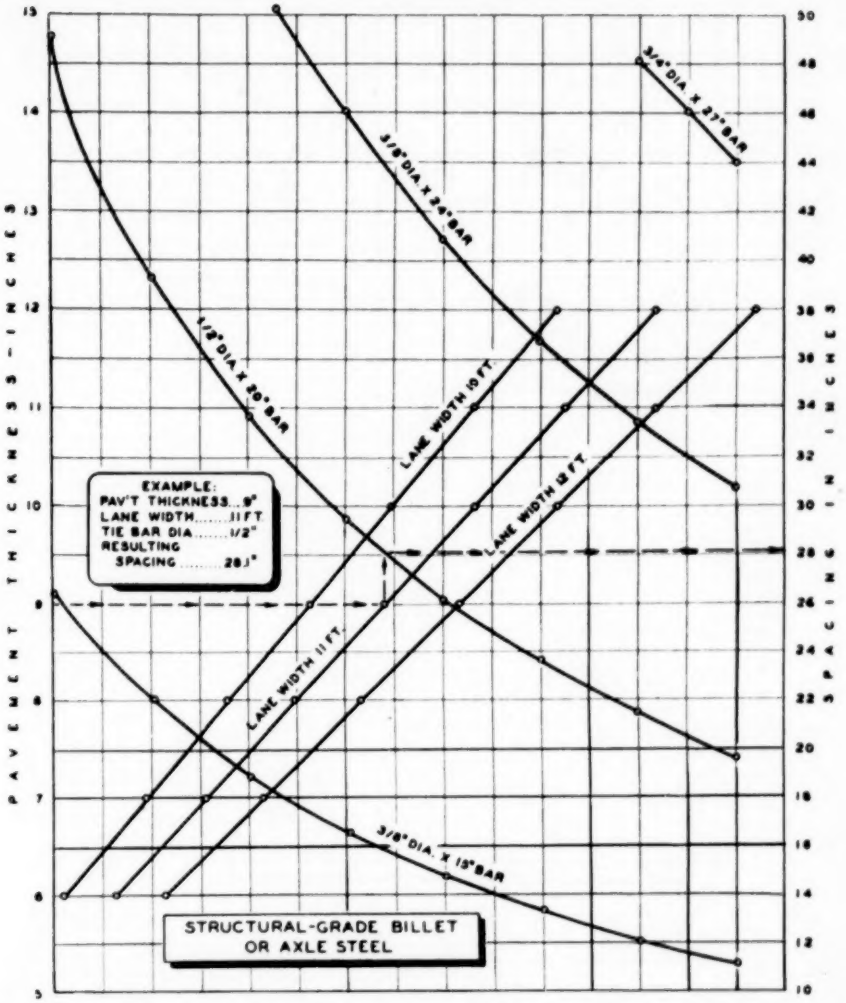

Fig. 6—Maximum spacing for typical tie bar diameters for various pavement thicknesses and lane widths—structural-grade billet or axle steel

DETERMINATION OF SIZE AND SPACING OF ROUND DOWELS

Determination of dowel diameter and design of the doweling system is based on the following recommended design criteria. The doweling system is designed with sufficient strength to transfer one-half of the assumed pavement design wheel load across the joint with a safe bearing pressure between the dowel and the supporting concrete.

1. The design wheel load is considered compatible with the supporting ability

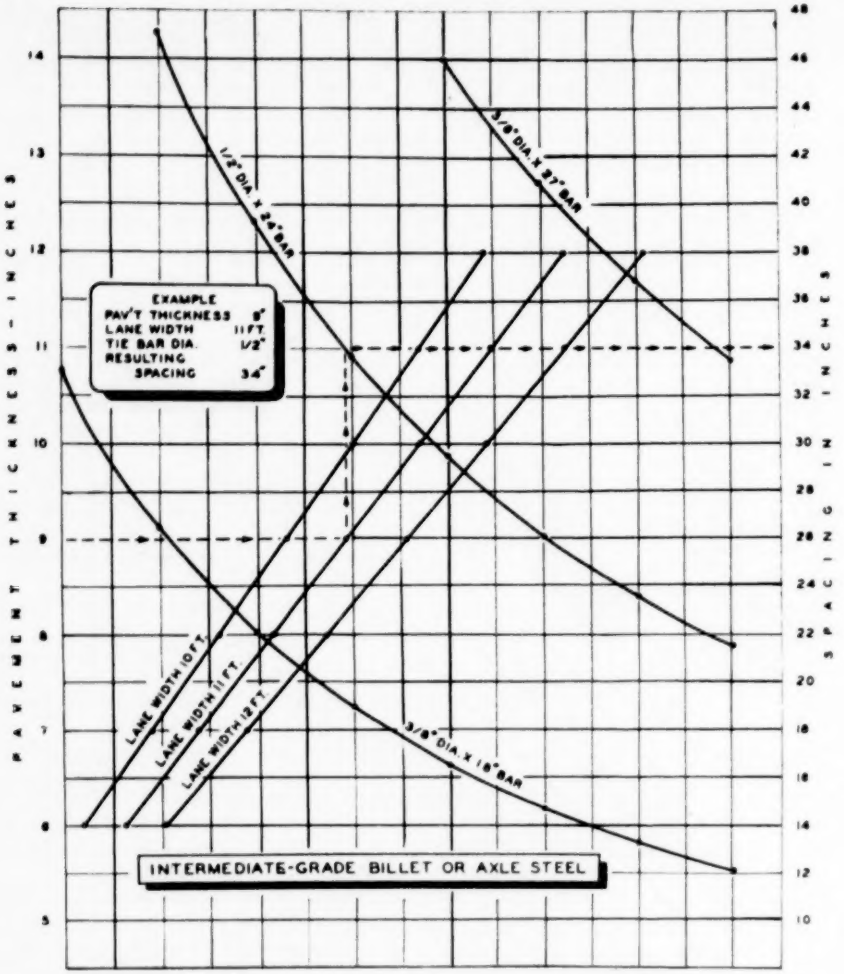
PAVEMENT THICKNESS - INCHES
TIE BAR SPACING - INCHES
EXAMPLE
PAV'T THICKNESS 9"
LANE WIDTH 11 FT.
TIE BAR DIA. 1/2"
RESULTING SPACING 34"
1/2" DIA X 24" BAR
5/8" DIA X 27" BAR
3/8" DIA X 18" BAR
LANE WIDTH 10 FT.
LANE WIDTH 11 FT.
LANE WIDTH 12 FT.
INTERMEDIATE-GRADE BILLET OR AXLE STEEL

Fig. 7—Maximum spacing for typical tie bar diameters for various pavement thicknesses and lane widths—intermediate-grade billet or axle steel

of the pavement structure and not necessarily with the legal wheel load.

2. The doweling system must be capable of transferring one-half the design wheel load.

3. The design wheel load is considered to be acting at corner of slab over the outside dowel.

4. Bearing pressure on the concrete rather than the bending stress or shearing in the dowel controls the design of the dowel.

5. Allowable bearing stress in the concrete at the joint face and under the dowel is based on theoretical considerations and laboratory experimentation developed by Friberg[2] and Marcus.[3]

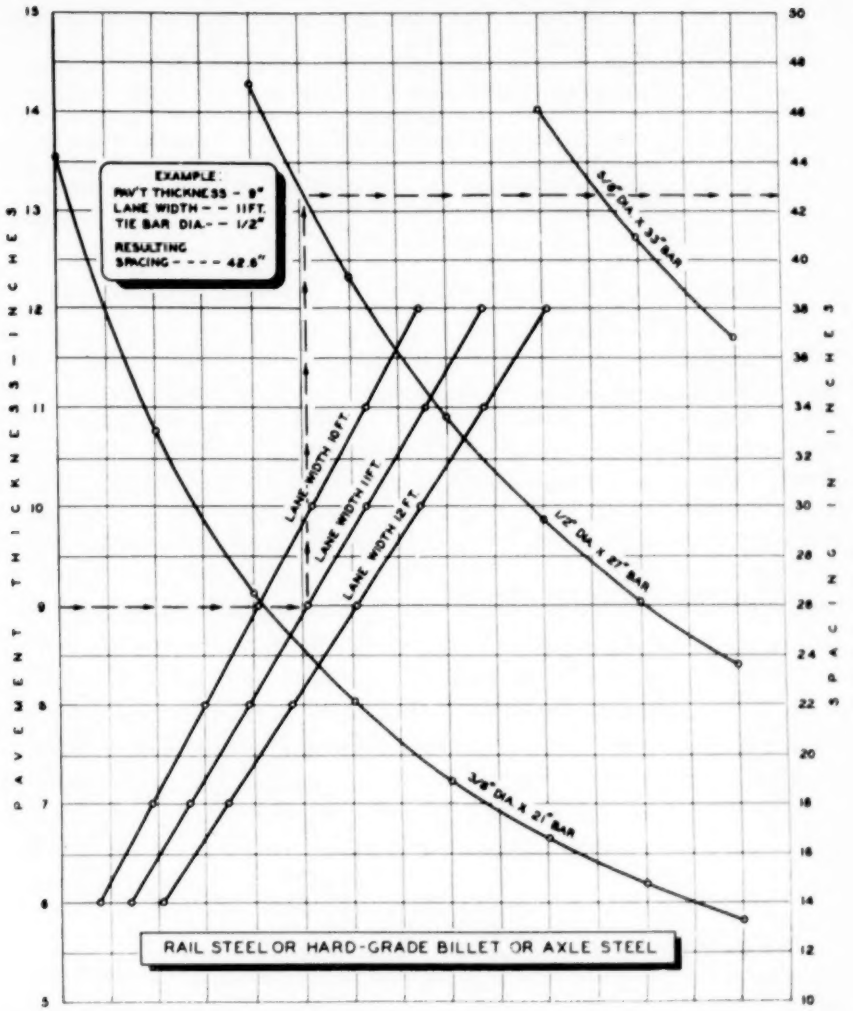
EXAMPLE:
PAV'T THICKNESS - 9"
LANE WIDTH - - 11FT.
TIE BAR DIA.- - 1/2"
RESULTING
SPACING - - - - 42.6"
LANE WIDTH 10 FT.
LANE WIDTH 11FT.
LANE WIDTH 12 FT.
5/8" DIA X 33" BAR
1/2" DIA X 27" BAR
3/8" DIA X 21" BAR
RAIL STEEL OR HARD-GRADE BILLET OR AXLE STEEL
PAVEMENT THICKNESS - INCHES

Fig. 8—Maximum spacing for typical tie bar diameters for various pavement thicknesses and lane widths—rail steel or hard-grade billet or axle steel

6. Capacity of a dowel to transfer load across a joint is based on the theory developed by Timoshenko and Lessels,[1] which is applicable to an elastic structure extending into an elastic mass an infinite distance from its boundary surface.

7. The number of effective dowels is determined in accordance with criteria developed by Friberg[4] in which the effectiveness of adjacent dowels decreases linearly to zero at a distance from the load equal to 1.8 times the radius of relative stiffness of the pavement slab. The radius of relative stiffness is a linear dimension relating the relative stiffness of the pavement slab to that of the sub-

grade. It is based on a physical concept necessary in the pavement design theory developed by Westergaard.[2]

8. The effective length of embedment is considered that portion of the dowel which is in direct bearing on the concrete. In the case of expansion joints, the length of dowel normally covered by the expansion sleeve is excluded. However, for practical reasons the length of embedment of dowels in expansion and contraction joints is considered to be the same. Tests indicate that in the case of ¾-in. dowels, maximum performance is obtained when the length of embedment is approximately 8 times the dowel diameter, but this value tends to decrease as the dowel diameter increases (see Fig. 14).

Load-transfer capacity of single dowels

The following analysis of the behavior of a round dowel and its capacity to transfer load across a joint is based on the theory developed by Timoshenko and Lessels[1] which is applicable to an elastic structure extending into an elastic mass an infinite distance from its boundary surface. A general mathematical solution for this condition has been developed by Friberg,[2] and applied to the deflection of dowels at joints in concrete pavements. The solution is presented in Fig. 9.

One of the problems involved in the analysis is a proper selection of the modulus of support G [Eq. (3), Fig. 9]. Table 5 indicates that previous investigations have produced a wide range of values for this term. Testing procedures have varied between investigators, but it also appears that G is susceptible to variation between specimens tested in a given way. A study of these investigations seems to indicate that the smaller diameter dowels produce a resulting G which is higher, and as the dowel diameter increases, the resulting G decreases. A value for the modulus of support G of 1,500,000 lb per cu in. has been selected for this recommendation. If the selection of G is too low, the calculated bearing pressure for a given amount of load transfer across the dowel will also be too low, thus reducing the factor of safety.

In selecting G it should be mentioned that we are considering only the effects of

TABLE 5—G VALUES FROM VARIOUS SOURCES

Modulus of dowel reaction, G		Source	Remarks	Bibliography
Range, lb per cu in.	Average, lb per cu in.			
0.3 to 1.5×10^6	———	Grinter	Estimation	2
Max. 2.5×10^6	500 f_c'	Friberg	Tests on embedded dowels—1938	4
0.71 to 1.17×10^6	0.92×10^6	MSHD*	Load-deflection test data—1947	5
0.78 to 5.89×10^6	2.30×10^6	MSHD*	Tests on embedded dowels—1947	Not published
0.89 to 8.3×10^6	2.56×10^6	Marcus	Dowels with uniform bearing pressure	3
Not known	2.45×10^6	Loe	Load-deflection tests—1952	6
0.9 to 8.6×10^6	2.5×10^6	MSHD*	Tests on embedded dowels—1954	Not published

*Michigan State Highway Department.

The relative stiffness of the dowel and the concrete mass is expressed by

$$\beta = \sqrt[4]{\frac{Gd}{4E_sI}} \quad \ldots\ldots (3)$$

G = modulus of support of concrete mass (1,500,000 lb per cu in.)
d = diameter of dowel
E_s = modulus of elasticity of dowel (29,000,000 psi)
I = moment of inertia of dowel
L_2 = length of primary bearing pressure wave on dowel, in.

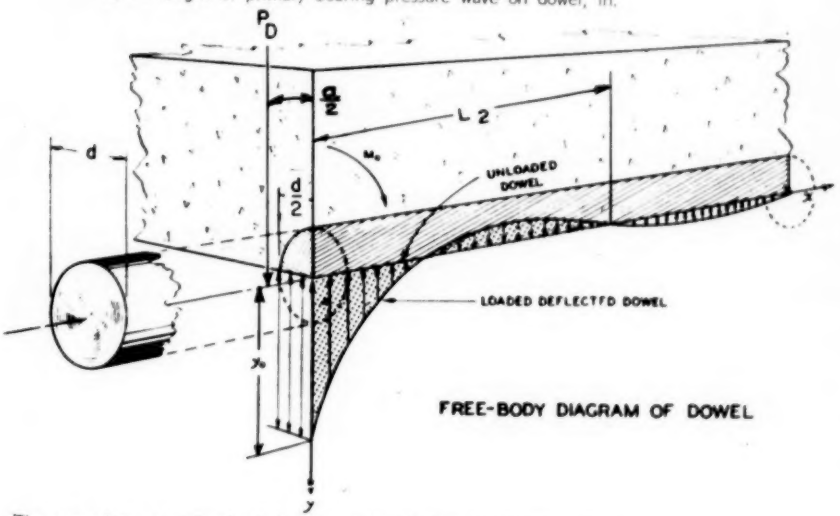

The general equation for the deflection of the dowel in the concrete mass is

$$y = \frac{e^{-\beta x}}{2\beta^3 E_s I} \{P_D \cos \beta x - \beta M_o (\cos \beta x - \sin \beta x)\} \quad \ldots\ldots (4)$$

e = base of Napierian logarithms
x = distance along the dowel from the slab face at the joint
P_D = concentrated load, lb, acting downward on the dowel at the center of the joint
M_o = bending moment in the dowel at the slab face, in.-lb. = P_D W/2

The moment and shear at any point in the dowel may be found from the following equations which are a development of the foregoing equation.

$$M = -E_sI\frac{d^2y}{dx^2} = -\frac{e^{-\beta x}}{\beta} \{P_D \sin \beta x - \beta M_o [\sin \beta x + \cos \beta x]\} \quad \ldots\ldots (5)$$

$$V = \frac{dM}{dx} = -e^{-\beta x} \{(2\beta M_o - P_D) \sin \beta x + P_D \cos \beta x\} \quad \ldots\ldots (6)$$

The maximum moment in the dowel occurs where $V = \frac{dM}{dx} = 0$

Then

$$M_{max} = -\frac{P_D e^{-\beta x_m}}{2\beta} \sqrt{1 + (1 + \beta W)^2} \quad \ldots\ldots (7)$$

W = joint width opening
x_m = distance from the slab face to the point of maximum moment in the dowel, where $\tan \beta x_m = 1/(1 + \beta W)$

Deflection of the dowel with respect to the concrete at the face of the joint is y_o, and equals y [Eq. (4)] when x = 0.

$$y_o = \frac{P_D}{4\beta^3 E_s I}(2 + \beta W)$$

S_b = bearing pressure on the concrete under the dowel at the slab face = Gy_o .... (8)

Fig. 9—Mathematical theory applicable to a round dowel in a concrete mass

TABLE 6—CONCRETE BEARING STRESSES IN RELATION TO DOWEL DIAMETER

Dowel diameter in.	Ultimate compressive strength of concrete f_c', psi	Bearing stress at failure f_b' psi	Ratio $\frac{f_b'}{f_c'}$	Allowable bearing stress* f_b', psi	Factor of safety, $\frac{f_b'}{f_b}$
¾	3780	9873	2.61	3200	3.08
⅞	—	—	—	3100	—
1†	3850	9020	2.34	3000	3.01
1⅛	—	—	—	2900	—
1¼	—	—	—	2800	—
1⅜	—	—	—	2650	—
1½†	3530	6450	1.83	2500	2.58
2†	3610	6410	1.78	2000	3.20

*As recommended by ACI Committee 325.
†Data from Marcus.[7]

TABLE 7—ALLOWABLE LOAD-TRANSFER CAPACITY OF DOWELS*

Dowel diameter, in.	Joint width, in.	Bearing stress for 1000 lb load-transfer, psi	Allowable bearing stress, psi	Allowable load-transfer capacity, lb	Dowel diameter, in.	Joint width, in.	Bearing stress for 1000 lb load-transfer, psi	Allowable bearing stress, psi	Allowable load-transfer capacity, lb
	0.00	2370	3200	1350		0.00	970	2800	2890
	0.25	2630		1220		0.25	1040		2680
¾	0.50	2890		1110	1¼	0.50	1120		2510
	0.75	3150		1020		0.75	1190		2350
	1.00	3420		940		1.00	1260		2220
	1.50	3940		810		1.50	1410		1980
	0.00	1810	3100	1710		0.00	820	2650	3230
	0.25	1990		1560		0.25	880		3010
⅞	0.50	2170		1430	1⅜	0.50	940		2830
	0.75	2350		1320		0.75	1000		2650
	1.00	2530		1230		1.00	1050		2520
	1.50	2880		1080		1.50	1170		2270
	0.00	1430	3000	2100		0.00	700	2500	3560
	0.25	1560		1920		0.25	760		3340
1	0.50	1690		1780	1½	0.50	800		3140
	0.75	1820		1650		0.75	840		2970
	1.00	1940		1540		1.00	890		2810
	1.50	2200		1360		1.50	980		2550
	0.00	1160	2900	2500		0.00	430	2000	4690
	0.25	1260		2300		0.25	450		4450
1⅛	0.50	1360		2140	2	0.50	470		4240
	0.75	1450		2000		0.75	490		4050
	1.00	1550		1870		1.00	520		3870
	1.50	1740		1670		1.50	560		3550

*Based on G = 1,500,000 lb per cu in.; E_s = 29,000,000 psi.

the concrete mass around the dowel. Some discussion has appeared in the literature on the effect of subgrade support beneath the pavement at the joint and its influence on G. The modulus of subgrade support k will influence the deflection and curvature of the pavement slab in the vicinity of the joint. It is our considered opinion, however, that the pavement curvature is of such a large radius that its influence on bending stress in the dowel and bearing pressure between the concrete and the dowel is not appreciable. Therefore, pavement curvature will have little effect on G.

It can be demonstrated by proper substitution in the equations in Fig. 9 that in every case the bearing pressure on the concrete rather than the bending stress or shearing stress in the dowel controls the design of the dowel. It has been shown by

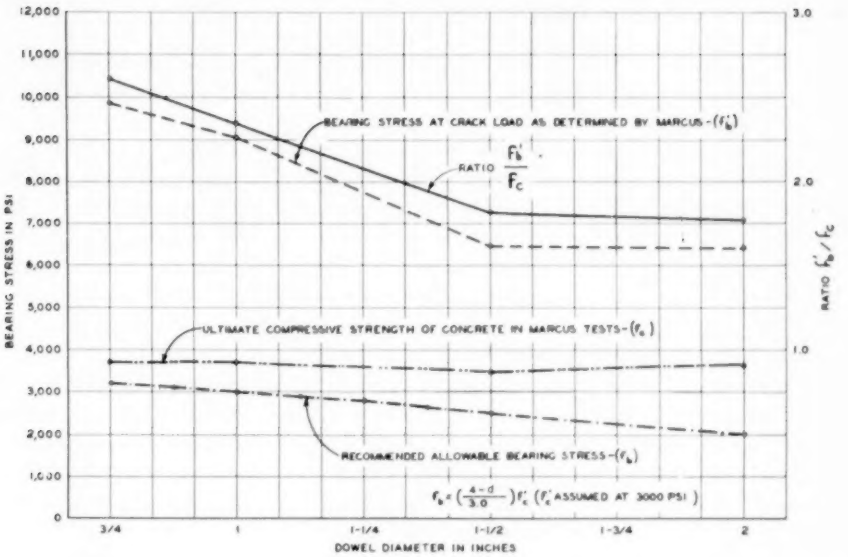

Fig. 10—Concrete bearing stresses in relation to dowel diameter

Marcus[3] that ultimate bearing stress varies also with the dowel diameter. Data determined by Marcus and others are shown in Table 6. Ultimate bearing stresses and recommended allowable bearing stresses for various dowel diameters are illustrated in Fig. 10.

Calculation of the bearing pressure on the concrete for 1000 lb of load transfer is illustrated below.

Example: 1-in. diameter dowel
0.25 in. width of joint opening
P = 1000 lb acting on dowel at slab face

$$I = \frac{\pi d^4}{64} = \frac{3.1416}{64}(1.0)^4 = 0.0491 \text{ in.}^4$$

$$\beta = \sqrt[4]{\frac{Gd}{4E_cI}} = \sqrt[4]{\frac{(1.5 \times 10^6)1}{4(29 \times 10^6)0.0491}} = 0.716 \text{ per in.}$$

$$y_o = \frac{P_D}{4\beta^3 E_c I}(2 + \beta W) = \frac{1000}{4(0.716)^3(29 \times 10^6)0.0491}[2 + (0.716)0.25] = 1.042 \times 10^{-3} \text{ in.}$$

$$S_b = Gy_o = 1.5 \times 10^6(1.042 \times 10^{-3}) = 1563 \text{ psi, say 1560 psi bearing stress}$$

Since the recommended allowable concrete bearing stress for a 1-in. dowel is 3000 psi, the allowable load-transfer capacity for a 1-in. dowel is:

$$\frac{3000}{1560} \times 1000 = 1923 \text{ lb, say 1920 lb}$$

In Table 7, similar bearing-pressure values and load-transfer capacity-values have been calculated for dowel sizes from ¾ to 2 in. and for variable joint widths.

Number of effective dowels

The number of dowels effective in transferring load across a joint depends on pavement thickness and modulus of subgrade support k, as well as spacing of the dowels. Since corner loading is the most critical condition from the standpoint of dowel design, this condition of loading is recommended as a basis for selecting the size and spacing of dowels. The wheel load is considered as acting over the outside dowel, which is a half dowel spacing from the edge of the pavement.

In this recommendation, the spacing of dowels has been standardized at the spacing which is most often used, that is, 12 in. For balanced load-transfer design between the edge of the pavement and the center, a variable spacing, smaller at the edges and greater at the center, would be the optimum. However, this is not practical and, therefore, a uniform spacing is recommended.

The number of effective dowels can be determined by using the criteria developed by Friberg[8] in which the effectiveness of the dowel directly under the point of loading is 1.0. The effectiveness of adjacent dowels decreases linearly as the distance between the dowel and the point of load application increases, until at a distance of $1.8l$ (l = radius of relative stiffness) from the load, effectiveness of the dowel is considered zero. This is illustrated in Fig. 11.

In cases where $1.8l$ exceeds the average center-to-center spacing between dual wheels, certain dowels are stressed due to both sets of dual wheels on one axle. This would result in overstressing of certain dowels unless a correction was applied in the design for the number of fully effective dowels as computed in Fig. 11. A case when it is necessary to apply such a correction is illustrated in Fig. 12.

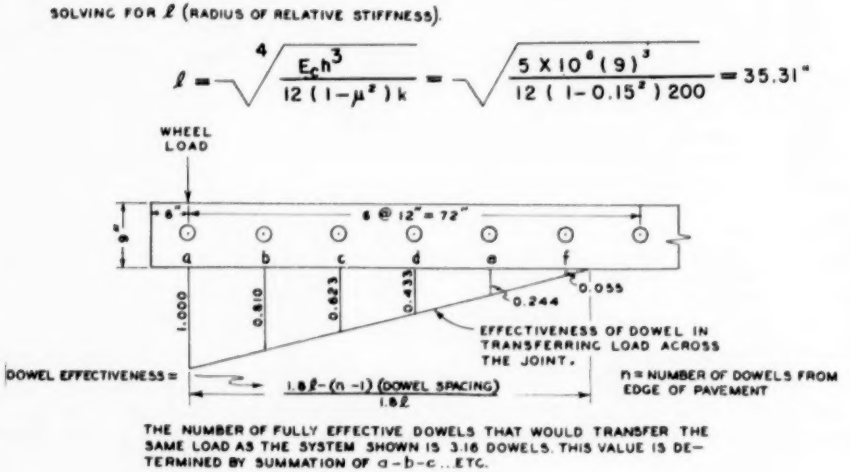

Fig. 11—Calculation of number of equivalent fully effective dowels

Example: 9-in. pavement
k = 200 lb per cu in.
Dowels spaced on 12-in. centers

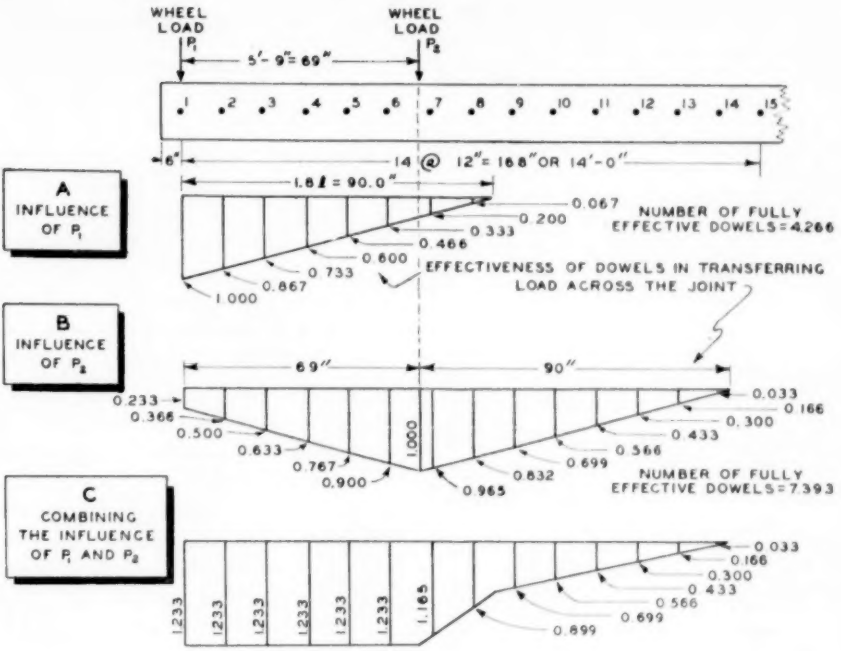

This correction is necessary when low values of k are used and for greater pavement thicknesses.

Example: 9-in. pavement

$k = 50$ lb per cu in.

Dowels spaced at 12 in.

Solving for l:

$$l = \sqrt[4]{\frac{E_c h^3}{12(1-\mu^2)k}} = \sqrt[4]{\frac{5 \times 10^6 (9)^3}{12(1-0.15^2)50}} = 50.03 \text{ in.}$$

$1.8\ l = 1.8(50.03) = 90.0$ in.

Average center-to-center spacing of dual wheels assumed to be 5 ft 9 in.

Computing the number of effective dowels on the basis of diagram A, where the influence of wheel load P_1 is shown, would give 4.266 fully effective dowels. However, due to the influence of wheel load P_2 as well as P_1 there is an overlapping effect which would lead to overstressing of dowels No. 1 through 6 by 23.3 percent. If we consider only 1/1.233 (4.266) = 3.46 dowels as fully effective and select the proper size of dowel on this basis, then the dowels will not be overstressed due to the overlapping effect of wheel loads.

Fig. 12—Calculation of number of effective dowels when 1.8 *l* exceeds the average center-to-center spacing of dual wheels

There are indications, however, that this theory may not hold true in practice. Load tests conducted by the Bureau of Public Roads[9] on doweled joints where the number of dowels was progressively reduced by cutting, indicated that two, or at most, four dowels did practically all the work. It is believed that this is due to departures in practice from the ideal conditions assumed in the theoretical treatment.

Common values for the radius of relative stiffness are shown in Table 8 based on E_c = modulus of elasticity of the concrete = 5,000,000 psi, and Poisson's ratio μ = 0.15. Table 9 contains the number of effective dowels for various design conditions.

TABLE 8—RADIUS OF RELATIVE STIFFNESS FOR VARIOUS PAVEMENT THICKNESSES AND SUBGRADE SUPPORT VALUES*

$$l = \sqrt[4]{\frac{E_c h^3}{12(1-\mu^2)k}} \quad \ldots\ldots\ldots\ldots\ldots\ldots\ldots\ldots (9)$$

Pavement thickness h, in.	Radius of relative stiffness (l), in.			
	k = 50	k = 100	k = 200	k = 300
6	36.82	30.97	26.06	23.58
7	41.39	34.83	29.28	26.45
8	45.79	38.48	32.40	29.33
9	50.03	41.96	35.31	31.94
10	54.17	45.58	38.25	34.53
11	58.13	48.80	41.09	37.10
12	61.96	52.13	43.77	39.61

*Based on modulus of elasticity of concrete = 5,000,000 psi; Poisson's ratio = 0.15.

TABLE 9—NUMBER OF EFFECTIVE DOWELS FOR LOAD TRANSFER ACROSS A JOINT FOR CORNER LOADING*

Pavement thickness, in.	Dowels spaced at 12 in.			
	k = 50	k = 100	k = 200	k = 300
6	3.29	2.85	2.47	2.29
7	3.36	3.12	2.72	2.49
8	3.37	3.38	2.95	2.73
9	3.46	3.38	3.16	2.91
10	3.54	3.39	3.38	3.10
11	3.63	3.44	3.38	3.31
12	3.72	3.50	3.38	3.36

*Based on modulus of elasticity of concrete = 5,000,000 psi; Poisson's ratio = 0.15. A reduction in the number of effective dowels has been made when 1.8 l exceeds the average center-to-center spacing of dual wheels which is taken as 5 ft. 9 in. This prevents overstressing of the dowels due to the overlapping effect on the wheels.

Selection of proper dowel size

The load-transfer capacity of a system of dowels of a given diameter is the product of (1) the individual capacity of the dowel and (2) the number of dowels which are effective in transferring wheel load across the joint. Items 1 and 2 have previously been evaluated for a wide range of dowel diameters and pavement design conditions. It is therefore possible to check and see whether a given size of dowel, at a 12-in. spacing between dowels, is sufficient to transfer one-half of the design wheel load across the joint. However, such a checking procedure would be tedious for design purposes, and therefore a direct method for determining the proper dowel diameter for load transfer for a given design wheel load and other related design considerations is shown in Fig. 13.

For example, knowing the design values for subgrade modulus, pavement thickness, design wheel load, and joint width, the proper dowel diameter can be determined from the graphs in Fig. 13 in the following manner:

Starting with a known k at the left edge of diagram A, proceed horizontally to the right to an intersection with a curve, indicating pavement thickness. At this point, proceed vertically to an intersection with a curve in diagram B representing load-transfer capacity, which is considered to be one-half of the design wheel load. From this point on the curve, project a line horizontally to the left until it intersects, in diagram C, a vertical line representing a certain joint width value. The position of the point of intersection of these two lines, with respect to a curve representing dowel diameter, will indicate the proper diameter of dowel to be used. An example, represented by dash lines and arrows on the graph, indicates that a dowel diameter of 1⅛ in. should be used for design conditions selected.

Checking this from the beginning, we may obtain from Table 7 that a 1⅛-in. dowel for a joint width of ¾ in. has an allowable load-transfer capacity of 2000 lb. Then from Table 9, for a pavement thickness of 9 in. and k = 200, we find that the number of effective dowels for transferring the design wheel load is 3.16. Therefore, 1⅛-in. diameter dowels spaced 12 in. apart are capable of transferring 2000 × 3.16 = 6320 lb of load across a transverse joint with a satisfactory bear-

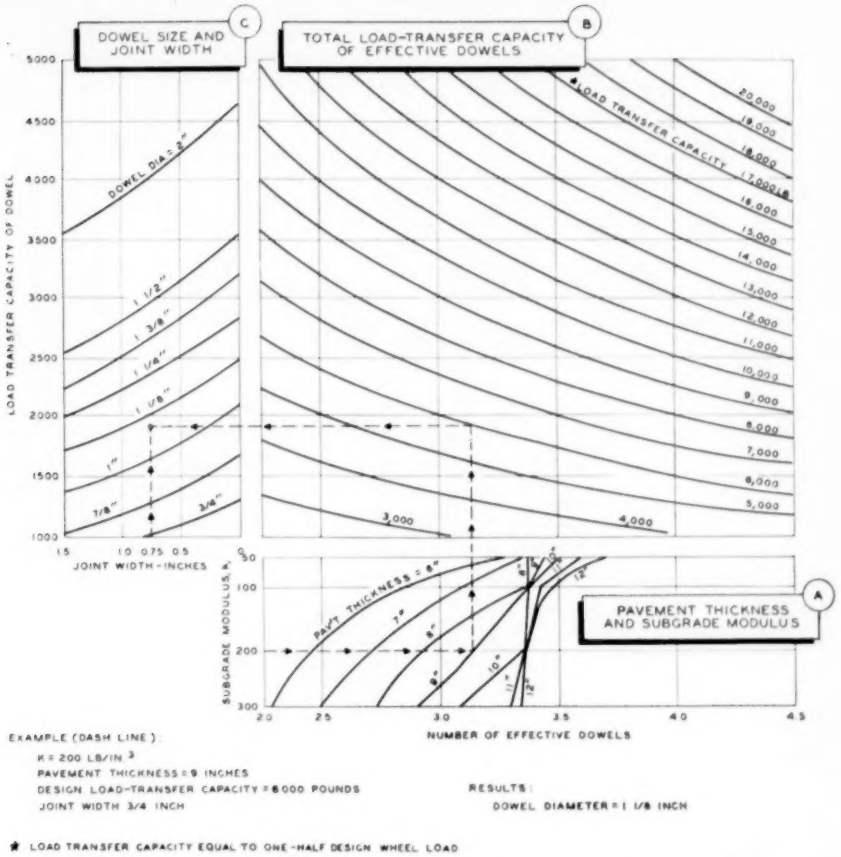

Fig. 13—Dowel diameter selection chart for dowels spaced 12 in. on center

G = 1,500,000 lb per cu in.

ing pressure between the concrete and the dowels. This 6320 lb is slightly more than one-half of an assumed design wheel load of 12,000 lb, which indicates that the dowel design is satisfactory, since this design procedure is based on one-half of the wheel load being transferred across the joint.

It is not intended at this point to discuss the proper selection of controlling conditions, *i.e.*, wheel load, pavement thickness, and subgrade modulus, which is necessary, and a prerequisite to the selection of the dowel size. However, it should be pointed out that the wheel load to be used for design purposes is not necessarily the maximum wheel load permitted by law, but rather it should be a wheel load compatible with the supporting ability of the pavement structure to insure a uniform continuity of support in slab and joint. For example, a 9-in. pavement slab with a subgrade modulus k of 200 will have a compatible design wheel load capacity of approximately 13,500 lb in accordance with Eq. (10).

TABLE 10—COMPARATIVE DIMENSIONS OF DOWELS REQUIRED FOR LOAD TRANSFER AT CONTRACTION AND EXPANSION JOINTS*

Pavement thickness, in.	Subgrade modulus k, lb per cu in.	Design wheel load,** lb	Dowel diameter, in.		Exact dowel length required, in.†	
			Contraction joints‡	Expansion joints§	Contraction joints‡	Expansion joints§
6	100	5400	¾	¾	12 ¼	13
	200	5900	¾	⅞	12 ¼	15
7	100	7400	¾	⅞	12 ¼	15
	200	8100	⅞	1	14 ¼	17
8	100	9300	⅞	1	14 ¼	17
	200	10600	1	1 ⅛	16 ¼	19
9	100	12300	1	1 ⅛	16 ¼	19
	200	13500	1 ⅛	1 ¼	18 ¼	21
10	100	15200	1 ⅛	1 ¼	18 ¼	21
	200	16500	1 ¼	1 ⅜	20 ¼	23

*Based on theoretical considerations; dowels spaced uniformly on 12-in. centers.
†Exclusive of length covered by expansion cap.
‡Based on a joint width of ¼ in. $(16 \times d) + \frac{1}{4}$ in.).
§Based on a joint width of 1 in. $(16 \times d) + 1$ in.).
**From Eq. (10).

To facilitate a study and comparison of the required sizes and lengths of dowels necessary at contraction and expansion joints for various pavement thicknesses and two common subgrade modulus values, Table 10 has been prepared. This table also gives the exact required length based on an embedded length of eight times the diameter of the bar on each side of the joint plus the joint width, to which length should be added the length covered by the expansion sleeve. The design wheel-load value used in the table was selected as the highest wheel load the pavement could withstand for unlimited repetition of loading without causing failure.

To obtain this value, use was made of the empirical equation for stress in a poorly supported slab corner as derived to fit observed data obtained in the Arlington test.[10]

$$f_t = \frac{3P}{h^2}\left[1 - \left(\frac{a_1}{l}\right)\right]^{1.2} \qquad (10)$$

where

f_t = maximum tensile stress, assumed to be 350 psi for design
P = wheel load, kips
h = slab thickness, in.
a_1 = $a\sqrt{2}$ where a = radius in inches of the circular area equivalent to the contact area of the tire with the pavement, which was obtained for dual tires from p. 22 of "Concrete Pavement Design" published by the Portland Cement Assn.[11]

$$l = \text{radius of relative stiffness (Westergaard)} = l\left[\frac{E_c h^3}{12(1-\mu^2)k}\right]^{1/4}$$

E_c = modulus of elasticity of concrete, assumed to be 5×10^6 psi
μ = Poisson's ratio, assumed to be 0.15
k = modulus of foundation support, lb per cu in.

In the equation the unit stress was selected as 350 psi so that the factor of safety would be 2.0, assuming a modulus of rupture of 700 psi. Fatigue studies have shown that test specimens can withstand unlimited repetition of load when the factor of safety is two.

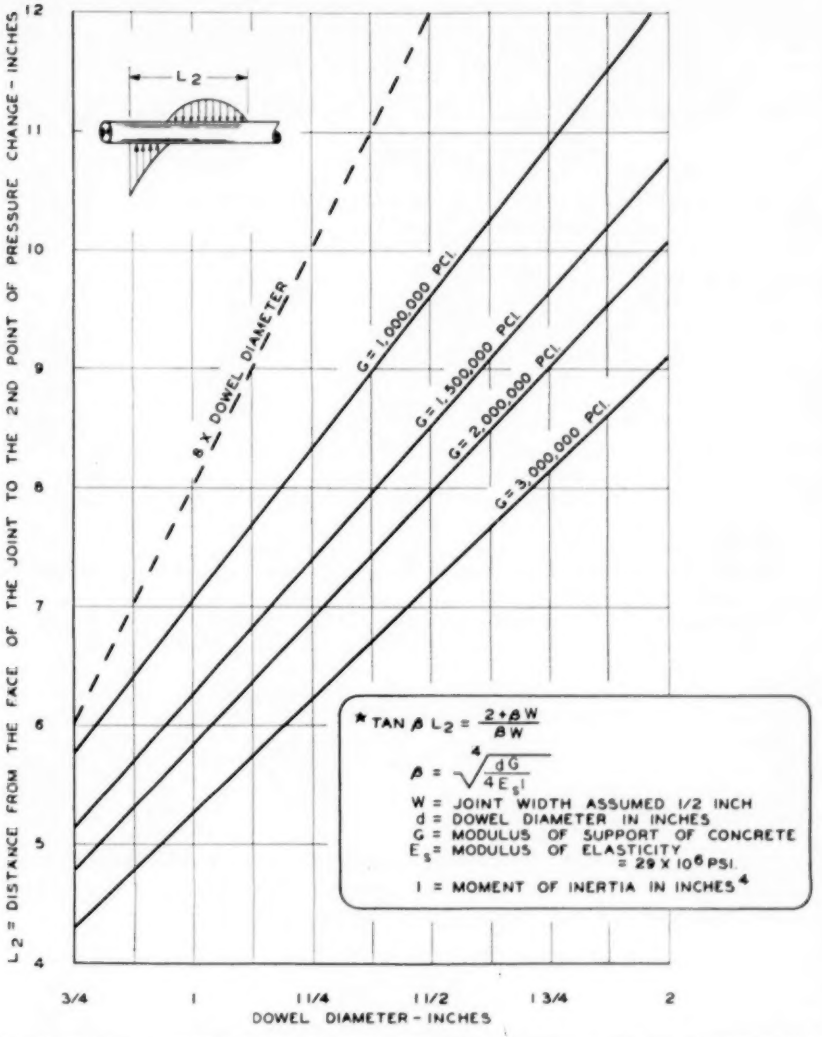

★ THEORY FROM "DESIGN OF DOWELS IN TRANSVERSE JOINTS OF CONCRETE PAVEMENTS" -B.F. FRIBERG, TRANSACTION A.S.C.E., 1940, P. 1079.

Fig. 14—Relation between L_2 and dowel diameter with variation in the modulus of support

Influence of dowel diameter and modulus of support on dowel length

Friberg[4] has shown that cutting the dowel at the second point of pressure change does not materially affect the maximum concrete bearing stress at the face of the joint. The distance from the face of the joint to the second point of pres-

sure change is shown in Fig. 14 for various values of the modulus of support G of the concrete. The length necessary to obtain eight times the dowel diameter is also shown in Fig. 14 to illustrate the fact that the required embedment length becomes less than eight times the dowel diameter as the dowel diameter increases.

REFERENCES

1. Timoshenko, S., and Lessels, J.M., *Applied Elasticity*, Westinghouse Technical Night School Press, East Pittsburgh, Pa., 1925, pp. 133-141.

2. Friberg, B.F., "Design of Dowels in Transverse Joints of Concrete Pavements," *Transactions*, ASCE, V. 105, 1940, pp. 1078-1080.

3. Marcus, Henri, "Load Carrying Capacity of Dowels at Transverse Pavement Joints," ACI JOURNAL, Oct. 1951, *Proc.* V. 48, p. 171.

4. Friberg, B.F., "Load and Deflection Characteristics of Dowels in Transverse Joints of Concrete Pavements," *Proceedings*, Highway Research Board, V. 18, Part 1, 1938, p. 154.

5. Finney, E.A., and Fremont, W.O., "Progress Report on Load-Deflection Tests Dealing with Length and Size of Dowels," *Proceedings*, Highway Research Board, V. 27, 1947, p. 171.

6. Loe, John A., "Dowel Bar Joints for Airfield Pavements," *Journal of Institution of Civil Engineers* (London), V. 1, Oct. 1952, p. 625.

7. Marcus, Henri, *loc. cit.*

8. Friberg, B.F., "Design of Dowels in Transverse Joints of Concrete Pavements," *op. cit.*, p. 1085.

9. Sutherland, E.C., Discussion on "Design of Load Transfer Joints in Concrete Pavements," *Proceedings*, Highway Research Board, V. 20, 1940, p. 496.

10. Kelley, E.F., "Application of the Results of Research to the Structural Design of Concrete Pavements," *Public Roads*, V. 20, July 1939, p. 89.

11. "Concrete Pavement Design," Portland Cement Assn., Chicago, 1951.

12. Van Breemen, William, "Report on Experimental Dowel Installations in New Jersey," *Proceedings*, Highway Research Board, V. 34, 1955, pp. 8-33.

13. Van Breemen, William, and Finney, E.A., "Design and Construction of Joints in Concrete Pavement Surfaces," ACI JOURNAL, June 1950, *Proc.* V. 46, pp. 789-820.

For such discussion of this paper as may develop please see Part 2, December 1957 *Journal*. In *Proceedings* V. 53 discussion immediately follows the June 1957 *Journal* pages.

A report of research sponsored by the Reinforced Concrete Research Council

Title No. 53-2

Shearing Strength of Reinforced Concrete Slabs*

By RICHARD C. ELSTNER and EIVIND HOGNESTAD†

SYNOPSIS

Presented as a research report without practical design recommendations, this paper reports the methods and results of experimental work on the shearing strength of reinforced concrete slabs subjected to a centrally located, concentrated load. Tests of thirty-nine 6-ft square slabs are reported. For 34 slabs, final failure was in shear by the column punching through the slab, in most cases after initial yielding of the tension reinforcement.

Major variables were: concrete strength, percentage of tension reinforcement, percentage of compression reinforcement, size of column, conditions of support and loading, distribution of tension reinforcement, and amount and position of shear reinforcement.

The test findings show that the shearing strength of slabs is a function of concrete strength as well as several other variables. An ultimate strength theory was developed, by which the slab behavior under load may be explained and the measured ultimate loads may be predicted with satisfactory accuracy.

INTRODUCTION

Historical review and object of investigations

Design of reinforced concrete slabs with respect to shear is based on a limited amount of factual knowledge concerning the effects of numerous variables involved. Therefore, design specifications for various countries differ considerably, not only with respect to quantitative limitations of allowable shearing stresses, but also in the basic methods of evaluating such shearing stresses.

Nearly all specifications employ the conventional beam formula for diagonal tension as a design formula for shearing stresses in slabs:

$$v = \frac{V}{bjd} \leq Kf_c' \qquad (1)$$

in which Kf_c' is an allowable shearing stress. Since the exact location of the shearing area cannot be observed in a slab, it is reasonable to expect disagreement

*Received by the Institute Mar. 22, 1956. Title No. 53-2 is a part of copyrighted JOURNAL OF THE AMERICAN CONCRETE INSTITUTE, V. 28, No. 1, July 1956, *Proceedings* V. 53. Separate prints are available at 50 cents each. **Discussion** (copies in **triplicate**) should reach the Institute not later than Nov. 1, 1956. Address 18263 W. McNichols Rd., Detroit 19, Mich.

†Members American Concrete Institute, Development Engineer and Manager, respectively, Structural Development Section, Portland Cement Assn., Chicago, Ill. (Formerly Research Associate and Research Associate Professor, respectively, Department of Theoretical and Applied Mechanics, University of Illinois, Urbana, Ill.)

among specifications in the determination of the shearing area, bjd, and the corresponding constant, K, which is required for a proper factor of safety. One or more of the following steps have been used to determine the shearing area:

1. The concept of an "equivalent width" in which b is the width of a fictitious beam strip of slab across which a concentrated load should be considered distributed to produce calculated shearing stresses equal to the maximum stresses that actually occur in the slab.

2. The nominal shearing area in which b is taken equal to the perimeter of an area concentric to the column or concentrated load area and located at a distance therefrom equal to the effective depth or some fraction of this depth.

3 The pure or punching shearing area in which b is the perimeter of the column or concentrated load area.

In this country, steps 1 and 3 were recommended in 1916 by the first Joint Committee on Concrete and Reinforced Concrete, but these steps were abandoned in 1924 by the second Joint Committee in favor of step 2 which has been used lately in most American design specifications. Steps 1 and 3 are still used in several European specifications.

Information regarding the behavior and ultimate strength of slabs failing in shear is believed to be of great importance in furthering the development of reinforced concrete design, especially since in recent years considerable progress has been made in design methods basing the safety of structures primarily on their ultimate strength. An ultimate flexural theory of slabs, the yield-line theory,[1] was developed in considerable detail during the 1940's. A fundamental assumption of this theory is that the slabs are designed so that sudden shear failures do not occur before the full flexural capacity of the slab is realized. Therefore, knowledge regarding the characteristics of shear failures is urgently needed so that effective steps may be taken in design to prevent such failures.

Most American tests of slabs failing in shear have been concerned with relatively thick footing slabs.[2,3] The results of these footing tests have been applied to shear design procedures for flat slabs, and an even further extrapolation has recently been made to flat plate floors, which are essentially flat slabs supported without column capitals or drop panels. Though practical experiences in flat plate construction have been satisfactory, these extrapolations may be questioned from a theoretical point of view since lower thickness-to-span ratios and higher moment-to-shear ratios are associated with floor slabs than with footings.

Hence, investigations reported herein were made to throw new light on the shearing strength of relatively thin reinforced concrete slabs subjected to concentrated loads or concentrated reactions. This paper describes test observations regarding the behavior and strength of such slabs and expresses the ultimate strength in mathematical terms. The paper is presented as a research report with no specific design recommendations.

Outline of tests

Two investigations subdivided into nine series of tests were made, involving a total of thirty-nine 6-ft square slabs 6 in. thick. Slabs were supported at the edges

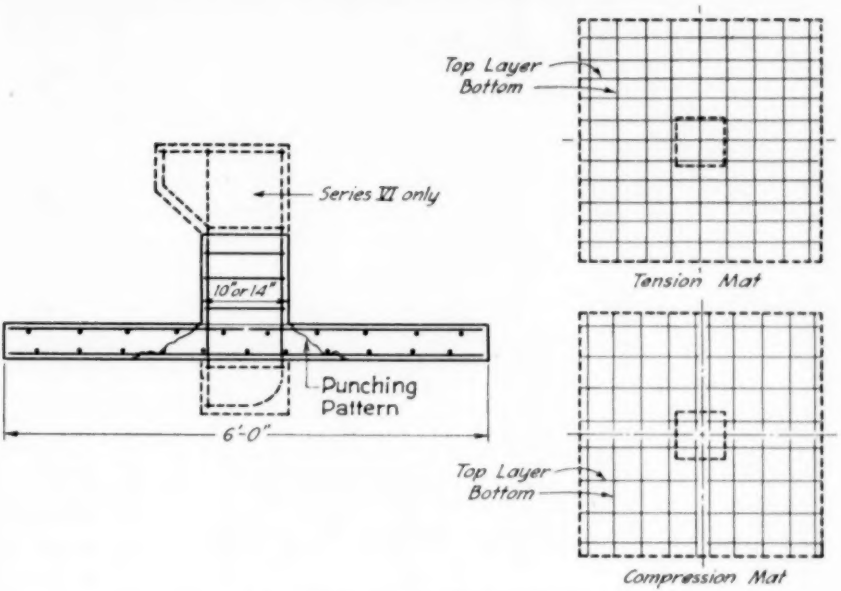

Fig. 1—Sketch of slab specimens

and loaded through a centrally located column stub as indicated in Fig. 1.

The first investigation, series I through VII, was conducted at Talbot Laboratory, University of Illinois, in 1952. An outline of these tests is given in Table 1. In series I, the principal test series, 13 slabs supported on all four edges were loaded through a 10-in. square column stub; variables were concrete strength and amount of longitudinal reinforcement. Series II introduced a change from a 10-in. to a 14-in. column, and series III and IV gave variations in support conditions. In series V, 50 percent of the tension reinforcement was concentrated directly under the column, and the slabs of series VI were loaded eccentrically. The single slab of series VII was lightly reinforced to obtain a flexural failure. In addition to the slab specimens, eight beam specimens were included representing 12-in. wide slab strips.

The second investigation, series VIII and IX, was conducted at the Research and Development Laboratories of the Portland Cement Assn. in 1954. An outline of these tests is given in Table 2. Series VIII extended the range of variables in series I, and the longitudinal compression reinforcement was omitted. Series IX introduced shear reinforcement, details of which are shown in Fig. 2.

MATERIALS, FABRICATION, AND TEST METHODS

Materials

Concrete mixtures—Type I portland cement, purchased from local dealers, was used in both investigations. In the University of Illinois tests Wabash River sand

TABLE 1—OUTLINE OF TESTS AT UNIVERSITY OF ILLINOIS, 1952*

Slab No.	Concrete design strength psi	Longitudinal reinforcement: Tension mat: Bar size, No.	Spacings: Bot., in.	Spacings: Top, in.	p, percent	Compression mat: Bar size, No.	Spacings: Bot., in.	Spacings: Top, in.	p, percent	Column stub: Size r, in.	Column stub: Reinforcement
Series I—Symmetrical support on four edges, 10-in. column											
A-1a	2000	6	9	7½	1.15	4	7	8	0.56	10	4-#5
A-1b	3500	6	9	7½	1.15	4	7	8	0.56	10	4-#5
A-1c	3500	6	9	7½	1.15	4	7	8	0.55	10	4-#5
A-1d	5000	6	9	7½	1.15	4	7	8	0.56	10	4-#5
A-1e	3500	6	9	7½	1.15	4	7	8	0.56	10	4-#5
A-2a	2000	8	8	6¼	2.47	6	7½	9	1.15	10	4-#5
A-2b	3500	8	8	6¼	2.47	6	7½	9	1.15	10	4-#5
A-2c	5000	8	8	6¼	2.47	6	7½	9	1.15	10	4-#5
A-7b	3500	8	8	6¼	2.47	6	7½	9	1.15	10	4-#5
A-3a	2000	8	5¼	4¼	3.70	6	7½	9	1.15	10	8-#6
A-3b	3500	8	5¼	4¼	3.70	6	7½	9	1.15	10	8-#6
A-3c	3500	8	5¼	4¼	3.70	6	7½	9	1.15	10	8-#6
A-3d	5000	8	5¼	4¼	3.70	6	7½	9	1.15	10	8-#6
Series II—Symmetrical support on four edges, 14-in. column											
A-4	3500	6	9	7½	1.15	4	7	8	0.56	14	4-#7
A-5	3500	8	8	6¼	2.47	6	7½	9	1.15	14	4-#7
A-6	3500	8	5¼	4¼	3.70	6	7½	9	1.15	14	4-#7
Series III—Symmetrical support on two opposite edges											
A-7	3500	8	8	6¼	2.47	6	7½	9	1.15	10	4-#5
A-8	3500	8	8	6¼	2.47	6	7½	9	1.15	14	4-#7
Series IV—Symmetrical support on four corners											
A-7a	3500	8	8	6¼	2.47	6	7½	9	1.15	10	4-#5
Series V—Concentrated reinforcement, four-edge support											
A-9	3500	8 8	2½ 12	2½ 9	7.02 1.64	6	7½	9	1.15	10	4-#5
A-10	3500	8 8	2½ 12	2½ 9	6.28 1.48	6	7½	9	1.15	14	4-#7
Series VI—Eccentric thrust on column, four-edge support											
A-11	3500	8	8	6¼	2.47	6	7½	9	1.15	14	4-#10
A-12	3500	8	8	6¼	2.47	8	8	6¼	2.47	14	4-#10
Series VII—Low reinforcement percentage, four-edge support											
A-13	3500	4	8	7¼	0.55	3	8¼	8¾	0.28	14	4-#5

*Depth from the compression surface of all slabs to the centroid of the bottom layer of the tension mat was 5 in. Depth from the compression surface to the centroid of the top layer of the compression mat was 1 in.

TABLE 2—OUTLINE OF TESTS AT PCA LABORATORIES, 1954*

Slab No.	Concrete design strength, psi	Tension mat: Bar size, No.	Bot., in.	Top, in.	p, percent	Shear reinforcement: Reinforcement	θ, deg.	A_v, sq in.	Column stub: Size r, in.	Column stub: Reinforcement
Series VIII—Symmetrical support on four edges, 10-in. column										
B-1	2000	4	9⅜	8⅜	0.50				10	4-#3
B-2	6500	4	9⅜	8⅜	0.50				10	4-#3
B-4	6500	5	7⅜	6⅜	0.99				10	4-#3
B-9	6500	7	7⅜	6	2.00				10	4-#8
B-11	2000	8	6½	5¼	3.00				10	4-#8
B-14	6500	8	6½	5¼	3.00				10	4-#8
Series IX—Shear reinforcement, symmetrical support on four edges										
B-3	2000	5	7⅜	6⅜	0.99	4-#3	45	0.88	10	4-#8
B-5	2000	7	7⅜	6	2.00	2-#4	45	0.80	10	4-#8
B-6	2000	7	7⅜	6	2.00	4-#4	45	1.60	10	4-#8
B-10	6500	7	7⅜	6	2.00	4-#4	45	1.60	10	4-#8
B-12	6500	8	6½	5¼	3.00	10-#3†	90	2.20	10	4-#8
						6-#3	90	1.32		
B-13	6500	8	6½	5¼	3.00	10-#5	20	6.20	10	4-#8
B-15	6500	8	6½	5¼	3.00	6-#4	45	2.40	10	4-#8
B-16	6500	8	6½	5¼	3.00	8-#4†	45	3.20	10	4-#3
						4-#4	45	1.60	10	4-#3
B-17	2000	6	7	6	1.50	4-#3	45	0.88	10	4-#8

*Depth from compression surface to centroid of the tension mat was 4.5 in. No compression reinforcement.
†Two rings of shear reinforcement.

with a fineness modulus of 3.21 and Wabash River gravel of 1-in. maximum size with a fineness modulus of 6.51 were used. For series VIII and IX the aggregates were a mixture of lake sand and Elgin sand with a fineness modulus of 2.82, and Elgin gravel of 1½-in. maximum size with a fineness modulus of 7.30.

The principal concrete mixes used are described in Table 3. All batching was by weight; the concretes were mixed 3 min in 6-cu ft nontilting drum mixers. Three 6 x 12-in. vibrated control specimens were made for each batch. Compressive strengths as determined by an average of 12 to 15 cylinders for each slab specimen

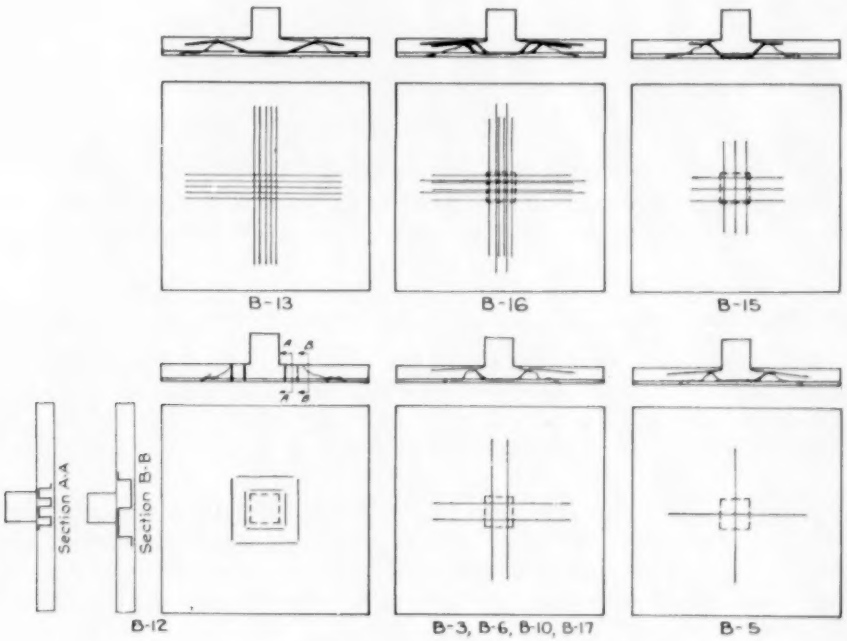

Fig. 2—Sketch of shear reinforcement

and 6 cylinders for each beam strip are listed with test results of these principal specimens in Table 4, 5, and 7.

Reinforcing steel—Deformed reinforcing bars meeting ASTM A 305-50T for deformations were used in both investigations. Yield point stresses as determined by tension tests are listed with test results of the principal specimens.

Fabrication and curing—Reinforcement was securely wired together and carefully placed in the forms so that correct distances were maintained. Cored holes were provided in the concrete at desired locations for 1-in. electric strain gages which were attached to the tension reinforcement after the concrete had hardened and dried. The compression reinforcement was supported from the form sides since steel chairs would act as shear reinforcement. Bends for the shear reinforce-

TABLE 3—CONCRETE MIXTURES

Design strength, psi	Mix ratio by weight, S.S.D.	Average slump, in.	Percent sand, by weight	Cement, sacks per cu yd	Water, lb per cu yd	w/c, by weight	Average f_c', psi
University of Illinois, 1952							
2000	1:4.72:6.55	3.0	41.9	3.21	303	0.99	2010
3500	1:3.45:4.81	3.4	41.9	4.79	300	0.74	3870
5000	1:2.67:3.71	3.9	41.9	5.41	281	0.55	5260
Portland Cement Assn., 1954							
2000	1:5.62:6.72	3.1	45.5	3.06	246	0.85	2100
6500	1:2.25:3.37	3.1	40.0	6.19	234	0.40	6840

ment were made around a pin of 1-in. diameter. All shear reinforcement was bent hot. Waterproofed ¼-in. electric strain gages were attached to the shear reinforcement at desired locations.

Concrete for both slab and control specimens was vibrated. All specimens, including control cylinders, were removed from the forms after 24 hr, cured with wet burlap for 7 days, then stored in the air of the laboratory until tested at an age of about 28 days.

Testing procedure

For convenience in conducting the slab tests at the University of Illinois, a special steel frame with four wheels was constructed, on which the slabs were supported through 2 x 1-in. maple strips. The steel frame was used as a vehicle to move the slabs in and out of the testing machine as well as a testing support for the slabs as shown in Fig. 3a.

In the Portland Cement Assn. tests a concrete frame 3 ft high was constructed to support the panels during testing. This made it possible to observe the formation of cracks on the tension surface of the slabs. The concrete frame, shown in Fig. 3b, served as a vehicle as well as a testing base on which the slabs were supported through 2 x 1-in. maple strips.

Slabs were loaded to failure in 10 to 15 increments. Strains in the reinforcement, deflections over a gridwork on the top surface of the slabs, formation of cracks, and the phenomena of failure were recorded.

The beam strips of the University of Illinois tests were simply supported and loaded to failure through a column stub, with strains and center deflections recorded.

RESULTS OF SLAB TESTS

Slab action in flexure

A flexural load-deflection diagram is given in Fig. 4 for the 6-ft square slab B-4, which was supported on all four edges and loaded through a 10-in. column. It is seen that there are four typical stages of slab behavior in flexure. In stage I the slab

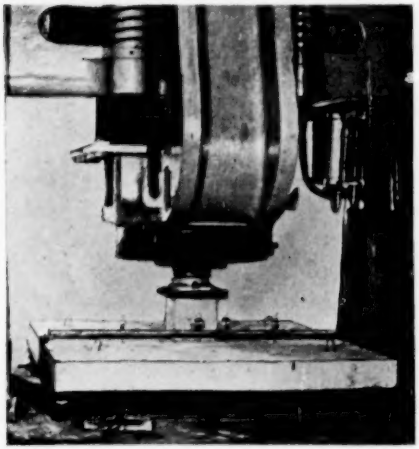

Fig. 3a—Testing arrangement, University of Illinois

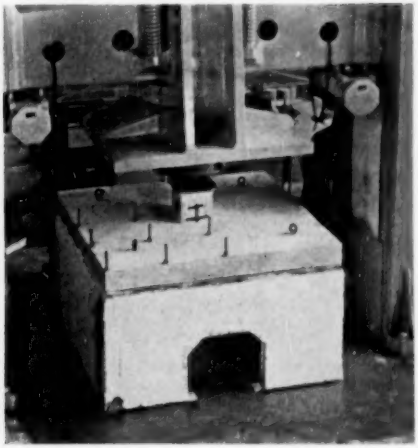

Fig. 3b—Testing arrangement, Portland Cement Assn.

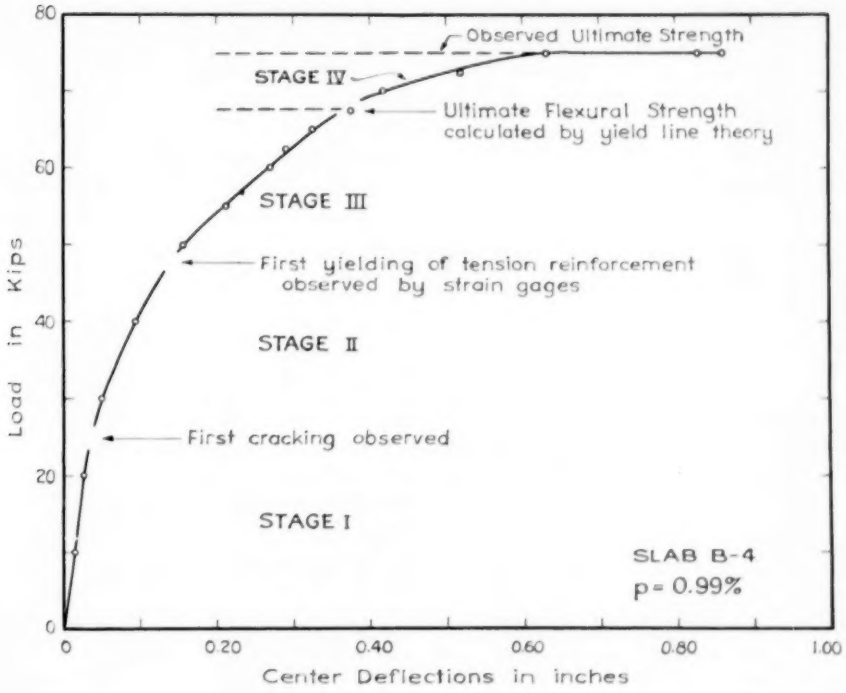

Fig. 4—Typical flexural load-deflection diagram

TABLE 4—RESULTS OF SLAB TESTS, SERIES I THROUGH VIII

Series	Slab No.	p, percent	d, in.	r, in.	f_c' psi	f_{sp} ksi	P_{test}, kips	Conventional procedure			v_2/f_c'	P_{yield}, kips	P_{flex}, kips	P_{test}/P_{yield}	P_{test}/P_{flex}	P_{calc}, kips	$\phi_3 P_{calc}/P_{flex}$	P_{test}/P_{calc}
								v_1, psi	v_1/f_c'	Factor of safety								
I	A-1a	1.15	4.63	10	2040	48.2	68	227	0.111	4.44	0.206	55	81.2	1.24	0.837	71.2	0.877	0.954
	A-1b	1.15	4.63	10	3660	48.2	82	274	0.075	3.00	0.138	60	86.6	1.37	0.947	82.6	0.954	0.993
	A-1c	1.15	4.63	10	4210	48.2	80	268	0.064	2.56	0.117	60	87.9	1.33	0.910	86.0	0.978	0.930
	A-1d	1.15	4.63	10	5340	48.2	79	264	0.049	1.96	0.091	55	89.2	1.44	0.886	92.5	1.037	0.854
	A-1e	1.15	4.63	10	2940	48.2	80	268	0.091	3.64	0.168	60	85.3	1.33	0.938	78.0	0.914	1.026
	A-2a	2.47	4.50	10	1980	46.6	75	251	0.127	5.08	0.240	—	131.0	—	0.573	77.2	0.589	0.973
	A-2b	2.47	4.50	10	2830	46.6	90	301	0.106	4.24	0.202	75	147.2	1.20	0.611	88.5	0.601	1.017
	A-2c	2.47	4.50	10	5430	46.6	105	350	0.064	2.56	0.123	80	165.1	1.31	0.636	110.9	0.672	0.946
	A-7b	2.47	4.50	10	4050	46.6	115	384	0.095	3.80	0.180	85	158.3	1.35	0.726	99.2	0.627	1.158
	A-3a	3.70	4.50	10	1850	46.6	80	267	0.144	5.76	0.274	—	147.6	—	0.542	77.9	0.528	1.026
	A-3b	3.70	4.50	10	3280	46.6	100	334	0.102	4.08	0.194	—	203.9	—	0.490	100.9	0.495	0.990
	A-3c	3.70	4.50	10	3850	46.6	120	401	0.104	4.16	0.198	115	214.6	1.04	0.559	107.9	0.503	1.111
	A-3d	3.70	4.50	10	5010	46.6	123	411	0.082	3.28	0.156	120	228.8	1.03	0.538	121.9	0.529	1.017
II	A-4	1.15	4.63	14	3790	48.2	90	249	0.066	2.64	0.105	75	93.9	1.20	0.958	108.8	1.159	0.827
	A-5	2.47	4.50	14	4030	46.6	120	331	0.082	3.28	0.135	100	171.2	1.20	0.701	127.9	0.747	0.938
	A-6	3.70	4.50	14	3630	46.6	112	309	0.085	3.40	0.140	—	228.0	—	0.491	135.4	0.594	0.827
III	A-7	2.47	4.50	10	4130	46.6	90	301	0.073	2.92	0.138	75	93.1	1.20	0.967	85.2	0.915	1.057
	A-8	2.47	4.50	14	3180	46.6	98	270	0.085	3.40	0.140	85	94.7	1.15	1.035	103.1	1.089	0.950
IV	A-7a	2.47	4.50	10	4050	46.6	63					—		—				
V	A-9	7.02 1.64	4.50	10	4330	46.6	100	334	0.077	2.56	0.147	—	147.8	—	0.677	99.5	0.673	1.006
	A-10	6.28 1.48	4.50	14	4310	46.6	110	304	0.071	2.36	0.116	—	157.0	—	0.701	127.5	0.812	0.863
VI	A-11	2.47	4.50	14	3760	46.6	119	328	0.087	3.48	0.143	65	155.7	1.83	0.764	122.4	0.786	0.972
	A-12	2.47	4.50	14	4120	46.6	119	328	0.080	3.20	0.131	80	158.2	1.49	0.752	125.9	0.796	0.945
VII	A-13	0.55	4.75	14	3800	42.6	53	Flexural Failure			0.060	40	44.1	1.33	1.202	—	2.176	—
VIII	B-1	0.50	4.50	10	2060	47.0	40.1	Flexural Failure			0.124	30	35.6	1.34	1.126	—	1.713	—
	B-2	0.50	4.50	10	6900	46.5	45.0	Flexural Failure			0.041	33	37.0	1.36	1.216	—	2.074	—
	B-4	0.99	4.50	10	6920	44.0	75.0	Flexural Failure			0.069	48	67.7	1.56	1.107	—	1.331	—
	B-9	2.00	4.50	10	6370	49.5	113.5	380	0.060	2.40	0.113	85	146.2	1.34	0.776	112.3	0.768	1.010
	B-11	3.00	4.50	10	1960	59.3	74.0	247	0.126	5.04	0.240	—	155.9	—	0.475	80.1	0.514	0.924
	B-14	3.00	4.50	10	7330	47.2	130.0	435	0.059	2.36	0.113	100	205.1	1.30	0.634	133.7	0.652	0.972

Avg P_{test}/P_{calc} = 0.972
Standard deviation = 0.077

is uncracked, in stage II flexural cracking of the slab is developing, in stage III yielding of the tension reinforcement is spreading from the loaded area toward the slab edges, and in stage IV the slab is in a plastic state of rapidly increasing deflection.

It has been found[4] that the shearing strength of a slab subject to concentrated loads or column reactions is different for these various stages of flexure. Therefore, shear and flexure must be considered as a combined loading problem, not as two separate cases. This is even more evident for an analogous problem, that of combined axial load and flexure in columns.

Because shearing strength is related to flexural behavior, it is necessary to define the terms shear failure and flexural failure clearly. In the discussions presented herein, a punching of the column stub through the slab is always regarded as a shear failure, unless such punching takes place after the full flexural strength of the slab by inelastic action has been developed so that the slab is in stage IV of flexure. A slab failure by rapidly increasing deflection (Fig. 4) in stage IV of flexure is regarded as a flexural failure.

Analytical approach in shear studies

In current design specifications such as ACI 318-51, shearing stresses, v_1, in flat slabs subjected to concentrated column reactions are computed by Eq. (1). If t is the total thickness of the slab at the vertical section in question, b in Eq. (1) is the circumference of a polygon concentric to the column area and located at a distance $t - 1.5$ in. therefrom. In a similar manner d in Eq. (1) is taken at $t - 1.5$ in. The corresponding allowable design stress given by ACI 318-51 is proportional to the cylinder strength f_c'. No other variables are considered, with the exception of concentrated reinforcement over the column.

Table 4 shows that the measured ultimate values of the ratio v_1/f_c' are not constant; v_1/f_c' decreases with decreasing reinforcement percentage and with increasing concrete strength. Similarly, the safety factor as computed with an allowable stress of $0.025f_c'$ ranges from about 2.5 to 5.5. It is considered, therefore, that improved expressions for the ultimate shearing strength of slabs are desirable.

A reanalysis of F. E. Richart's footing tests[3] was carried out and reported in a previous paper.[4] For that series of tests it was found that a shearing stress, v_2, computed at zero distance from the column faces is a better measure of shearing strength than the conventional shearing stress, v_1. It was further found that the ultimate value of v_2/f_c' decreases with increasing concrete strength and with increasing flexural capacity in a manner given by

$$\frac{v_2}{f_c'} = \frac{P_{ultimate}}{\frac{7}{8}bdf_c'} = 0.035 + \frac{130}{f_c'} + \frac{0.07}{\phi_o} \qquad (2)$$

in which

f_c' = cylinder strength, psi
b = circumference of column
d = effective depth of slab

$\phi_o = P_{shear}/P_{flex}$
P_{shear} = ultimate shear capacity
P_{flex} = ultimate flexural capacity of the slab computed by the yield-line theory without regard to a shear failure

It was anticipated that the general structure of Eq. (2), which was derived from Richart's thick footings, would also be applicable to the relatively thin slabs of these investigations. However, for concrete strengths greater than 4500 psi, computed values of v_2/f_c' using Eq. (2) were higher than actual test values, and by statistical analysis* of all slabs except series IX it was found that v_2/f_c' could be better expressed as

$$\frac{v_2}{f_c'} = \frac{P_{shear}}{\frac{7}{8} bdf_c'} = \frac{333}{f_c'} + \frac{0.046}{\phi_o} \qquad (3)$$

In checking the applicability of Eq. (3) against test results it is desirable to use this equation to predict the ultimate load of test slabs for comparison with an observed load. Since the shearing strength, P_{shear}, appears both in v_2 and ϕ_o, Eq. (3) must be solved for ϕ_o and the shearing strength. It is then convenient to refer to a calculated shearing strength as P_{calc} and an observed ultimate load as P_{test}. We have from Eq. (3)

$$\frac{v_2}{f_c'} = \frac{P_{calc}}{\frac{7}{8} bdf_c'} = B\phi_o = A + \frac{0.046}{\phi_o}$$

in which

$$A = \frac{333}{f_c'}; \quad B = \frac{P_{flex}}{\frac{7}{8} bdf_c'}; \quad \phi_o = \frac{P_{calc}}{P_{flex}}$$

Solving these equations for ϕ_o and P_{calc} we obtain

$$\phi_o = \frac{A + \sqrt{A^2 + 0.184B}}{2B} \qquad (4)$$

and

$$P_{calc} = \phi_o P_{flex}$$

The flexural ultimate load, P_{flex}, was computed using the yield-line theory as outlined in Appendix 1. It should be noted that Eq. (4) is a mathematical aid to check the applicability of Eq. (3); it should not be regarded as a design equation. Theoretically, a value of ϕ_o greater than one corresponds to a flexural failure. However, since ϕ_o is a calculated quantity dependent upon the empirical constants in Eq. (3), it is subject to experimental scatter. Therefore, only those slabs exhibiting obviously large deflections at failure are considered flexural failures, independent of the calculated value of ϕ_o.

*The statistical methods used are described in Appendix 2.

From series IX it was found that for slabs with shear reinforcement v_2/f_c' could be expressed as

$$\frac{v_2}{f_c'} = \frac{P_{max}}{\frac{7}{8}bdf_c'} = \frac{333}{f_c'} + \frac{0.046}{\phi_s} + (q_s - 0.050) \qquad (3a)$$

in which

$$q_s = \frac{A_v f_v \sin\theta}{\frac{7}{8}bdf_c'}$$

where A_v and f_v are the area and yield point of the shear reinforcement and θ is the angle between the shear reinforcement and the plane of the slab. Thus, A in Eq. (4) becomes

$$A = \frac{333}{f_c'} + q_s - 0.050$$

Series I

The 13 slabs of this series were loaded centrally through a 10-in. square column and were supported on four edges with corners free to lift. Tension reinforcement percentages* were 1.15, 2.47, and 3.70 and concrete strengths varied from about 2000 to 5000 psi as indicated in Table 4.

Flexural cracking was indicated at 15 to 25 percent of ultimate load by audible cracking sounds and by breaks in both load-deflection curves and load-steel strain curves. At about 50 percent of the ultimate load the slab corners lifted, preceded by vertical cracks at the slab edges 15 to 18 in. from the corners.†

Distributions of strain in the tension reinforcement typical for series I are shown in Fig. 5. The highest strains and consequently initial yielding generally occurred below the column. Yielding spread gradually from the center to the edges of the slab with increased application of load. The degree of yielding at failure ranged from none for slabs with a high tension reinforcement percentage and low concrete strength to practically full yielding for slabs with a low percentage and a high concrete strength. Final failure of all slabs took place by the column punching through the slab in a manner similar to that described by Richart for footings.[3]

Slab deflections were measured by a deflection bridge along four lines on the top surface. A typical deflection pattern for series I is shown in Fig. 6. At approximately 50 percent of ultimate capacity the corners of the slabs lifted from the supports. Maximum deflection of the slab was at the column; this deflection is shown also in Fig. 7, which gives load-deflection curves for all slabs of series I. This figure shows that the slope of the deflection curve increases with concrete strength and reinforcement percentage. Also, breaks in the curves are seen at initial flexural cracking, and at first yielding which is indicated by arrows in the figure.

The pertinent data involved in the ultimate strength analysis are given in Table

*The average percentage for two layers of reinforcement is computed by Eq. (c) of Appendix 1.

†The theoretical location of these cracks is 18.1 in. as computed by Eq. (d) of Appendix 1.

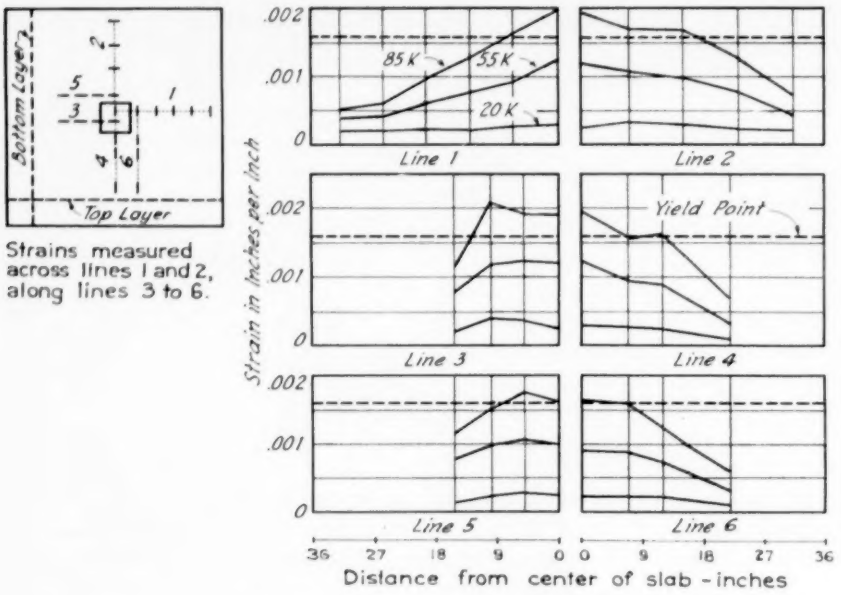

Fig. 5—Strain distribution, slab A-2b

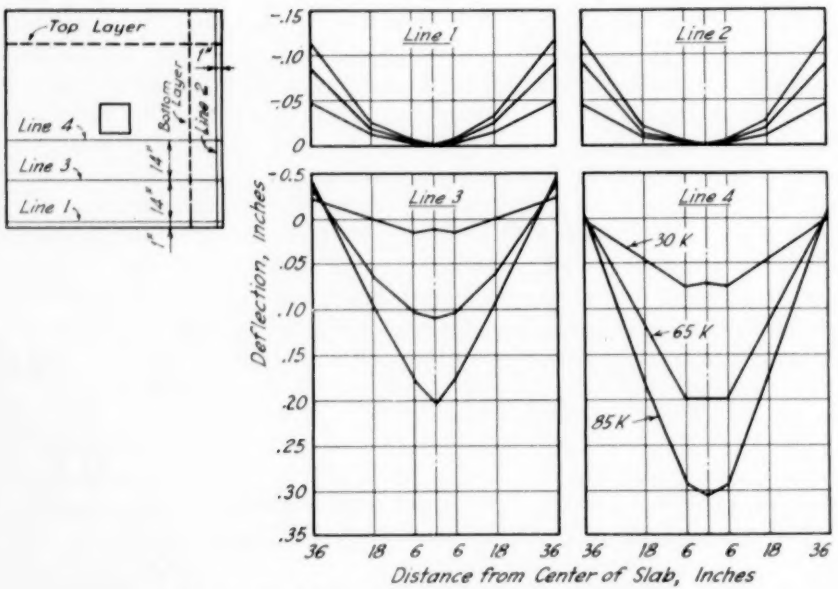

Fig. 6—Distribution of deflections, slab A-2b

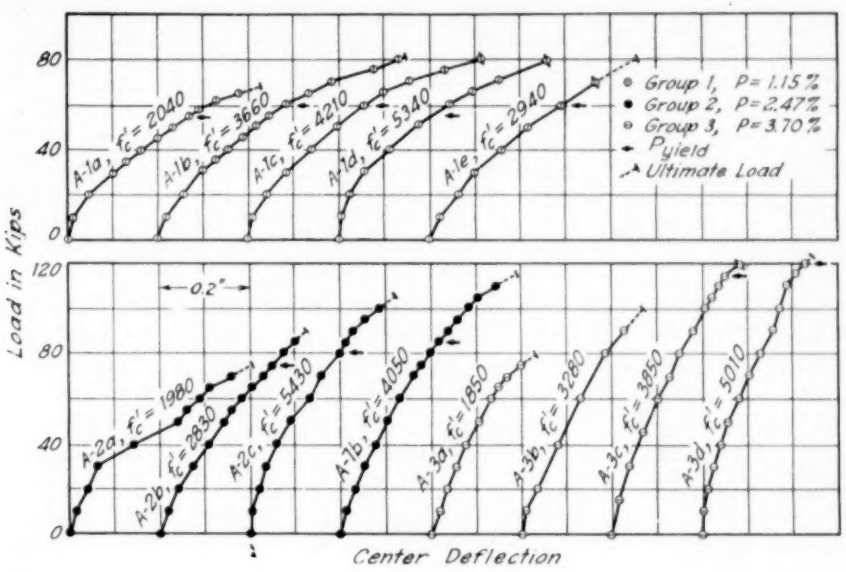

Fig. 7—Load-deflection curves, series I

4. For a majority of the slabs P_{test}/P_{yield} is greater than one and P_{test}/P_{flex} is less than one; that is, most slabs failed in shear while yielding was spreading from the center toward the slab edges. Only three slabs, A-2a, A-3a, and A-3b failed prior to yielding, though measured strains in all three cases indicated that yielding was imminent. Although ϕ_o is slightly greater than one for slab A-1d, neither the load-deflection curve nor the ratio P_{test}/P_{flex} indicates a flexural failure.

Series II

The three slabs of this series were loaded at the center through a 14-in square column stub and were supported on four edges with corners free to lift. Except for the increased size of column stub and the slight difference in concrete strength, slabs A-4, A-5, and A-6 are identical to series I slabs A-1b, A-7b, and A-3c, respectively.

The general behavior of these slabs under load was similar to that of the slabs in series I. According to calculated results slab A-4 should have been a flexural failure since ϕ_o was greater than one. However, the center deflection of the slab was not exceptionally large at failure and P_{test}/P_{flex} was less than one; therefore, it is classed as a shear failure. The behavior of slab A-6 at failure departed from the general pattern. Punching took place suddenly and without the slight drop of load indicated by the testing machine dial as was the usual case. After testing, the bar spacing, size of bars, workmanship, and testing procedure were examined closely; but no reason for the unusual behavior could be found.

Load-deflection curves are compared to corresponding slabs of series I in Fig. 8. As would be expected, the increase in column size increased the slab stiffness and thereby increased the slopes of the load-deflection curves. Slab A-6 again is abnormal.

Observed and predicted ultimate loads are compared in Table 4. By comparison with corresponding slabs in series I it is seen that P_{test} increased with column size, with the exception of the abnormal slab A-6.

Series III

The two slabs of this series were supported on only two opposite edges. Otherwise slab A-7 with a 10-in. column is similar to slab A-7b of series I, and slab A-8 with a 14-in. column may be compared to slab A-5 of series II.

Flexural cracking was initiated at about 10 percent of the ultimate load and cracks appeared at the unsupported edges at a load of about 45 percent. Maximum strains in the tension reinforcement occurred in the bars perpendicular to the supported edges and near the column stub. The reinforcement of both slabs was yielding near the column at failure, but the yielding had not spread to the slab edges.

The deflection pattern for slab A-7 is shown in Fig. 9. It is seen that the corners rose relatively little and that the slab tended to act as a one-way slab. Load-deflection curves are compared in Fig. 8 with corresponding slabs with four-edge supports.

According to the mathematical analysis presented herein, two-edge support as compared to four-edge support decreases P_{flex}, increases ϕ_o, and decreases P_{calc} for the slabs of this investigation. This predicted behavior was born out by test results.

Series IV

The single slab of this series was loaded centrally through a 10-in. square column and was supported at four corners on 3.5 x 3.5-in. oak blocks.

This slab failed suddenly near three corner supports. Since no reinforcement passed directly over these support blocks, the failure was a local one and is fundamentally different from the failures of reinforced slabs studied in this paper. Therefore, the strength results are not included in the analyses.

Only local damage at the corners resulted from the failure; reinforcement was not yielding. Therefore, slab A-7a was retested with four-edge support as slab A-7b and added to series I.

Series V

Slabs A-9 and A-10 are similar to A-7b and A-5, respectively, except that 50 percent of the tension reinforcement is concentrated under the column. When such a concentration of reinforcement is provided, ACI 318-51 permits a 20 percent increase in allowable shearing stresses for flat slabs.

The two slabs behaved under load much like the slabs of series I and II. However, due to the concentration of tension reinforcement, they were slightly stiffer,

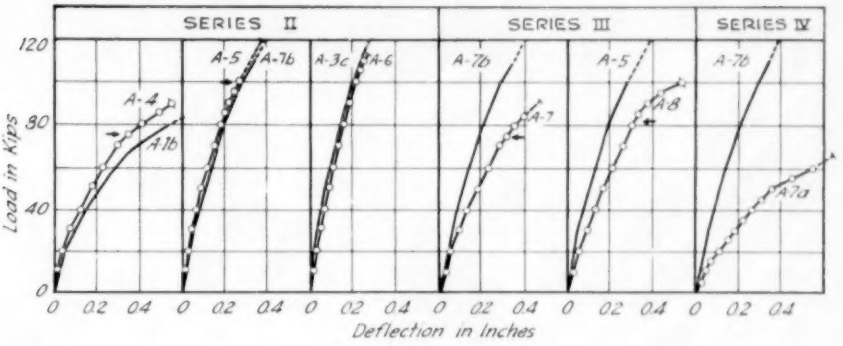

Fig. 8—Load-deflection curves, series II, III, and IV

as shown in the load-deflection curves in Fig. 10, and the steel strains near the column were lower. Furthermore, the tensile strains at the center of the first interior dispersed bars were about 20 percent higher than those in the concentrated reinforcement under the columns. In both slabs first yielding was imminent at failure.

By the mathematical procedures outlined in this paper, P_{flex}, ϕ_o, and P_{calc} are in no way affected by steel concentration. Test results show this to be true; in fact, for the slabs investigated, concentration of tension reinforcement tended to lower somewhat the ultimate shearing capacity, rather than increase it. It is felt, therefore, that further investigation of reinforcement concentration is desirable.

Series VI

This series introduced column moment as a new variable. While the columns of all other slabs were loaded concentrically, slabs A-11 and A-12 were loaded by a line load at the edge of the 14-in. column, that is, the eccentricity of load was 7 in.

The tension reinforcement of both slabs was identical to that of slab A-5 of series II. In slab A-11 the compression mat was also identical to that of slab A-5 except that the bars were not cut off at the centerlines, and in slab A-12 the percentage of reinforcement in the compression mat was doubled.

The behavior of both slabs of this series was similar to that of their concentrically loaded counterpart, slab A-5, except that strains and deflections were slightly higher at the loaded edge of the column than at the opposite edge. Both slabs failed in shear after yielding had begun near the column, but before yielding had spread to the slab edges. It was noted that the loaded column edge seemed to punch through the slab first, but this was followed rapidly by punching around the entire column perimeter.

The ultimate strength of both eccentrically loaded slabs was 119 kips as compared to 120 kips for slab A-5. These tests indicate, therefore, that an eccentricity up to one-half the column size has little or no effect on the ultimate shearing strength of

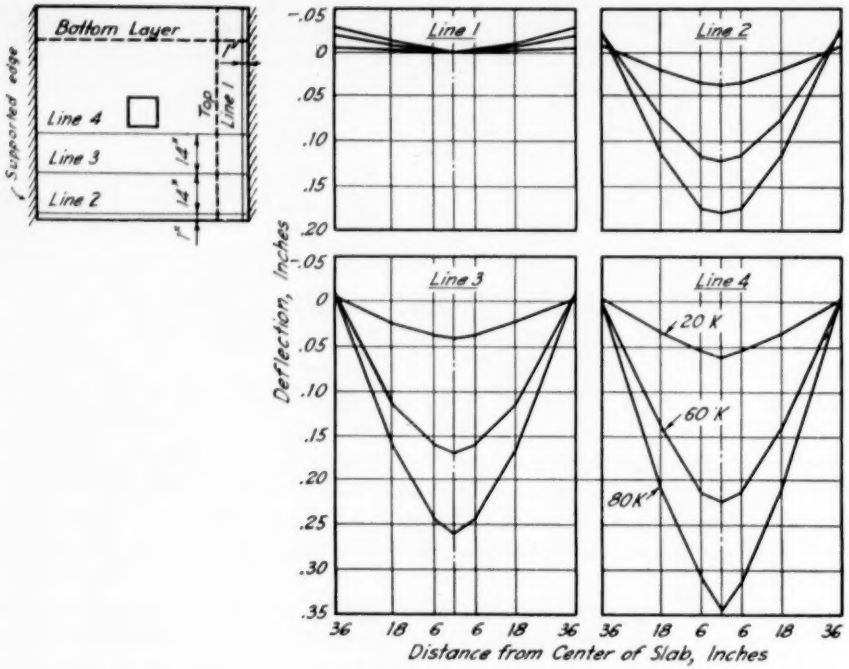

Fig. 9—Distribution of deflections, slab A-7

a slab subjected to a concentrated load through a column, and that increase in the percentage of compression reinforcement likewise has little effect.

Series VII

The single specimen of this series was designed with a low percentage of reinforcement to study the behavior and mode of failure in a slab fully yielding at failure.

This slab was similar to slab A-4 of series II in all respects except that both tension and compression reinforcement were reduced by 50 percent.

The load-deflection curve given in Fig. 10 provides a good illustration of the four stages of flexural slab behavior. Each stage is sharply defined by changes in the slope of the load-deflection curve as well as by physical changes in the slab itself. Below the cracking load of about 7 kips the slab behaved essentially in an elastic manner. This range is referred to as the elastic stage. The cracking stage extended from 7 to 40 kips. At 40 kips the tension reinforcement at the center of the slab reached yielding. The yielding stage ranged from 40 to about 50 kips during which yielding spread from the center to the edges of the slab. In the final phase, the plastic stage, yielding was fully developed along the yield-lines, and deflections in-

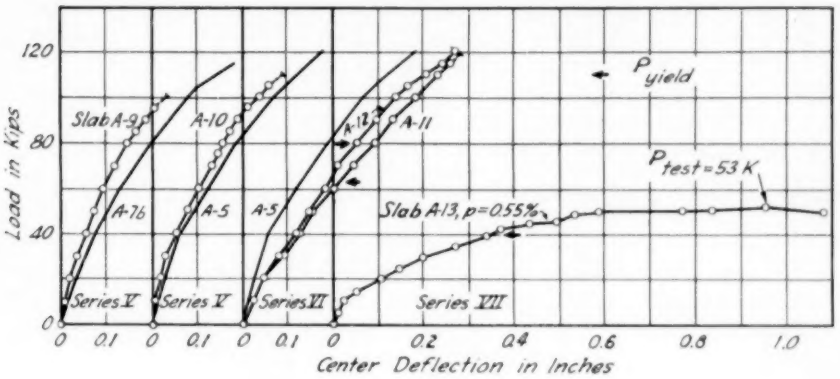

Fig. 10—Load-deflection curves, series V, VI, and VII

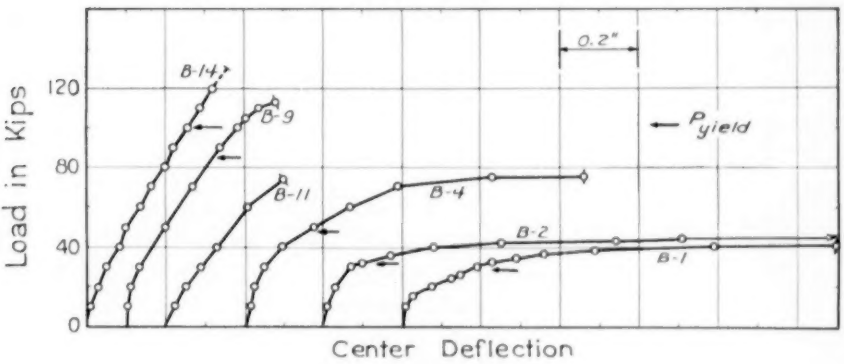

Fig. 11—Load-deflection curves, series VIII

creased considerably under a nearly constant load. Throughout the plastic stage the slab was in flexural distress; however, the slab was able to maintain load until the center deflection reached about 1 in., when a secondary and final failure took place by the column punching through the slab.

The shearing failure was a secondary phenomenon and Eq. (3) does not apply. As indicated in Table 4, P_{test} is 20 percent higher than P_{flex} computed by the yield-line theory. This 20 percent excess strength is reasonable since the yield-line theory as used herein did not consider strain hardening of the reinforcement and membrane action of the slab due to the excessive slab deflections, both of which will tend to increase load-carrying capacity in flexure.

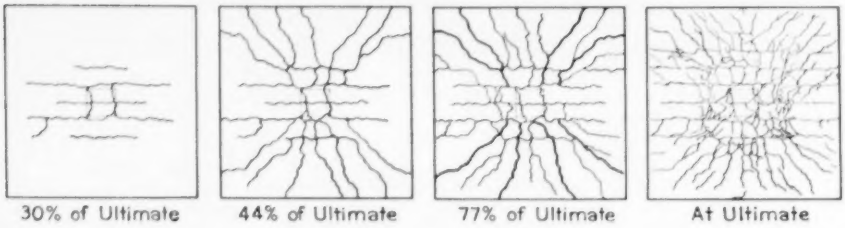

Fig. 12—Formation of cracks, slab B-14

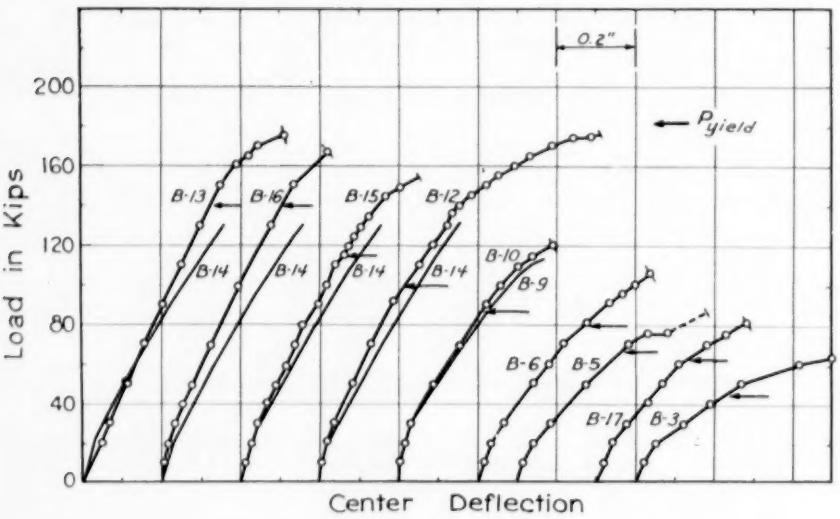

Fig. 13—Load-deflection curves, series IX

Series VIII

The six slabs of this series were designed primarily to extend the range of series I both in concrete strength and in percentage of tension reinforcement. They are similar to the slabs of series I, concentrically loaded through a 10-in. square column and supported on four edges with corners free to lift, except that the compression reinforcement was eliminated. Also in slab B-11 tension reinforcement with a higher yield point was used.

The general behavior of these slabs was the same as that of slabs in series I. Load-deflection curves are shown in Fig. 11. Because the slabs were supported 3 ft above the base of the testing machine, it was possible to observe the crack pattern on the tension surface of the slabs. Fig. 12 shows a typical pattern of the crack formation. What was assumed to be flexural cracking in series I at 15 to 25 percent of ultimate load was verified by these observations. As shown in Fig. 12, the initial flexural

cracking developed in the vicinity of the column stub along the lines of the tension reinforcement. These cracks were much more pronounced along the parallel lines of reinforcement close to the tension surface. As load increased, cracks radiated from the vicinity of the column to the slab edges not unlike the assumed yield-line pattern shown as Case I in Fig. A1 of Appendix 1. When the radial cracks had reached the slab edges, usually at about 50 percent of ultimate, development of new cracks diminished; however, the major radial cracks widened considerably as load increased. Prior to ultimate load, it was impossible to predict the location of the punching crack which seemed to be completely independent of the cracks formed beforehand.

Of the six slabs tested in this series three definitely failed in flexure since deflections and tensile strains were quite large. These three slabs, B-1, B-2, and B-4, followed the same pattern as slab A-13. It should be noted that, as was the case for slab A-13, P_{test} was 10 to 20 percent larger than calculated by the yield-line theory because of membrane action and strain hardening. The type of strain gages and recording equipment used made it impossible to measure the tensile strains at failure; however, they were greater than 0.02 in. per in.

Pertinent data involved in the ultimate strength analysis are given in Table 4. Comparison of results of slabs B-9, B-11, and B-14 to the slabs of series I indicate favorable agreement. It can be concluded, therefore, that the ultimate shearing capacity of these slabs is not dependent upon compression reinforcement.

Series IX

The nine slabs of this series were loaded concentrically through a 10-in. column and were supported on four edges with corners free to lift. The slabs were similar to those of series VIII except that shear reinforcement was provided. This shear reinforcement, details of which are shown in Fig. 2 and Table 2, was added steel and not bent-up tension reinforcement. The bend in these added bars was generally directly under the column edges, and the top cover was ¾ in. In slab B-16, the second bend began 4½ in. from the column edge. For slab B-12, the two rows of vertical stirrup reinforcement were located 2¼ and 6¾ in. from the column edge, respectively.

Slabs B-12, B-13, B-15, and B-16 of series IX, and B-14 of series VIII, are comparable, all having the same percentage of tension reinforcement and about the same concrete strength. The only variable was type and amount of shear reinforcement. Slab B-14, with no shear reinforcement, failed in shear in the normal manner at 130 kips, and P_{calc} as computed by Eq. (3) and (4) was 133 kips. Slab B-15 with six # 4 bar stirrups at an angle of 45 deg and an anchorage length of 7 in. past the top bend failed in shear at 155 kips. The punched-out section for this slab was much larger than the corresponding slab with no shear reinforcement (Fig. 2). The shear crack ran along the tops of the stirrups rather than through the stirrups. Examination after failure indicated that failure may have been caused by local crushing of the concrete under the top bend of the stirrups or by insufficient anchorage length. Anchorage length was increased to 15 in. in succeeding slabs. In slab

B-16 the amount of stirrup steel was increased and a second row of stirrups provided. Ultimate shearing capacity was raised to 168 kips, but the shearing crack ran along the tops of the first and second row of stirrups. Anchorage was sufficient, but local crushing at the bends of the stirrups was again noted. Slab B-13 with stirrups at 20 deg but with approximately the same vertical force component, $A_v f_v \sin \theta$, as slab B-16 failed at 175 kips. Again the shearing crack was well toward the tops of the stirrups pushing the punched section out almost to the edges of the slab. Local crushing under the bends of the stirrups was not obvious. For slab B-12 two rows of vertical stirrups were provided such that the shearing force component was approximately equal to the diagonal stirrups of slab B-16. Less than ¼ in. of top cover was provided for these stirrups so that the shear crack would have to run through the stirrups rather than along the tops of the stirrups. Failure was at 177 kips and the shear crack was outside the second row of stirrups. In all these slabs electric strain gages were attached to the centers of the stirrup length. None of the stirrups in these slabs reached yielding at this location at failure. Whether the stirrups yielded at the shear crack near the top bend of the stirrups can only be presumed.

Slabs B-5 and B-6 of series IX and B-9 of series VIII, all with 2 percent tension reinforcement, are comparable. Slabs B-5 and B-6, both with about 2000-psi concrete, failed at 85 kips and 105.3 kips, respectively. Slab B-5 had two # 4 bar stirrups at 45 deg; slab B-6 had twice as much stirrup steel. Slab B-9 with no stirrups but with 6300-psi concrete failed at 113.5 kips, so in this case raising the concrete strength was more effective than adding shear reinforcement.

Slab B-3 with 2000-psi concrete and 0.99 percent tension reinforcement would have been close to flexural failure even without shear reinforcement. The addition of four # 3 bar stirrups did not increase the ultimate load appreciably even though the stirrups were definitely yielding at failure.

Load-deflection curves for slabs of this series are compared to similar slabs without shear reinforcement in Fig. 13. As one would expect, diagonal shear reinforcement increased the slab stiffness and raised P_{yield}. Vertical shear reinforcement did not change slab stiffness.

Pertinent data for the ultimate load analysis in which Eq. (3a) and Eq. (4) were used are given in Table 5. A comparison of these data to that of similar slabs without shear reinforcement shows that stirrups increase the ultimate load capacity of slabs as much as 30 percent, but in no case was enough shear reinforcement provided to cause flexural rather than shear failure.

Even though it would be desirable to fully develop the flexural capacity of relatively thin slabs supported on slender columns, to do so with shear reinforcement may be impractical. In some cases the required stirrup steel area may be abnormally large so that it may be impractical to meet the accepted requirements for minimum spacing, minimum diameter of bends, and minimum concrete cover. Slab thickness, concrete strength, and column dimensions should therefore probably be so chosen in design that only a small amount of shear reinforcement, if any at all, is needed in thin slabs.

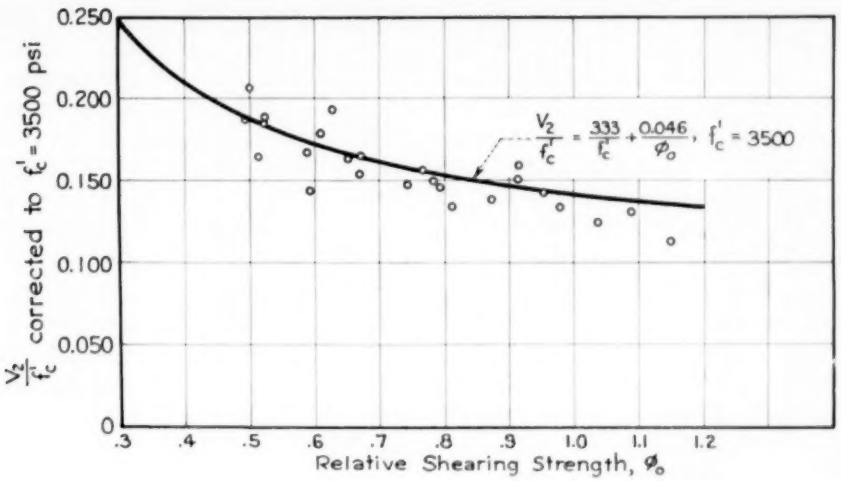

Fig. 14—Influence of relative shearing strength, series I through VIII

Summary of ultimate shearing strength analysis

Twenty-five slabs without shear reinforcement failed in shear. They may be studied on the basis of Eq. (3); the observed shearing stresses are plotted as a function of ϕ_o in Fig. 14 and as a function of concrete strength in Fig. 15. The test data are corrected to $f_c' = 3500$ psi or $\phi_o = 1.0$, respectively, in accord with Eq. (3). Thus,

$$\frac{v_2}{f_c'} \text{ (corrected to } f_c' = 3500) = \frac{v_2}{f_c'} \text{ (observed)} - \frac{333}{f_c'} + \frac{333}{3500}$$

$$\frac{v_2}{f_c'} \text{ (corrected to } \phi_o = 1.0) = \frac{v_2}{f_c'} \text{ (observed)} - \frac{0.046}{\phi_o} + 0.046$$

Also shown in Fig. 15 is a comparison of Eq. (3) which was used in this analysis and Eq. (2) which was used in the analysis of Richart's footing tests. Between 3000 and 4500 psi, the range in which 75 percent of Richart's footings are located, the difference between Eq. (3) and Eq. (2) varies from +5 to −9 percent. Thus, it can be concluded that Eq. (3), developed from the data reported herein, could be applied to Richart's footings with a reasonable degree of accuracy.

The agreement between observed and predicted values in Fig. 14 and 15 is satisfactory. For these 25 slabs failing in shear the average P_{test}/P_{calc} ratio based on Eq. (3) is 0.972 with a corresponding standard deviation of 0.077. Using Eq. (2) the average P_{test}/P_{calc} is 0.951 with a standard deviation of 0.095. Although the latter values are acceptable in concrete research, it can be seen from Fig. 15 that the standard deviation for Eq. (2) would have been much larger if more test points were available for concrete strengths greater than 4500 psi and less than 3000 psi.

The nine slabs with shear reinforcement all failed in shear. Using Eq. (3a) the

average P_{test}/P_{calc} ratio is 0.992 with a standard deviation of 0.067. Considering the range and number of variables the results are quite satisfactory.

Eq. (3a) can be further substantiated by applying it to the results of tests conducted in Germany in 1935-36 and reported by Otto Graf in 1938.[5] Graf tested eight slabs of which six had shear reinforcement. These slab specimens were about 5-ft square, were supported on all four edges, and were loaded through 7.9- and 11.8-in. square columns at the center of the slab. In these respects Graf's slabs were similar to those reported herein. However, Graf's specimens were much thicker, having effective depths of 10.7 and 18.8 in.

The pertinent data for Graf's slabs and the analysis of the test results using Eq. (3a) is presented in Table 6. The average P_{test}/P_{calc} ratio of 1.025 is satisfactory.

Observed v_z/f_c' corrected to $f_c' = 3500$ psi and $\phi_v = 1.0$, is plotted against q_v in Fig. 16 for both series IX and Graf's tests. Agreement between observed and calculated results is quite satisfactory. This figure also shows that v_z/f_c' can be increased considerably by increasing q_v. However, the increase in q_v is limited by the amount of shear steel that can be effectively placed across the shear section. For thick slabs such as Graf's it was possible to place two rows of reinforcement across the shear section and to use bars ¾ and ⅞ in. in diameter. Such is not the case for thin slabs because of space and bending limitations.

RESULTS OF BEAM STRIP TESTS

As part of the investigation of slabs reported herein, eight beam specimens representing center strips of the slabs of series I were tested to study possible relationships between the behavior and strength of such beam strips and of corresponding slabs.

All beams were 6 ft long, 12 in. wide, and 6 in. deep. They were simply supported at the ends on maple strips similar to those used for the slabs and were loaded at midspan through an integrally cast 10-in. square column stub. Properties of the specimens are given in Table 7. Percentages of tension reinforcement were 1.03, 2.00, and 3.00, and corresponding percentages of compression reinforcement were 0.50, 1.00, and 1.00, respectively. None of the beams had shear reinforcement of any kind.

Six of the eight beam strips failed in flexure either by yielding of the tension reinforcement followed by a secondary compression failure, or by yielding of the tension reinforcement followed by a bond failure. Only in beam B2a did a diagonal crack appear before yielding of the tension reinforcement. However, shear failure occurred after the reinforcement was yielding. For beam B1c, the final shear failure was probably a secondary failure.

The behavior during loading of all beams was typical for simple beams loaded at midspan. Major tensile cracks formed at the bottom of the beams, usually directly under the edges of the column stub, at approximately 50 percent of ultimate load. Other cracks formed progressively closer to the beam ends as the load increased. Except for beam B2a, deflections at failure were several inches.

TABLE 5—TEST RESULTS FOR SERIES IX*

Slab No.	p, percent	f_c', psi	f_{sp}, ksi	A_r, sq in.	f_r, ksi	θ, deg.	q_r	P_{test}, kips	$\frac{v_2}{f_c'}$	P_{yield}, kips	P_{flex}, kips	$\frac{P_{test}}{P_{yield}}$	$\frac{P_{test}}{P_{flex}}$	P_{calc}, kips	$\frac{\phi_o P_{calc}}{P_{flex}}$	$\frac{P_{test}}{P_{calc}}$
B-3	0.59	1930	43.3	0.88	46.9	45	0.096	64.5	0.212	45.0	61.1	1.43	1.056	77.5	1.269	0.832
B-5	2.00	2080	60.9	0.80	48.0	45	0.083	85.0	0.259	67.0	138.2	1.27	0.615	86.9	0.629	0.978
B-6	2.00	2450	55.1	1.60	48.0	45	0.141	105.3	0.273	80.0	137.1	1.32	0.768	109.8	0.801	0.959
B-10	2.00	6730	48.6	1.60	48.0	45	0.051	120.0	0.113	87.0	144.2	1.38	0.832	115.1	0.798	1.043
B-12	3.00	6650	48.1	2.20	46.9	90	0.099	177.0	0.169	100.0	206.5	1.77	0.857	164.0	0.794	1.079
B-13	3.00	6960	47.6	6.20	54.1	20	0.105	175.0	0.160	140.0	205.5	1.25	0.852	172.6	0.840	1.014
B-15	3.00	7090	48.1	2.40	48.0	45	0.073	155.0	0.139	115.0	208.3	1.35	0.744	148.5	0.713	1.044
B-16	3.00	6570	49.2	3.20	48.0	45	0.105	168.0	0.162	140.0	210.5	1.20	0.798	169.0	0.803	0.994
B-17	1.50	2100	44.6	0.88	46.9	45	0.088	80.3	0.243	63.0	90.4	1.27	0.888	81.8	0.905	0.982

Avg P_{test}/P_{calc} = 0.902
Standard deviation = 0.067

*For all slabs d = 4.5 in. and r = 10 in.

TABLE 6—GRAF'S 1935-36 SLAB TESTS

Slab No.	p, percent	f_c', psi	d, in.	r, in.	f_y, ksi	A_r, sq in.	f_r, ksi	θ, deg.	q_r	P_{test}, kips	$\frac{v_2}{f_c'}$	P_{flex}, kips	$\frac{P_{test}}{P_{flex}}$	P_{calc}, kips	$\frac{\phi_o P_{calc}}{P_{flex}}$	$\frac{P_{test}}{P_{calc}}$
1355	0.83	2210	10.7	7.9	40.1	5.74	39.1	45	0.243	271.2	0.415	276.9	0.979	257.0	0.928	1.055
1356	0.82	2210	10.8	7.9	40.1	5.70	39.1	45	0.240	288.8	0.441	277.0	1.043	313.0	0.923	1.130
1376	0.50	2370	18.7	7.9	40.0	10 40	38.8	60	0.289	507.2	0.418	514.2	0.986	504.4	1.005	0.981
1377	0.50	2210	18.7	7.9	40.0	10.40	38.8	60	0.310	496.1	0.437	512.4	0.968	490.4	1.012	0.957
1361	1.17	2380	10.7	11.8	39.0	8.03	38.5	45	0.208	388.0	0.369	402.0	0.965	424.5	0.914	1.067
1363	0.70	2380	18.5	11.8	38.8	13 87	38.1	60	0.253	679.1	0.375	746.8	0.909	714.7	0.950	0.957

Avg P_{test}/P_{calc} = 1.025
Standard deviation = 0.064

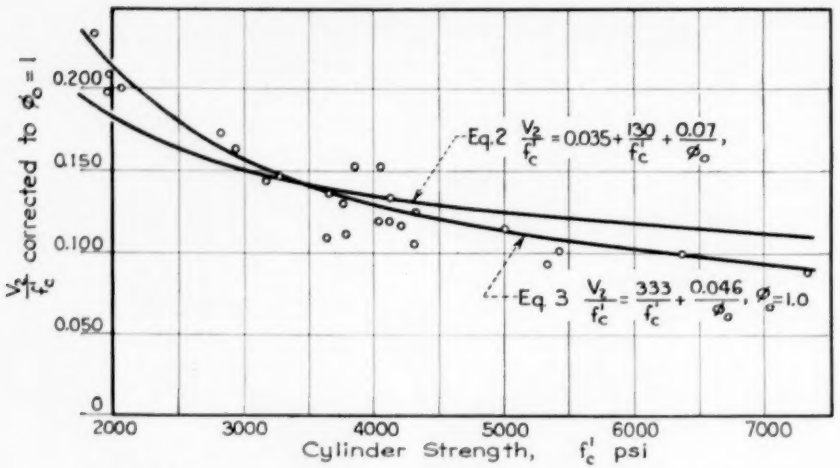

Fig. 15—Influence of concrete strength, series I through VIII

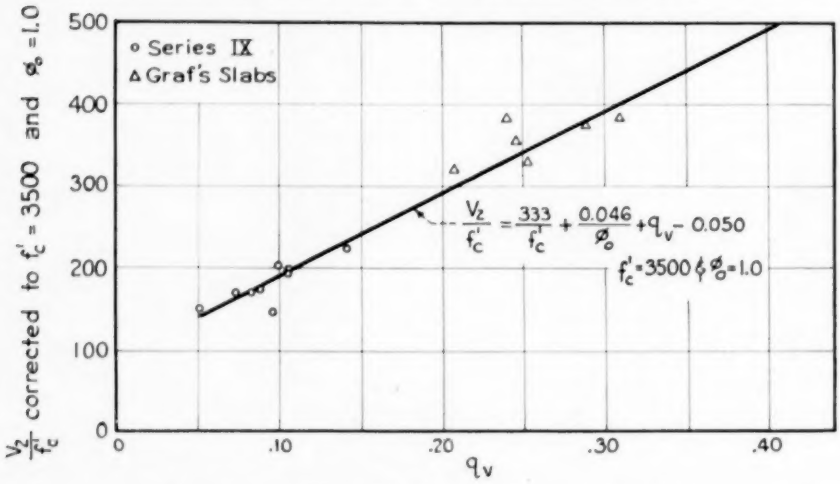

Fig. 16—Influence of shear reinforcement index

A study of the ultimate strength of the beam strips is given in Table 7. Theoretical flexural strength, P_{flex}, was computed on the basis of Eq. (b) and (g) of Appendix 1. The ratios P_{test}/P_{flex} are 10 to 30 percent greater than one. In this connection it is pertinent that the beams were loaded through a monolithically cast stiff column stub at midspan. Thus, at the large deflections preceding failure a concentration of plastic rotation existed at the edge of the column with the result that the reinforcement was strained into the work hardening range.

Six of the eight beams failed in flexure while the corresponding slabs of series I failed in shear. Thus, the behavior of beam strip specimens does not reflect the be-

TABLE 7—RESULTS OF BEAM STRIP TESTS*

Beam No.	Concrete strength f_c' psi	Tension reinforcement			P_{test}, kips	P_{yield}, kips	P_{flex}, kips	$\frac{P_{test}}{P_{yield}}$	$\frac{P_{test}}{P_{flex}}$	Mode of failure†
		p, percent	Yield f_{sy} ksi	Index q						
B1a	1600	1.03	48.7	0.314	9.8	7.3	8.2	1.34	1.20	T
B1b	3830	1.03	48.7	0.131	11.8	8.8	9.1	1.34	1.30	T
B1c	5640	1.03	48.7	0.089	12.0	8.6	9.3	1.40	1.29	T,S
B2a	1520	2.00	45.6	0.600	15.2	11.8	12.4	1.29	1.23	T,S
B2b	3460	2.00	45.6	0.263	17.7	13.5	15.3	1.31	1.16	T,B
B2c	4520	2.00	45.6	0.202	17.4	13.0	15.8	1.34	1.10	T
B3b	3530	3.00	45.6	0.388	25.3	20.0	21.4	1.27	1.18	T
B3c	4730	3.00	45.6	0.289	25.9	19.5	22.6	1.33	1.14	T

*Simply supported and loaded at the center through a 10-in. square column, all beams were 6 ft long, 12-in. wide, and 5-in. effective depth.
†T = tension failure; S = shear failure; B = bond failure.

havior and mode of failure of a corresponding slab. Beam strips are therefore unsuitable to evaluate the shearing strength of slabs. Analyses based on the concept of "equivalent width" may be good tools in elastic studies, but this concept tends to confuse rather than aid studies of ultimate strength of slabs.

SUMMARY

1. Object of the investigations reported herein was to throw new light on the behavior under load and shearing strength of reinforced concrete slabs. Thirty-nine 6-ft square slabs were loaded to failure through a centrally located column stub. Major variables were: concrete strength (2000 to 7000 psi), percentage of tension reinforcement (0.50 to 3.70 percent), percentage of compression reinforcement (0 to 1.00 percent), size of column (10 and 14 in.), conditions of slab support and loading, distribution of tension reinforcement, and amount and position of shear reinforcement. Final failure of 34 slabs was by the column punching through the slab; in most cases such punching took place after initial yielding of the reinforcement in the vicinity of the column.

2. The test results confirm the findings of the re-evaluation[4] of Richart's footing investigation[3] to the effect that the shearing strength is a function of concrete strength as well as of several other variables.

3. Ultimate shearing stress for slabs without shear reinforcement can be expressed as:

$$\frac{v_n}{f_c'} = \frac{V}{\frac{7}{8}bdf_c'} = \frac{333}{f_c'} + \frac{0.046}{\phi_o} \qquad (3)$$

For slabs with shear reinforcement:

$$\frac{v_n}{f_c'} = \frac{V}{\frac{7}{8}bdf_c'} = \frac{333}{f_c'} + \frac{0.046}{\phi_o} + (q_s - 0.050) \qquad (3a)$$

where

$$q_s = \frac{A_s f_s \sin\theta}{\frac{7}{8}bdf_c'}$$

in which b is the circumference of the loaded area, and ϕ_o is the ratio between the

ultimate shear capacity and the ultimate flexural capacity computed without regard to shear. The ultimate flexural capacity of the slab may be computed with the aid of the yield-line theory.[1]

Eq. (3) is similar to that derived from the reanalysis of Richart's footing tests and can be applied to those tests with a reasonable degree of accuracy, even though the footings were thicker, more lightly reinforced, and supported differently.

4. A concentration of 50 percent of the tension reinforcement directly over a column did not increase the shearing strength for the conditions represented by the test slabs.

5. Eccentric loading, by applying a live load at an edge of a centrally located column, had a negligible effect on shearing strength as compared to corresponding concentric loading.

6. Compression reinforcement had no effect on the ultimate shearing strength of the slabs.

7. For slabs which failed in flexure the measured ultimate capacity was 10 to 20 percent greater than predicted by the yield-line theory, probably due to membrane action and strain hardening of the reinforcement.

8. Tests of beam strips representing a narrow slab section and supported as a beam indicated that the use of such concepts as "beam strip analogy" and "equivalent width" does not necessarily lead to a correct prediction of the mode of failure for the corresponding slabs.

ACKNOWLEDGMENT

The first of these investigations was carried out during 1952 in the Department of Theoretical and Applied Mechanics, University of Illinois, under the sponsorship of the Reinforced Concrete Research Council of the Engineering Foundation. Credit for initiating and planning this first investigation belongs to the ACI-ASCE joint committee on shear and diagonal tension.

The second investigation was carried out as part of the structural development program of the Portland Cement Assn. during 1954.

REFERENCES

1. Hognestad, E., "Yield-Line Theory for the Ultimate Strength of Reinforced Concrete Slabs," ACI JOURNAL, Mar. 1953, *Proc.* V. 49, pp. 637-656.

2. Talbot, A. N., "Reinforced Concrete Wall Footings and Column Footings," *Bulletin* No. 67, University of Illinois Engineering Experiment Station, Urbana, 1913, 114 pp.

3. Richart, F. E., "Reinforced Concrete Wall and Column Footings," ACI JOURNAL, Oct. and Nov. 1948, *Proc.* V. 45, pp. 97-127 and 237-260.

4. Hognestad, E., "Shearing Strength of Reinforced Concrete Column Footings," ACI JOURNAL, Nov. 1953, *Proc.* V. 50, pp. 189-208.

5. Graf, O., "Versuche über die Widerstandsfähigkeit von allseitig aufliegenden dicken Eisenbetonplatten unter Einzellasten," Heft 88, Deutscher Ausschus für Eisenbeton, Berlin, 1938, 26 pp.

APPENDIX 1

In the analysis of shearing strength presented herein, shear and flexure were considered as a combined loading problem. It was therefore necessary to estimate the ultimate flexural strength the various slabs would have had if premature shear failures had not taken place. The yield-line theory as developed primarily by Dr. K. W. Johansen was used for this purpose. It is assumed in this theory that yielding of the tension reinforcement is concentrated across certain lines in the slab plane, the yield lines, the locations of which depend primarily on loading and boundary conditions. An outline of the yield-line theory has been given in a previous ACI JOURNAL paper.[1] The conditions of support and loading considered are shown in Fig. A1.

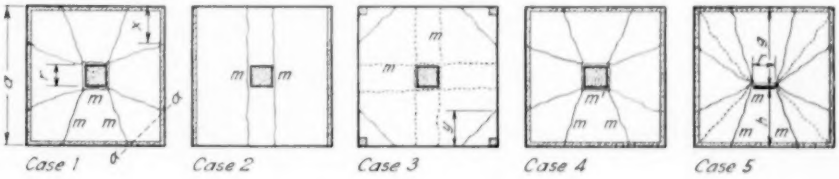

Fig. A1—Yield-line patterns

1. Square slab supported along four edges

Corner levers will form permitting the slab corners to lift by rotation about the axes a-a. Assuming a deflection of unity at the column, the principle of virtual work gives:

$$P = 4m(a - 2x)\frac{2}{a - r} + 4mx\sqrt{2}\frac{\sqrt{2}}{a - r - x} \quad \text{(a)}$$

in which m is the ultimate flexural moment per unit width:

$$m = pf_{yy}d^2\left(1 - \tfrac{1}{2}p\frac{f_{yy}}{f_c'}\right) = q(1 - \tfrac{1}{2}q)d^2f_c' \quad \text{(b)}$$

when the tension reinforcement index

$$q = p\, f_{yy}/f_c'$$

For the test slabs considered herein the average percentage of reinforcement, p, for the two layers is computed by

$$pd^2 = \tfrac{1}{2}(p_1d_1^2 + p_2d_2^2) \quad \text{(c)}$$

where the subscripts 1 and 2 refer to the two layers of reinforcement and $d = \frac{1}{2}(d_1 + d_2)$.

A yield-line pattern will develop corresponding to a value of x giving a minimum value of P in Eq. (a).

$$\frac{\partial P}{\partial x} = 0 \text{ gives } x = (1 - \tfrac{1}{2}\sqrt{2})(a - r) \quad \text{(d)}$$

which substituted into Eq. (a) gives:

$$P_{flex} = 8m\left(\frac{1}{1 - \frac{r}{a}} - 3 + 2\sqrt{2}\right) \quad \text{(e)}$$

If the corners are tied down, the yield lines must go through the corners, that is, $x = 0$, and

$$P_{flex} = 8m \frac{1}{1 - \frac{r}{a}} \quad \text{(f)}$$

2. Support along two opposite edges

The governing pattern is shown in Fig. A1. With a deflection of unity at the column we obtain by virtual work:

$$P_{flex} = 2ma \frac{2}{a - r} = 4m \frac{1}{1 - \frac{r}{a}} \quad \text{(g)}$$

3. Support at four corners

Two types of yield-line patterns are possible. If the lines form across the corners, we obtain by virtual work:

$$P_{flex} = 4my\sqrt{2} \frac{\sqrt{2}}{y} = 8m \quad \text{(h)}$$

For the dotted pattern, on the other hand, we obtain:

$$P_{flex} = 4m \frac{a - r}{2} \sqrt{2} \frac{\sqrt{2}}{a - r} + 4mr \frac{4}{a - r} = 4m \left(1 + \frac{4}{\frac{a}{r} - 1} \right) \quad \text{(i)}$$

The equation giving the smallest P_{flex} will govern. Thus, Eq. (h) applies when $r \geq a/5$, and Eq. (i) applies when $r \leq a/5$.

4. Concentration of reinforcement over column

In this case a higher moment m' exists at the column edge than the m in the rest of the slab. Eq. (e) must therefore be modified as follows:

$$P_{flex} = 4m(a - 2x) \frac{2}{a - r} = 4mx \sqrt{2} \frac{\sqrt{2}}{a - r - x} + 4(m' - m)r \frac{2}{a - r} \quad \text{(j)}$$

The new term in Eq. (j) does not contain x, and differentiation will therefore still give Eq. (d). Thus:

$$P_{flex} = 8m \left(\frac{1}{1 - \frac{r}{a}} - 3 + 2\sqrt{2} + \frac{\frac{m'}{m} - 1}{\frac{a}{r} - 1} \right) \quad \text{(k)}$$

The ratio m'/m may by Eq. (b) be expressed as:

$$\frac{m'}{m} = \frac{q'(1 - \frac{1}{2}q')}{q(1 - \frac{1}{2}q)} \quad \text{(l)}$$

The percentage of concentrated reinforcement, p', is quite large as indicated in Tables 1 and 6. Thus, a maximum value of q' $(1 - \frac{1}{2}q')$ of 1/3 should be used recognizing compression failures by Whitney's equation $M/bd^2 = 1/3\ f_c'$.

5. Eccentric loading, four-edge support

With an eccentricity of $r/2$, we consider the load a line load at the column edge. A mathematical solution is then somewhat complex if the corners are left free to

lift. An approximate solution may be obtained by considering the corners tied down, the dotted yield lines in Fig. A1. Later a correction factor equal the ratio between Eq. (e) and (f) may be applied, which ratio is 0.865 for $a = 72$ in. and $r = 14$ in. For the corners tied down, we obtain:

$$P_{flex} = ma\left(\frac{1}{h} + \frac{1}{g} + 2\frac{2}{a - r}\right) \qquad \text{(m)}$$

For the corners free to lift:

$$P_{flex} = 0.865m\left(\frac{a}{h} + \frac{a}{g} + \frac{4}{1 - \frac{r}{a}}\right) \qquad \text{(n)}$$

APPENDIX 2

Statistical Analysis of Test Results

By Paul Seligmann*

The test results were assumed to fit an equation of the form

$$\frac{v_2}{f_c'} = a + \frac{b}{f_c'} + \frac{c}{\phi_o}$$

where

$$\phi_o = \frac{7}{8}\frac{bdf_c'}{P_{flex}}\frac{v_2}{f_c'}$$

The quantities b, d, f_c', and P_{flex} were assumed to be without error. Solution of this equation for v_2/f_c' would lead to a form of function to which ordinary least squares methods are not applicable. Accordingly, a method of least squares using successive approximations† was applied.

The constants a, b, and c were assumed to have approximate values a_1, b_1, *and* c_1. The function

$$F = \frac{v_2}{f_c'} - a_1 - \frac{b_1}{f_c'} - \frac{c_1}{\phi_o}$$

has the partial derivative

$$\frac{\partial F}{\partial a_1} = -1, \quad \frac{\partial F}{\partial b_1} = -\frac{1}{f_c'}, \quad \frac{\partial F}{\partial c_1} = -\frac{1}{\phi_o}, \quad \frac{\partial F}{\partial \frac{v_2}{f_c'}} = 1 + \frac{c_1}{\frac{v_2}{f_c'}\phi_o} = \sqrt{L}$$

The corrections A, B, and C were obtained by solution of the normal equations

$$A\sum_{i=1}^{N}\frac{1}{L_i} + B\sum_{i=1}^{N}\frac{1}{f'_{ci}L_i} + C\sum_{i=1}^{N}\frac{1}{\phi_{oi}L_i} = -\sum_{i=1}^{N}\frac{F_i}{L_i}$$

$$A\sum_{i=1}^{N}\frac{1}{f'_{ci}L_i} + B\sum_{i=1}^{N}\frac{1}{f'^2_{ci}L_i} + C\sum_{i=1}^{N}\frac{1}{f'_{ci}\phi_{oi}L_i} = -\sum_{i=1}^{N}\frac{F_i}{f'_{ci}L_i}$$

$$A\sum_{i=1}^{N}\frac{1}{\phi_{oi}L_i} + B\sum_{i=1}^{N}\frac{1}{f'_{ci}\phi_{oi}L_i} + C\sum_{i=1}^{N}\frac{1}{\phi^2_{oi}L_i} = -\sum_{i=1}^{N}\frac{F_i}{\phi_{oi}L_i}$$

*Senior Research Physicist, Applied Research Section, Portland Cement Assn., Chicago, Ill.
†Deming, W. E., "Statistical Adjustment of Data," John Wiley and Sons, Inc., New York, 1943, Chapter VIII.

where the subscript i refers to the values obtained from ith test results and N is the total number of tests.

The corrected values were obtained from

$$a_2 = a_1 - A$$
$$b_2 = b_1 - B$$
$$c_2 = c_1 - C$$

The process was repeated by considering the corrected values as a new initial approximation. Since the method converges quite rapidly, two approximations were sufficient to give the proper degree of accuracy.

For such discussion of this paper as may develop please see Part 2, December 1957 *Journal*. In *Proceedings* V. 53 discussion immediately follows the June 1957 *Journal* pages.

Title No. 53-3

Prestressed Concrete Pavement for Airfields*

By THOMAS CHOLNOKY†

SYNOPSIS

Construction and testing of a 500 ft long and 12 ft wide experimental prestressed concrete slab are described. Loads on the prestressing tendons, development of prestressing in the slab, its load-carrying capacity, and the effect of heat thereon were studied. The results proved the superior behavior of the slab in all respects, and indicated that such construction could be utilized in future airfield pavement construction.

INTRODUCTION

The increasing use of jet planes and heavy wheel loads creates new problems in design of rigid airfield pavements. Elimination of expansion joints becomes a requirement in view of the maintenance problems caused by jet blast on joint materials. Also, current design methods lead to excessive pavement thickness under the heavy wheel loads of some new airplanes.

In 1952, as a part of the continuing search for better and more economical pavements, the Bureau of Yards and Docks undertook a research and development program on the possible use of prestressed concrete for airfields. Preliminary investigations and studies led to the building of an experimental prestressed concrete slab at the Patuxent River Naval Air Station, Md., during the summer of 1953. The test program commenced in September of the same year and was completed in May, 1955.

Description of test slab

The slab was 500 ft long, 12 ft wide, and 7 in. thick. It had 23 longitudinal strands, 0.6 in. in diameter, composed of seven wires. Transverse prestressing was provided using the same type strands, but only at three selected locations, called "test areas," where the instruments were concentrated (Fig. 1).

Post-tensioning of the strands was selected because it was considered an economical means of prestressing, and, with the type of strand anchorage used, stressing and releasing of strands was possible whenever desired.

---

*Presented at the ACI 51st annual convention, Milwaukee, Wis., Feb. 23, 1955. Title No. 53-3 is a part of copyrighted JOURNAL OF THE AMERICAN CONCRETE INSTITUTE, V. 28, No. 1, July 1956, *Proceedings* V. 53. Separate prints are available at 50 cents each. **Discussion** (copies in **triplicate**) should reach the Institute not later than Nov. 1, 1956. Address 18263 W. McNichols Rd., Detroit 19, Mich.

†Member American Concrete Institute, Consultant, Frederic R. Harris, Inc., Consulting Engineers, New York, N. Y.

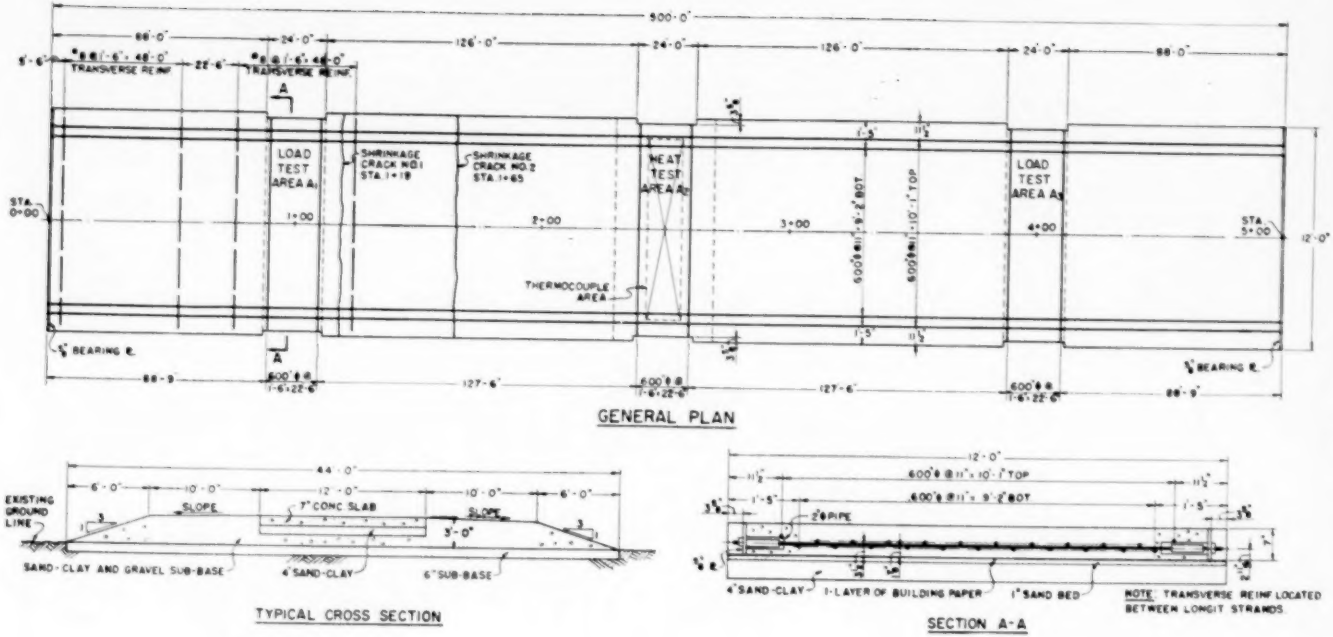

Fig. 1—General plan of experimental prestressed concrete pavement slab

Longitudinal strands were installed in lower and upper sets. Each set, stressed independently, could produce compressive stresses in the slab in excess of 300 psi. The two sets were used both independently and in combination. The slab also had ordinary transverse reinforcement consisting of # 8 bars, spaced at 18 in., in two locations only (Fig. 1).

Test program

Testing of materials was considered a basic requirement for the proper evaluation of any strain or stress measurements. Preliminary friction tests were made at the construction site to determine the approximate value of base friction under the slab, and to compare the relative merits of various friction-reducing layers.

Actual testing of the slab was centered around four basic problems: (1) loads on the strands; (2) development of prestressing in the concrete and losses due to base friction; (3) load carrying capacity; and (4) effect of heat on the slab.

Testing of the slab started immediately after casting in September, 1953, and was concluded in May, 1955, when the heat tests were performed. During this period work was interrupted only between April and December of 1954, mainly because the original loading equipment with 100,000-lb capacity proved to be inadequate and had to be replaced.

MATERIALS

Subbase

The test slab was placed on a 2 ft deep sand-clay and gravel subbase. A 4-in. layer of sand-clay directly under the slab was deposited on the finished surface of the subbase course. All material was placed in lifts of not more than 5 in. and each layer was compacted to 100 percent maximum density as determined by the modified Proctor compaction test. The finished surface of the sand-clay layer was required to have no projections or depressions greater than ⅛ in. when tested with a 10-ft straightedge.

Friction reducing layer

A friction-reducing layer consisting of 1 in. of local sand covered with building paper was placed immediately beneath the slab as a result of preliminary tests performed on small slabs. The sand was quite uniform in grain size, 94 percent of the material passing the 40-mesh and retained on the 80-mesh sieves.

Concrete

Composition of the concrete was determined by trial mixes. Specifications called for an average flexural strength of 760 psi and an average compressive strength of 5500 psi.

The final mix used 7 bags of cement per cu yd of concrete with about 34.5 gal. of water. Coarse aggregate consisted of crushed limestone with a maximum size of 1½ in. Plastiment at the rate of ¾ lb per bag of cement and Darex, to produce 4 to 5 percent entrained air, were required in the concrete.

The quality and characteristics of the concrete were subject to special study. Specimens were taken at various stations of the slab during placing and tested over a period of 1 year in the laboratory. These specimens were field cured to simulate conditions prevailing in the slab.

Compressive and flexural strengths and modulus of elasticity were determined at concrete ages of 3, 7, 14, 28, 60, 90, 180, and 360 days. Flexural strength of the concrete "in place" was determined from two specimens cut out at station 0+60 and 4+48 at the concrete age of 580 days.

Shrinkage measurements were made on three specimens over a period of 560 days. These specimens were also field cured and the measured variations include the effect of temperature changes and variations in moisture content. After the 200th day the specimens were laboratory cured for 90 days. Thermal expansion coefficients of the concrete were determined on three specimens at concrete ages of 28, 360, and 580 days. In each case, measurements were made with dry and saturated specimens. Results of these tests are given in Table 1.

TABLE 1—CONCRETE DATA*

Age of concrete, days	Flexural strength, psi	Compressive strength, psi	Modulus of elasticity, psi	Shrinkage, millionths	Thermal expansion, in. per in.
3	395	3070	—	—	—
7	610	3560	—	440	—
14	720	4830	3,240,000	510	—
28	805	5180	3,350,000	560	0.00000616
60	850	5300	3,560,000	500	—
90	875	5370	3,730,000	520	—
180	885	5970	4,070,000	410	—
360	965	6470	4,220,000	330	0.00000654

*Average values shown. Shrinkage values represent increases and were obtained from field specimens.

Prestressing tendons

Prestressing tendons 0.6 in. in diameter and weighing 0.737 lb per ft consisted of seven, hot-galvanized steel wires. The recommended initial stress for these strands is 140,000 psi and they have a guaranteed minimum modulus of elasticity of 24,000,000 psi. The strands were manufactured by J. A. Roebling's Sons Corp. and were delivered with their standard end-fittings.

Covering used on prestressing tendons

In designing the test slab, two materials seemed to be most promising for forming the conduit around the prestressing tendons. One was Sisalkraft paper, which represented low material cost but high labor cost. As an alternate solution and after careful investigation, a plastic material, Aeroflex tubing, which was more costly but seemed to be more economical of labor, was selected.

PRELIMINARY FRICTION TESTS

During the design of the test slab the need for preliminary investigations to determine the most suitable and economical friction reducing expedient became apparent. Therefore, specifications called for the installation of four 8 ft x 3 ft x 7 in. thick test slabs at the site as soon as some portion of the prepared base became available. These slabs were placed on:

Slab No. 1—1 in. of sand covered with one layer of building paper
Slab No. 2—two layers of building paper
Slab No. 3—two layers of copper-clad Sisalkraft paper, with the coppered faces turned together with powdered soapstone between them
Slab No. 4—the prepared base directly, with no intermediate devices

The setup used for pulling the test slabs and to measure their movement is shown in Fig. 2. The pulling force was provided by the same hand jack later used for prestressing. The pulling load exerted on the slabs was measured on a specially calibrated link, similar to those used for measuring loads on strands.

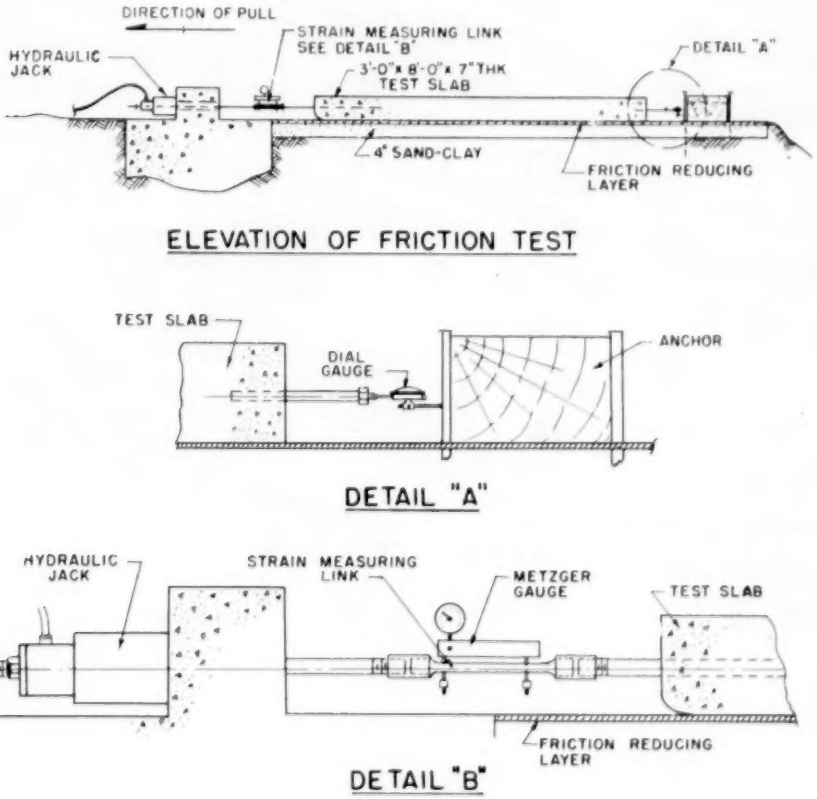

Fig. 2—Friction test

Failure was produced in about 5 min in slabs with friction reducing devices. It took somewhat longer to produce failure in the friction surface under the slab placed directly on the prepared base. The test results are listed in Table 2 which gives the maximum friction coefficients at the moment of failure and also that measured when the slabs were sliding. As a result of these tests 1 in. of sand covered with one layer of building paper (slab No. 1) was selected as the best solution.

TABLE 2—FRICTION TESTS

Slab No.	Coefficient of friction		Movement before failure, in.
	At failure	During sliding	
1	0.72	0.60	0.045
2	1.13	0.55	0.004
3	0.77	0.63	0.018
4	5.15	1.10	0.012

INSTRUMENTATION

Carlson strain meters were positioned in the concrete at test areas A_1 and A_3 as shown in Fig. 3 to determine strains and corresponding stresses in the concrete section during the various load tests. Carlson stress meters were placed in the same areas to determine pressures under the slab (Fig. 3). Longitudinal strain variations of the slab were determined primarily from readings made on Carlson strain meters, called "L" meters, at four stations of the slab (Fig. 4). Four of these meters were positioned at each station. Both the strain and stress meters could be used to determine temperatures in the concrete at any time.

Loads on the strands were measured by gages on the hydraulic stressing jack, and also by measuring elongation of special links inserted in certain strands (Fig. 5). The elongations on these special calibrated links were measured with Metzger gages.

The effect of jet heat and its dissipation throughout the depth of the slab was measured with thermocouples. The 38 thermocouples were attached to 19 dual temperature recording instruments. These were assembled in a panel, and a movie camera made recordings every second during the heat test.

Dial gages were used for deflection measurements during load tests. Such gages were used also during short periods to determine the over-all length variation of the slab.

CONSTRUCTION

Preparation of the base and the installation of the friction reducing layer was not an unusual task.

Handling and wrapping of the 500 ft long prestressing tendons proved to be quite cumbersome and time consuming. Both the paper and plastic tubing used for covering the strands had to be applied by hand in the field, which made this operation

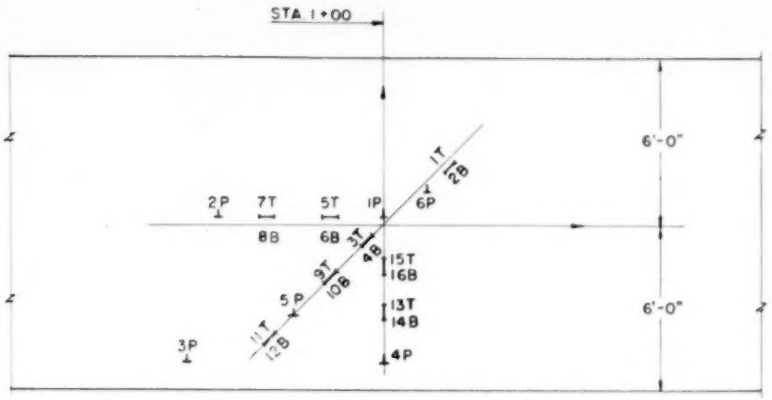

PLAN OF LOAD TEST AREA A_1

LOAD TEST AREA A_3 SIMILAR

LIST OF SYMBOLS

— STRAIN METER

⊥P PRESSURE METER

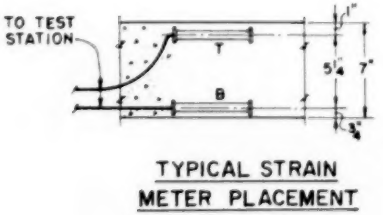

TYPICAL STRAIN METER PLACEMENT

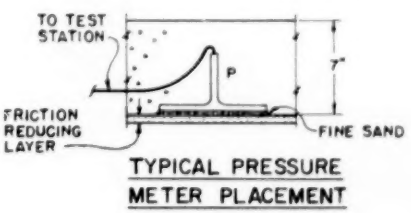

TYPICAL PRESSURE METER PLACEMENT

Fig. 3—Plan of load test area A_1

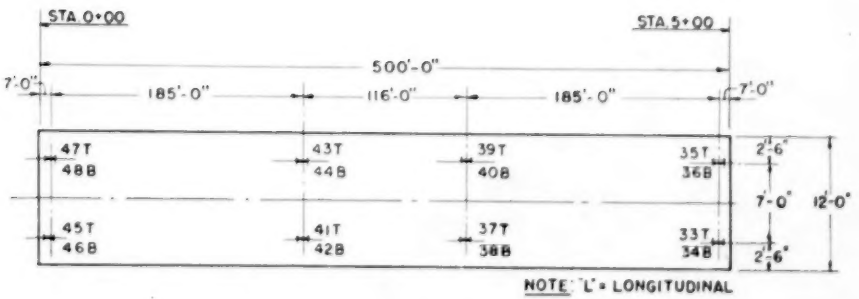

NOTE: 'L' = LONGITUDINAL

Fig. 4—Location of "L" strain meters

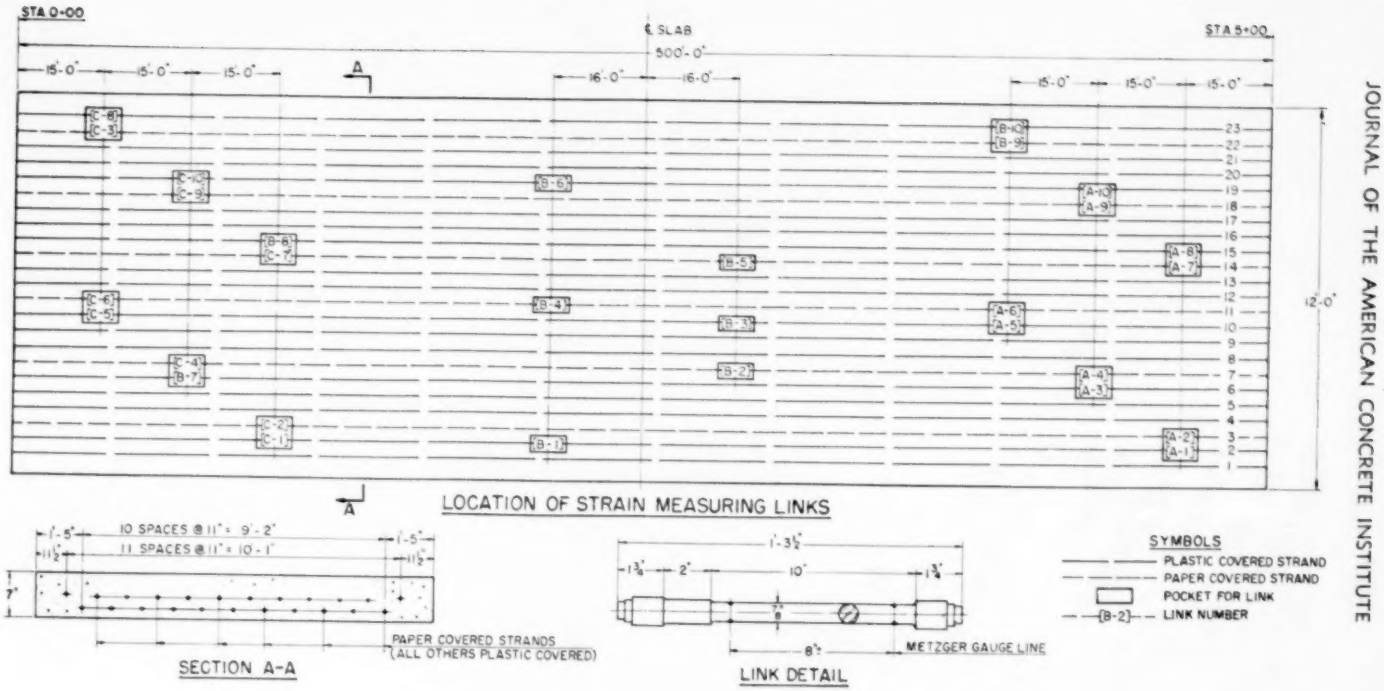

Fig. 5—Location of strain measuring links

costly. Even with special work benches it was difficult to handle the 500 ft long elements. Their placing also created some problems.

Prior to placing the longitudinal strands temporary anchors were set at the ends of the slab, with turnbuckles attached. After placing the strands, they were connected to these anchors, and a preliminary pull of 1500-2000 lb was applied on each by means of the turnbuckles (Fig. 6) to straighten the strands. They were also supported by chairs placed 6 ft on centers to eliminate any sag, and to make the conduit as straight as possible.

Concreting was completed in about 11½ hr (Fig. 7). For easier spreading and finishing of the concrete, the slump was increased gradually to 3½ in.

The finished surface was inspected the day following concreting. Two transverse shrinkage cracks, which extended full depth, were observed across the slab. One of these shrinkage cracks was at station 1+19, the other at station 1+65.

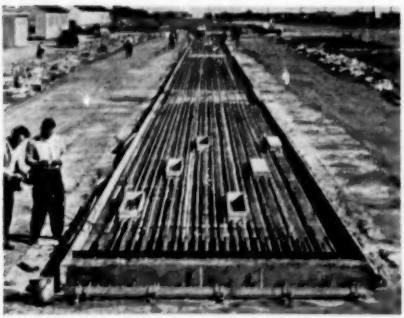

Fig. 6—Prestressing strands in place for concreting

Fig. 7—Placing of concrete in experimental slab

STRESSING OF THE STRANDS

The temporary anchorage was released and removed 1 day after the concrete was placed. Following this, the strands were checked one by one by pulling them through their conduits. None showed any sign of bonding or binding.

The first prestressing was applied the third day after concreting. First the upper strands were stressed starting at the center with strand No. 11 and proceeding alternately toward the two edges of the slab, *i.e.*, to strands No. 1 and 23. After stressing of the upper set was completed, jacking started on the lower strands in a similar manner. Two jacks were used; one was electric driven, the other hand operated. In general, the electric jack proved to be more efficient, considering the fact that each strand had to be stretched about 36 in.

The procedure during this first jacking was more complicated than that of later stressing operations because of the numerous measurements on the strain measur-

ing links. During the first stressing operation, strand elongation and not loads was the determining factor to the limits of stressing. Loads, of course, were checked with jack gages at both ends of each strand, and also at the strain measuring links.

The strands never were stressed or jacked from both ends simultaneously. All strands were stretched from one end to about 50 percent of the elongation corresponding to the design load of 30,000 lb. The remaining 50 percent elongation was produced thereafter at the other end of the strand. This procedure was later altered somewhat, when an additional step was added because it became apparent that loads introduced from one end did not develop uniformly along the strands. Therefore, as a third step, the load at the first jacking end was checked again and the final load was introduced there, if necessary.

LOADS ON STRANDS AND LOSSES DURING PRESTRESSING

During the first prestressing operation and the following release, the problem of developing and maintaining the desired load on the strands was carefully checked.

Twelve of the 23 strands were equipped with special strain measuring links as shown in Fig. 5. These 12 strands represented four distinct groups:

1. Three strands in the upper layer covered by plastic tubing
2. Three strands in the upper layer wrapped in paper
3. Same as 1, but in the lower layer
4. Same as 2, but in the lower layer

The layout of these strands was such that in certain cases the losses in load between the jacking end and the anchoring end could be measured. Six strands had a strain measuring link at one intermediate location also (Fig. 5). During stressing of the strands measurements on these links were made each time the hydraulic jack had to be reset, *i.e.*, after each elongation of 6 in.

Results of these measurements are presented in Fig. 8, representing strands wrapped in both plastic tubing and in paper. The loads measured on the links are plotted as a function of elongation at the jacking end. The diagrams indicate also the end or station from which the strands were stressed. The theoretical line given on these diagrams represents the strain-load relation of the strands based on the minimum guaranteed modulus of elasticity of 24,000,000 psi, if the applied load were evenly distributed throughout the entire length.

The results of these first tests indicated considerable friction losses for paper wrapped strands, particularly in the lower layer. On the other hand, these tests proved that friction losses can be kept to a negligible value on 500 ft long post-tensioned strands if they are lubricated and covered with fairly stiff material.

The most unfavorable conditions were observed in group 4, where in two extreme cases practically no load was transferred from one end to the other after approximately one-half the stretching was completed, and the jacking ends were reversed. The actual friction losses were lower when the induced load was low because at that stage the strands were relatively flexible. Friction losses observed on

strands in groups 2 and 3 showed similar results and stressing characteristics although the actual friction losses were lower.

The most favorable results were obtained with the plastic covered strands in the upper layer; average final friction loss was not more than 5 percent. In the lower layer, strands with the same covering showed an average loss of 19 percent. The paper covered strands in the same sets indicated a relative friction loss of 15 and 62 percent. There was no binding or bond between concrete and strands.

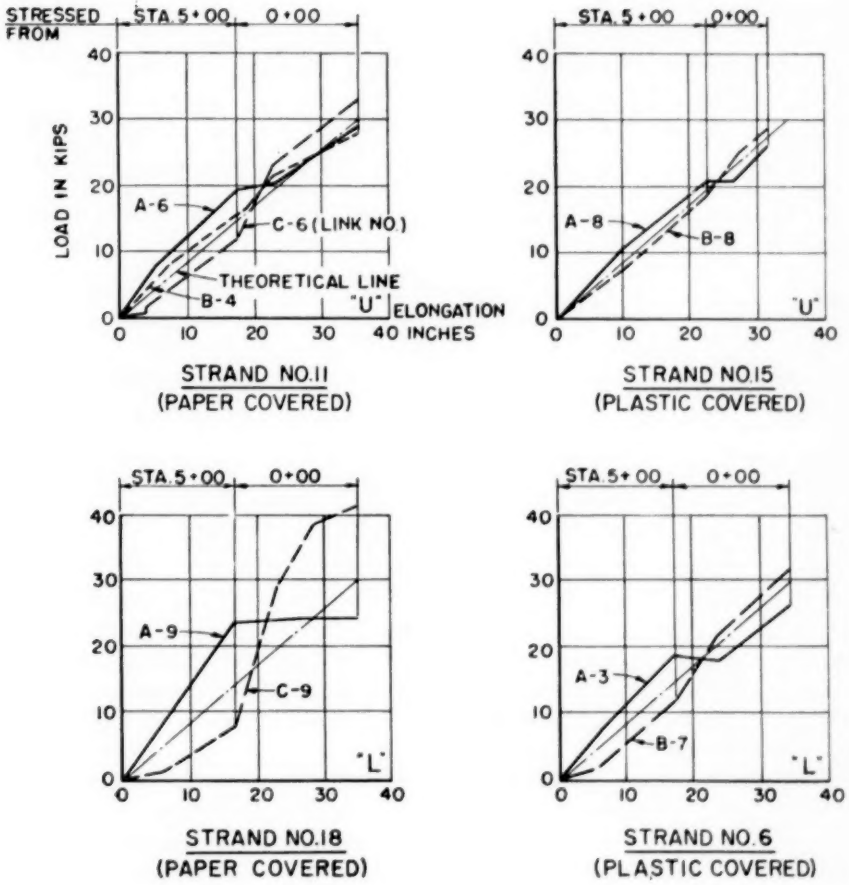

Fig. 8—Stressing of strands. U = upper strand; L = lower strand

LOSSES AFTER PRESTRESSING

Loads on the strands were checked several times before they were released, about 60 days after the first prestressing started. Due to the various conditions under which the strands were stressed, with different loads and with initial differentials between their two ends, it is difficult to express the losses over this 60-day period in an over-all percentage figure. As the strands had differentials in load between their ends, as well as minimum loads at intermediate points, any measured drop in load is more likely the result of the leveling off of such differentials rather than the result of losses due to elastic or plastic deformation in concrete or steel.

Only in the cases of strands No. 15, 19 and 23, which indicated least friction loss, would the difference of the average loads measured on both ends at the first stressing and release be indicative of the actual losses due to shrinkage, creep in the concrete, and creep in the strands. The average of losses on these three strands was 10 percent. Corresponding figures for strands No. 2, 6 and 10, strands No. 3, 7 and 11, and strands No. 14, 18 and 22 are 9, 10, and 15 percent, respectively.

Total shortening of the slab during this 60 days was not more than 2.0 in. Since prestressing of all strands was completed only after the first 30 days, it may reasonably be assumed that average shortening of the slab affecting the strands was not more than 1 in. This shortening would represent a loss of about 800 lb or 3 percent loss from the average initial load of 29,000 lb. It can be assumed that relaxation of the steel led to 6-7 percent loss, and the total result comes close to the measured 10 percent loss.

DEVELOPMENT OF PRESTRESSING IN THE SLAB; BASE FRICTION

When strands are tensioned, they exert loads on the two ends of the slab and these loads create stresses in the concrete section. These stresses are accompanied by strains which result in the shortening of the slab. Such shortening is resisted by the base friction. Therefore, the applied loads cause stresses that are reduced by the effect of friction forces. To study development of prestressing in the slab along its length, strain meters were installed at four stations (Fig. 4).

It is obvious that factors other than prestressing also create longitudinal strain variations, and must be considered in evaluating test results. Most important are thermal changes and variations in moisture content. Both produce volumetric changes in the concrete that may occur without accompanying stresses unless such changes are restrained, as in the case of any interior section of the slab where base friction is present.

The possible effect of temperature variations can be expressed by the thermal expansion coefficient of the concrete. Values obtained from specimens indicate a range of 6.22-5.13 millionths and 6.38-5.28 millionths for dry and saturated specimens, respectively. These figures indicate that a change of 50 deg in temperature would create strain in the order of 300 millionths.

It is considerably more difficult to evaluate the possible effect of shrinkage or variation in moisture content. Measurements on shrinkage specimens were made under

field conditions and for a short period under laboratory conditions. The results of measurements made under field conditions obviously include the effect of temperature changes also. After necessary temperature corrections, the results would indicate an extreme variation in the order of 200 millionths. Initial shrinkage which occurred during the first 28 days was disregarded.

The above figures are considerably higher than the strains which correspond to the maximum of 690 psi, to which the slab was stressed. Therefore, it is evident that errors made in determining the strain due to temperature and moisture content variations must have had considerable influence on the strains indicating the effect of prestressing.

Strain readings at the two ends of the slab presented a lesser problem because there it could be assumed that all strains developed freely. At interior sections of the slab, these strains could not develop freely because of base friction.

It is obvious that prior to application of prestressing, thermal changes and variations in moisture content create stresses in the concrete. These stresses are in equilibrium with the base friction, which is not constant but varies under sustained loads and with changes in temperature and moisture content of the base. Volumetric changes of the concrete, especially those due to temperature variations, are subject to daily and seasonal fluctuations. These fluctuations cause consequent contraction and expansion in the slab. Friction forces vary accordingly and alternately have a decreasing and increasing tendency.

The actual or governing stress condition in the slab when prestressing is applied will influence the efficiency with which the introduced stress can be distributed throughout the entire slab length. The fact that the restrained volumetric changes and base friction represent a stress condition in equilibrium would indicate that, by virtue of simple superimposition, the prestressing forces could be developed practically without losses.

The increasing or decreasing tendency of friction forces and the cyclical variation of contraction and expansion are, however, of real importance when the development of prestressing is to be determined. Losses in prestressing should be a minimum when prestressing is applied during that period when the slab has a tendency to contract and when most of the friction resistance of the base is dissipated by the restrained volumetric changes—in other words, at a time when the slab is as short as possible.

The preliminary friction tests, conducted before construction of the slab, obviously did not give the friction values to be expected under a 500 ft long pavement strip.

After preliminary observation, a detailed test program was set up to study the development of prestressing from December, 1954, to May, 1955. The slab was stressed and released several times and numerous strain meter readings were made before and after each of these operations. The mean values of these readings were used and seemed to be satisfactorily indicative.

Results indicate low losses in each case from December to April. In most of the cases it is fairly safe to assume that, with the assistance of low temperatures, prestressing was developed practically without loss.

This condition changed considerably after April, when increasing temperatures caused expansion of the slab and counteracted to a degree free development of prestressing forces. This was clearly indicated when the slab was released from 600 to 0 psi and then restressed to 690 psi. During the release there seemed to be no residual compression left at the interior stations. Strain indications at these stations were less, however, when the slab was prestressed, in which case strains were some 20 to 25 percent lower than the values registered at the end. By extrapolation these values indicate a loss of 30 percent at the center of the 500 ft long slab which would amount to 175 psi and give a friction coefficient somewhat lower than 0.7.

The final tests were made to determine the effect of repeated prestressing. The release of May 1, 1955, indicated a residual compression of 280 psi at the center of the slab. After the repeated prestressing performed on May 4, the measured strains indicated an additional 510 psi compression at the center. Since the total of these stresses amounts to 790 psi, which is more than the introduced 690 psi prestressing, it must be assumed that the residual compression of 280 psi decreased somewhat during the 3-day interval.

Results of these tests indicate clearly, however, that by repetition the efficiency of prestressing can be increased considerably.

The test indicated also that there is no constant factor which can express the prestressing losses with a friction coefficient at a given time. The maximum measured value of 0.7 seems to be a safe limit, but it is believed that by introducing prestressing when the volumetric changes have a tendency to produce contraction in the pavement, this friction coefficient can be reduced considerably. It is believed also that for future use a friction coefficient of 0.5 should be used and the prestressing repeated several times to increase the efficient development of prestressing in the pavement with a minimum of loss.

A much more evident effect of the development of prestressing forces was demonstrated at the two shrinkage cracks. These cracks opened up somewhat more than 1/16 in. before the first prestressing but closed gradually as prestressing was applied. These cracks remained tight and hardly visible for the entire time the first prestressing was in effect. The cracks opened up after the first release, but closed again as soon as prestressing was again applied. Some spalling around the irregular edges was observed after this second prestressing.

The actual length variation of the slab was determined from strain measurements. These readings were not continuous and did not coincide with extreme conditions. It is believed, however, that the weighted average of these readings gives a fairly accurate picture of the over-all length changes of the slab during the various test periods. The maximum measured shortening of the slab occurred in December, 1954, when the slab was prestressed to 300 psi. At that time, the slab shortened 2.6 in. The mean temperature measured in the slab at that time was 27 F compared with the original temperature of 75 F at the beginning of strain measurements.

LOAD TESTS

Summary

A total of 29 load tests were performed on the test slab. These tests were made under different conditions, varying the amount of prestressing, plate size, and location. The tests are summarized in Table 3.

Most of the tests were performed at the centers of the two load test areas A_1 and A_3, where the strain and pressure meters were concentrated. It was obvious that the narrow width of the slab, with unrestrained edges, would not produce the exact conditions to be found in airfield pavements. Still, the geometry of the slab was such that the deflection would approximate that of a slab infinite in both directions. Some tests were made on the edges of the slab, and to determine the effects of cracking, the load-carrying capacity of the slab was investigated at the two shrinkage cracks.

The diameter of plates with which the loads were applied varied between 2 and 20 in. The amount of transverse and longitudinal prestressing available in the slab was also subject to variation during the tests. During these load tests, deflections were measured close to the plate on which the load was applied. During load tests performed at the two load test areas, readings were made on the strain and pressure meters as well.

Load tests on interior of slab

The first seven load tests were performed on test areas A_1 and A_3 with varying amounts of prestressing and sizes of plate (Table 3). Results of these tests were in close agreement and no indication could be found as to the effect of plate size or amount of available prestressing on deflections. The conclusion from these tests was that the then available load of 100,000 lb was much below the actual load-carrying capacity of the slab. Therefore, a 100,000-lb load was applied on a 3-in. plate (test No. 11) and then on a 2-in. plate (test No. 12). Both these tests were made at station 1+43 where 300 psi longitudinal, and no transverse, prestressing was available. These tests were in close agreement and produced considerably higher deflections than those measured previously. However, they further proved the high moment and shear resistance of the slab because the applied load was high and was applied on small areas with concentrations of 14,000 and 30,000 psi. The only visible sign left on the slab after these tests was a small imprint about ⅛ in. deep under the 2-in. plate.

The actual effect of these loads was observed several months later when a longitudinal crack was observed on both sides of the point of load application. It is likely that this was the result of initial cracking on the bottom of the slab, which worked its way through the entire section as a result of cyclical volumetric changes (Fig. 9).

After new loading equipment of 200,000-lb capacity became available, four load tests were performed (tests No. 15, 17, 18, and 21).

The transverse deflection profile of the slab was quite different for the two tests made without prestressing. At station 3+60 where no transverse reinforcing was

TABLE 3—SUMMARY OF LOAD TESTS

	TEST NUMBER	DATE	LOCATION	APPLIED LOAD WITH INCREMENT (KIPS)	PLATE	PRESTRESSING IN SLAB (KIPS)		MAXIMUM DEFLECTION (INCHES)	MAXIMUM "k" Psi per in.
						LONGITUDINAL STRANDS	TRANSVERSE STRANDS		
LOAD APPLIED AT INTERIOR OF SLAB	1	10-20-53	A_3	10-20-30-40-50	20"	550	200	.036	–
	3	12-17-53	A_3	20-35-50-75-100	20"	250	200	.063	–
	4	12-18-53	A_3	10-20-30-40-50	8"	250	200	.032	270
	5	4-27-54	A_3	25-50-75-100	8"	250	200	.063	420
	2	11-17-53	A_1	10-20-30-40-50	20"	550	200	.030	–
	6	4-28-54	A_3	12^5-25-37^5-50-62^5-75-87^5-100	20"	250	200	.055	–
	7	4-28-54	A_1	25-50-75-100	8"	250	200	.053	420
	11	4-29-54	STA. 1+43	10-20-30-40-50-60-70-80-90-100	3"	300	0	.088	–
	12	4-29-54	STA. 1+43	50-60-70-80-90-100	2"	300	0	.076	–
	13	4-30-54	STA. 1+43	10-20-30-40-50-60	2"	300	0	.045	–
	15	12-8-54	A_1	50-100-125-150-182-200	20"	250	240	.157	280
	17	12-10-54	A_3	50-75-100-125-150-175-189	8"	250	240	~.150	400
	18	2-1-55	STA. 3+60	50-100-150-185	20"	0	0	~.459	–
	21	2-3-55	STA. 0+83	100-125-150-175	20"	0	0	.282	–
	22	3-29-55	A_1	200 (8 TIMES)	20"	280	240	.200	250
	23	3-30-55	STA. 3+94	200 (12 TIMES)	20"	280	240	.287	–
	24	4-19-55	STA. 3+94	200 (18 TIMES)	20"	600	240	.234	–
	26	4-20-55	A_1	200 (10 TIMES)	20"	600	240	.157	–
	29	4-20-55	A_1	50-100-150-200	8"	600	240	.177	–
	27	4-20-55	A_1	50-100-150-200	20"	600	240	.154	450
AT SHRINKAGE CRACKS	8	4-28-54	STA. 1+65	12^5-25-37^5-50-62^5-75-87^5-100	8"	300	0	.103	–
	9	4-29-54	STA. 1+65	12^5-25-37^5-50-62^5-75-87^5-100	8"	300	0	.086	–
	10	4-29-54	STA. 1+65	12^5-25-37^5-50-62^5-75-87^5-100	8"	300	0	.091	–
	16	12-9-54	STA. 1+65	50-75-100-125-150-175-200	20"	250	0	.288	–
	20	2-2-55	STA. 1+19.875	25-50-75-100-125-150-180	20"	0	0	.262	–
EDGE LOADING	14	4-30-54	STA. 1+45	20-40-60-80-95	8"	300	0	~.250	–
	19	2-1-55	STA. 3+60	25-37^5-50-100	8"	0	0	.192	–
	25	4-19-55	STA. 3+94	50-75-100-125-130	8"	600	240	~.177	–
	28	4-20-55	STA. 1+00	50-100-132	8"	600	240	249	–

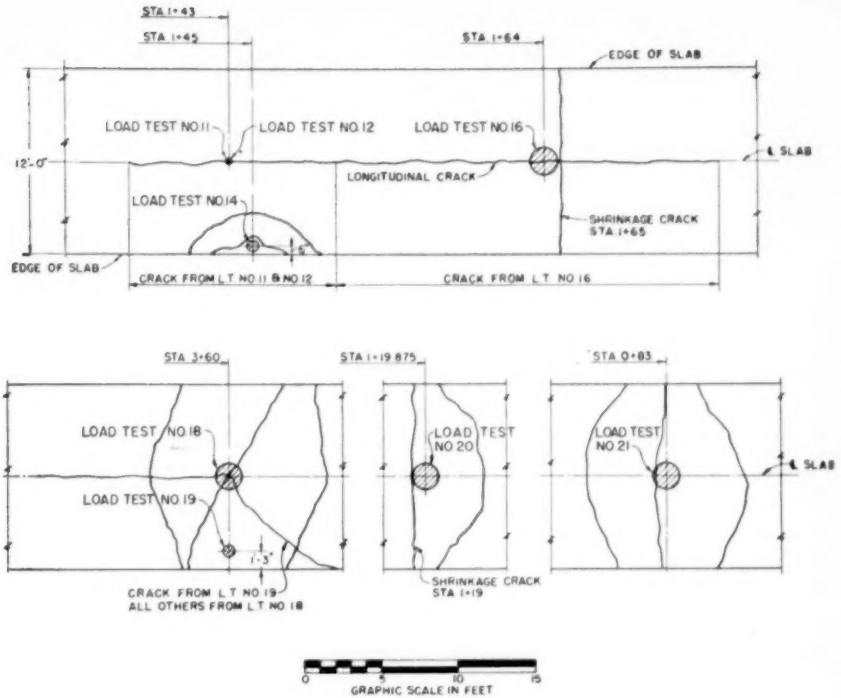

Fig. 9—Load test crack pattern

available, deflections increased suddenly between loads of 100,000 and 150,000 lb. Furthermore, characteristics of the deflection curves changed, showing a tendency to uplift at the edges after the load exceeded 100,000 lb. This can be expected if it is understood that the first cracking in the slab took place in the form of a longitudinal crack on the bottom of the slab. Such cracking probably developed at station 0+83 also, but there transverse reinforcement offered sufficient resistance against the increase of this crack and thereby reduced deflections. In both tests similar cracks were observed on the surface at a load of about 180,000 lb. (Fig. 9).

The presence of transverse reinforcement proved to be definitely beneficial. Although it was impossible to establish how much it added to the load-carrying capacity, measured deflections under the same load were sufficiently indicative.

The 200,000-lb load did not prove to be sufficient to produce moment failure in the prestressed slab. Load tests No. 15 and 17, performed with 300 psi longitudinal and 240 psi transverse prestressing, resulted in comparable deflections, even though the first was made with a 20-in. and the second with an 8-in. plate.

The fact that during test No. 17 the plate punched through the slab under a load of 189,000 lb should not be misleading. This is by no means an indication of the strength of the slab, because failure occurred by shear under an extremely high concentration of load, close to 4000 psi, at a location where the concrete section had been considerably weakened by the inserted strain and pressure meters. The fact that the concrete strength at this station was somewhat lower than that of the concrete at test area A_1, and that the latter test area had transverse reinforcement, should be considered also.

The rate of measured deflection at the test areas where two-way prestressing was available can be compared favorably with that measured under loads at stations without prestressing. Such comparison indicates that the prestressed slab deflected under a maximum load of 200,000 lb in a manner similar to the slab without prestressing under a load of 80,000 lb (Fig. 10).

Based on the deflection characteristics of the slab without prestressing it could be predicted that the prestressed slab would not fail under a load less than 350,000 lb. This assumption does not take into full consideration the considerable strength margin usually observed in prestressed concrete members, but anticipates large deflection without excessive local stresses. It is believed, furthermore, that the full advantage of prestressed concrete pavements could be utilized by allowing temporary cracking of the concrete sections. Such cracking would produce only temporary discontinuity of the pavement, and the integrity of the slab would be restored after the removal of excessive loads, by virtue of its inherent compressive energy.

A remarkable phenomenon observed during these tests was the high recovering ability of the prestressed slab after the maximum applied loads were removed. In-

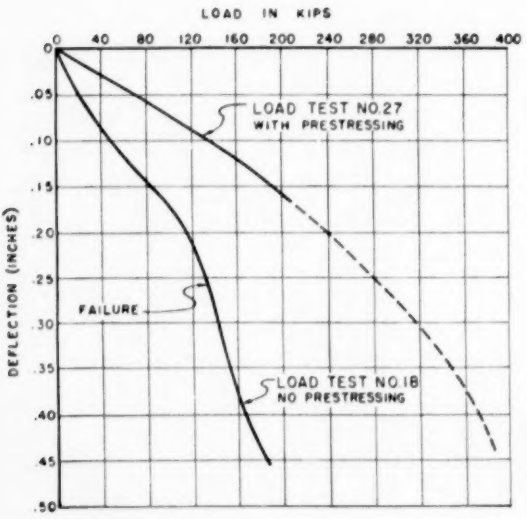

Fig. 10—Deflection versus load, with and without prestressing

stantaneous recovery, after removal of loads, was never less than 85 percent and occurred despite that fact that the subbase could not recover within the range of observed deflections.

Since it was considered impractical to obtain loading equipment with a capacity of 300,000 to 400,000 lb, the last series of load tests was made with the maximum available load of 200,000 lb, applying this load in short cycles and measuring deflections for each cycle (load tests No. 22, 23, 24, and 26).

These tests, although they did not clarify the problems under investigation, did demonstrate the high load-carrying capacity of the slab and its recovering ability. No limiting conditions were reached which would have proved the effect of the 300 or 600 psi prestressing.

The last load test (No. 29) was performed on an 8-in. plate using the maximum available load of 200,000 lb. The slab carried this maximum load even with such increased concentration without any sign of deterioration. The measured maximum deflection, however, showed an increase as compared to that obtained under the same load but applied on a 20-in. plate.

Pressure meters installed at load test areas A_1 and A_3 were used to determine the base reaction and distribution under the loaded portion of the slab. With the known deflection contour for given loads, it was possible to establish the relation between pressure and deflection at various points in the test area. This relation, known as the K value (lb per sq in. per in. of deflection) or the supporting capacity of the base, proved to be variable and showed an increasing tendency, with increasing pressure in the higher range of deflections.

This finding indicated that the basic assumption used in the Westergaard theory concerning pressures as varying proportionally with the deflection is not applicable in this case.The explanation for this is that the assumption holds true only for a limited range of pressures. The actual behavior follows a more nearly logarithmic relation between pressure and voids ratio.

A typical case is shown in Fig. 11, load test No. 5, where the relation between deflection and pressure indicates a K of 80 in the deflection range of 0.01 to 0.02 in. and a considerably higher K of 420 for deflections exceeding 0.05 in. This demonstrates the increased compaction produced by the greater load on the base. Under these extreme deflection conditions total recovery of the base could not be expected, even though the slab itself indicated excellent performance. It was assumed that after the first excessive deflection and removal of the load a void remained between the base and the slab.

This assumption was proved later when a special load test (No. 27) was performed, applying the maximum load of 200,000 lb in several increments and measuring simultaneously the maximum deflections and maximum pressure adjacent to and directly under the load. The result of this test clearly indicated that there was no contact between the face of the pressure meter at the lower surface of the slab and the base until deflections reached 0.08 in. under an approximate load of 100,000 lb. At this point the initial K was 200 and increased to 450 under the maximum load of 200,000 lb and a deflection of 0.154 in. (Fig. 12).

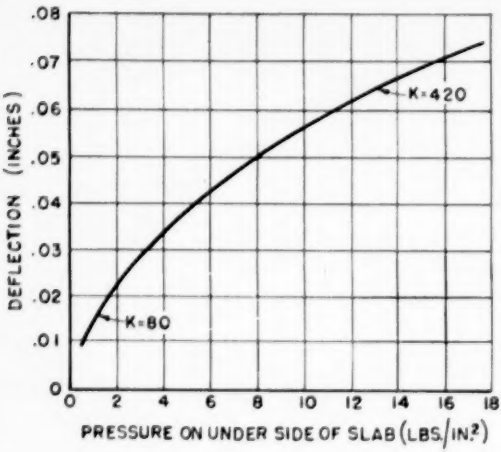

Fig. 11—Variation of K—Load test No. 5

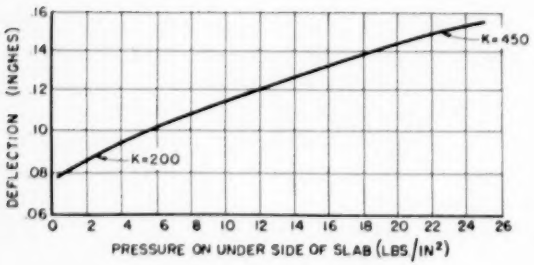

Fig. 12—Variation of K—Load test No. 27

Actual stress in the concrete section of the load test areas was measured with strain meters. Readings were made during various load tests. These measurements were used in comparison with deflection profiles, mainly to determine maximum stresses in the concrete. They indicated also the point at which cracking occurred in the concrete sections.

Due to deformation of the slab in the loaded area, some restraining movements can develop and may influence the readings considerably where the strains are low. Since many load tests were made on the two test areas, the increasing number of cracks progressively influenced the strain meter readings. For these reasons, strain meter readings were considered primarily as auxiliary measurements to compare the stresses derived from them with the deflection profiles.

Typical stress results, shown in Fig. 13, were observed during load test No. 6 on meters 3T and 4B. They indicate maximum concrete stresses of 660 to 680 psi. The maximum observed flexural stresses were in the same order as long as the concrete section proved to be homogeneous. Registration of higher real stresses became impossible because of the accompanying cracks which developed adjacent to or at the strain meters.

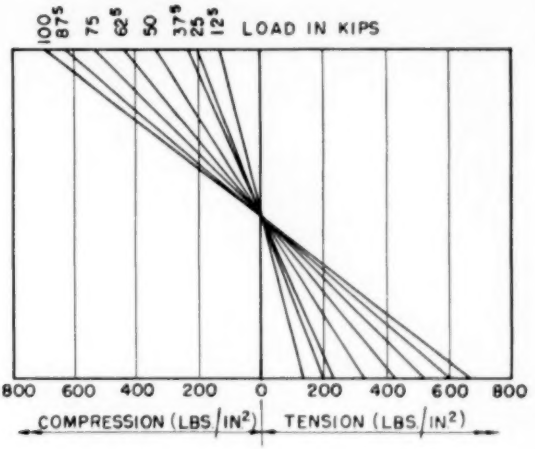

Fig. 13—Concrete stress—Load test No. 6

Load tests at shrinkage cracks

Five load tests were performed at the two shrinkage cracks. The first three tests, No. 8, 9 and 10, were performed at station 1+65 with an 8-in. plate, 300 psi longitudinal prestressing, and a maximum load of 100,000 lb. There was no indication during these tests of any shifting along the crack, and the crack seemed to behave as a hinge. The measured deflection showed little difference as a result of variation in plate location.

The fourth test (No. 16) was performed at the same location with a 20-in. plate, 250-psi longitudinal prestressing, and a maximum load of 200,000 lb. Deflections were sizable (Fig. 14), but even under such high loads no shifting could be observed through the cracks and the recovery in deflection immediately after removal of load was 86 percent.

An entirely different behavior of the crack was observed during load test No. 20, when the load was applied at station 1+19.875 without prestressing in the slab. The interlocking action of aggregates across the cracked section lost its effectiveness soon after the first load increment was applied. The loaded side of the slab behaved more like a free edge than part of a continuous slab. Shifting across the slab increased gradually with increase of the load and a crack finally occurred on the top of the slab, representing failure due to negative moment (Fig. 9). The deflections indicate clearly that cracking started after a load of 125,000 lb was applied (Fig. 15).

The tests demonstrated the beneficial effect of prestressing across a cracked section. The prestressing elements provided tension capacity which, together with the remaining concrete compression, formed a couple able to resist moments. Since such a section lost most of its rigidity after cracking, it allowed considerable deformation without increase in moments and behaved as a plastic hinge, leading to a

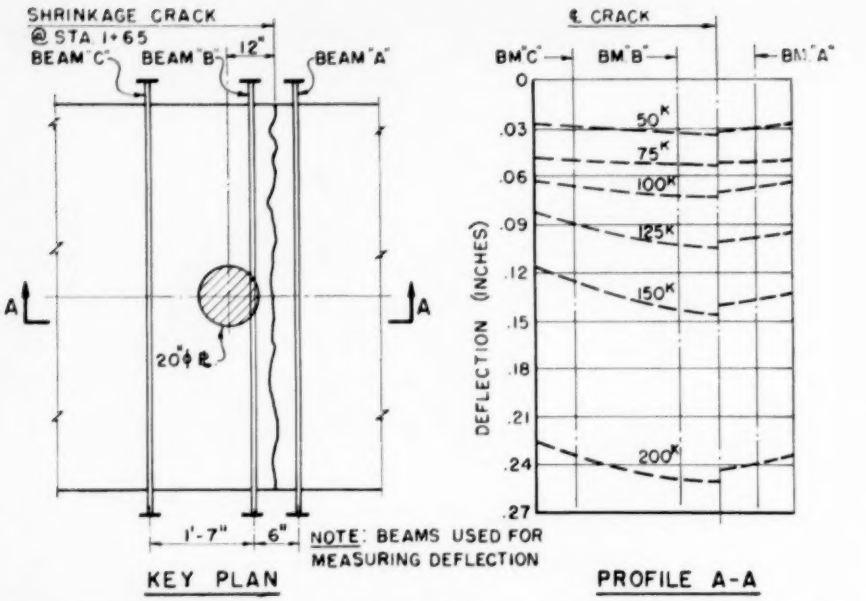

Fig. 14—Load test No. 16. Longitudinal prestressing = 250 psi. Transverse prestressing = 0 psi

redistribution of moments in a more efficient manner than that of an unreinforced concrete slab. The high recovering ability of such a cracked section with prestressing is also remarkable. It is unfortunate that no means were available to investigate the ultimate load carrying capacity of such a cracked section with prestressing.

Load tests at edge of slab

Four load tests were performed at the edge of the slab; in each case the load was applied with an 8-in. plate.

The first test (No. 14) was performed at station 1+45, where no transverse prestressing was available, but the slab was compressed longitudinally only to approximately 300 psi. Failure occurred after the load exceeded 75,000 lb. The crack which was observed on the top of the slab (Fig. 9) justified the theory that longitudinal prestressing increases the load-carrying capacity of a narrow strip even at the edges. This theory was further justified when no transverse cracking developed at the bottom of the slab under the applied load.

Unfortunately, the edge load test (No. 19) made on the slab at station 3+60, when there was no prestressing applied, proved to be inconclusive because cracking developed at adjacent sections as the result of another load test made at the

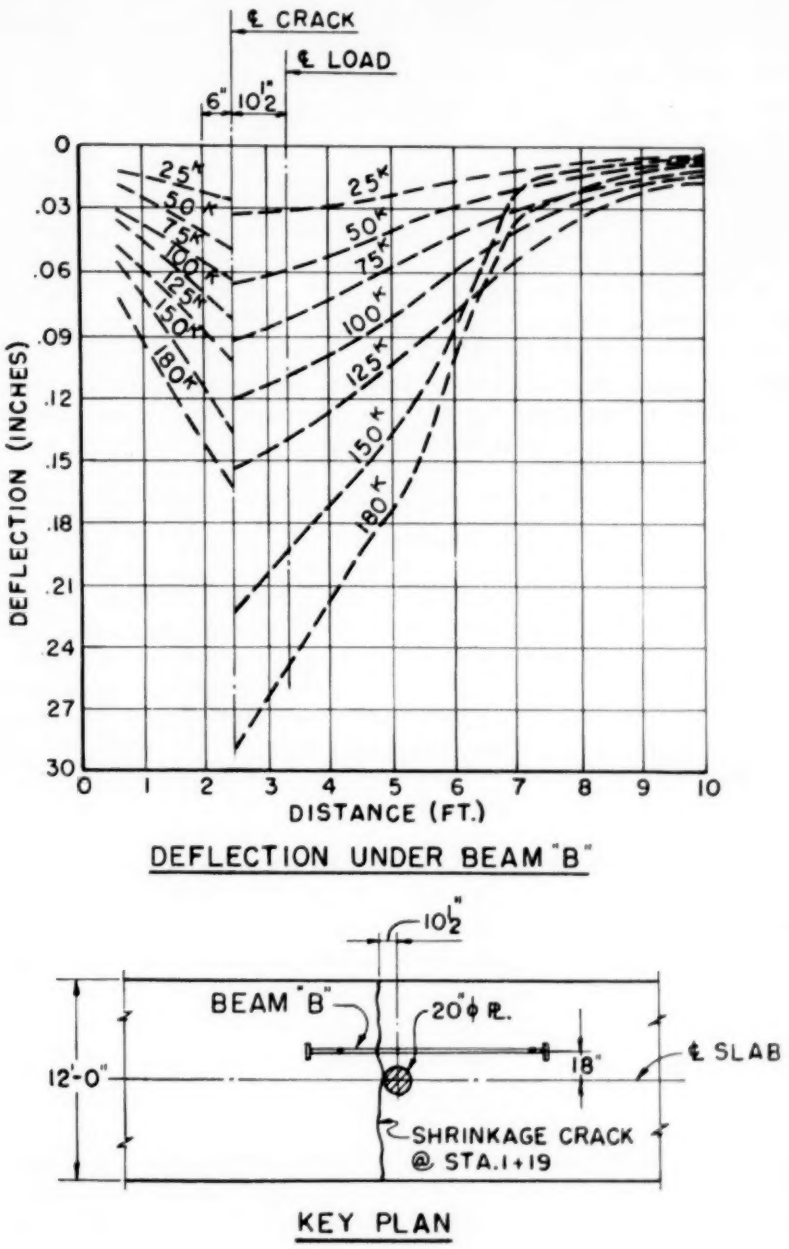

Fig. 15—Load test No. 20; no prestressing in slab

center of the slab at the same station. Since edge conditions were not of primary interest in the test program, the repetition of this test, which would have involved the complicated relocation of the loading rig, was omitted.

The other two edge load tests (No. 25 and 28) were performed at test areas A_1 and A_2, respectively, with 600 psi longitudinal and 240 psi transverse prestressing. Shear failure developed during test No. 25 at a load of 125,000 lb and measured deflection of 0.17 in. To that point deflections and loads had increased proportionally. No failure was observed during load test No. 28 when the maximum available load of 132,000 lb was applied. Measured deflection under this load was about 0.25 in. and showed a rapidly increasing tendency, which would indicate near cracking and possible failure. Unfortunately the available load was not sufficient to produce failure and permit investigating limit conditions for edge loadings.

The three tests indicate that prestressing is beneficial in resisting edge loads applied on narrow strips of pavements, even when prestressing is applied in one direction only. Prestressing applied in two directions greatly increased the load-carrying capacity of the edge.

HEAT TEST

The effect on the slab of heat and blast from jet planes was tested using the after burners of the plane (Chance Vought Aircraft—F7U-3, type a/c) for 10 sec in nine and five consecutive cycles. Maximum temperatures measured by thermocouples placed ¼ in. below the top surface of the slab were close to 600 F, somewhat higher than the maximum temperatures given by the manufacturer's jet wake profile. Temperatures close to the bottom at the same location did not exceed 100 F. The temperature gradient between these two points had a rapid decrease and it is believed that under the test condition maximum temperatures at the center of the slab were about 125 F.

The prestressing strands are said by the manufacturer to maintain their maximum design strengths under temperatures up to 600 F. Consequently, the test results would indicate that with ½ in. of concrete cover, adequate protection can be afforded to protect the prestressing tendons from the detrimental effect of excessive heat.

CONCLUSIONS

Construction

Construction of the test slab pointed to problems which must be overcome to make this type of construction competitive with present conventional methods. If post-tensioning is to be used, tendons should be delivered to the construction site with adequate wrapping or tubing. Presently available sheet-metal tubing seems to be a satisfactory solution. No attempt was made to prove the advantage in using pre- or post-tensioning of tendons for such construction.

Materials

All materials used for the test slab proved to be satisfactory. The friction-reducing layer used proved to be easy to install, economical, and performed as expected.

Prestressing operation

The considerable elongations of the tendons warrant the use of special equipment. A proper sequence in stressing the elements from both ends should be established to secure uniform distribution of stresses throughout the entire length of the tendons.

Load on strands

Losses in post-tensioning during the jacking operation can be kept to a minimum if tendon conduits can be kept fairly straight. Losses after prestressing should not be excessive, and should not exceed 10 percent for conditions as used in the test slab.

Development of prestressing in the slab; base friction

Efficient development of prestressing forces depends primarily on the effectiveness of the friction reducing layer. For layers similar to that used, a friction coefficient of 0.5 can be assumed. Base friction conditions under the slab are affected by numerous factors of which the tendency toward volumetric change in the concrete itself is the most important.

Repeated prestressing seems to be beneficial in developing the prestressing loads uniformly along the entire length of the slab.

Load-carrying capacity

The tests proved that the slab had a load-carrying capacity well beyond normal design practice. Deflections which correspond to ultimate conditions are so excessive that great deflections in the base, not permissible in conventional practice, may take place without detriment to the structural elements.

No moment failure could be obtained at intermediate points with loads up to 200,000 lb when the slab was prestressed. The indication is that the slab could resist loads up to 350,000 lb.

The slab showed superior behavior under loads placed at shrinkage cracks and at the edges.

The load tests were not conclusive as to the effect of varying the amount of prestressing and positioning of the tendons. It is believed that a minimum of 100 psi should be provided in the slab in addition to the stresses which may be dissipated by base friction. Actual positioning of tendons seemed to be satisfactory from both the theoretical and practical viewpoints.

Heat tests

Results of the heat test indicate that the tendons as positioned in the slab would not be subject to detrimental temperatures due to jet blasts.

ACKNOWLEDGMENT

The project was sponsored by the Bureau of Yards and Docks, Department of the Navy, for which H. H. Dutton acted as project manager. L. A. Palmer, consultant to the Bureau, supervised all technical problems in connection with the planning and execution of the test program.

Cdr. J. S. Marsh, P.W.O. at Patuxent River Naval Air Station, acted as officer in charge of construction. Ayer-Hagan-Booth were the contractors for the test slab. Testing of the concrete was performed by Froehling & Robertson Laboratories, Richmond, Va. Raymond E. Davis and David Pirtz, University of California, Berkeley, acted as special consultants during the planning and installation of the instrumentation.

The late G. M. Hilpert, associated at that time with Frederic R. Harris, Inc., initiated this project and deserves much of the credit. Design of the test slab and the entire test program was completed by Frederic R. Harris, Inc., Consulting Engineers, for which the writer acted as project engineer, assisted by S. Sedlmaier.

For such discussion of this paper as may develop please see Part 2, December 1957 *Journal*. In *Proceedings* V. 53 discussion immediately follows the June 1957 *Journal* pages.

Title No. 53-4

Earthquake Resistant Design Based on Dynamic Properties of Earthquakes*

By G. W. HOUSNER†

SYNOPSIS

A method of earthquake resistant design is proposed that takes into account the dynamic properties of earthquake ground motion and the dynamic properties of the structure. The method is applied to reinforced concrete cantilever chimneys and by appropriate simplifications the method is made sufficiently simple to be usable in ordinary design practice. The bending moments and shears given by this method differ markedly from those given by the percent g method of design. In particular, they give more economical designs for tall, flexible chimneys.

INTRODUCTION

Building codes in active seismic regions usually specify that structures be designed to resist certain static lateral forces. Sometimes the lateral forces are specified to be a constant percentage of the weight of the structure (percent g), which is strictly correct only if the structure is rigid. At other times some allowance is made for the dynamic properties of the structures; for example, by specifying smaller lateral forces for tall buildings than for short buildings or by specifying a percent g factor that is variable over the height of building. The lateral forces specified by the codes are not intended to represent the actual forces that might be acting during an earthquake, but rather are intended to provide strength adequate to withstand the deformation produced by strong ground motion. The rather limited experience obtained during strong earthquakes with structures designed by these methods indicates that the behavior of ordinary structures is satisfactory but that a more detailed dynamic analysis is desirable for extraordinary structures. The particular structure with which this paper is concerned is the reinforced concrete cantilevered chimney, but it will be seen that the same method of analysis and design can be applied to structures of other types.

A thorough analysis of the behavior of a cantilever chimney during an earthquake requires that it be treated as a vibration problem in which the motion of the ground excites the structure into oscillation. Since the precise characteristics

*Presented at the ACI Seventh Regional Meeting, Los Angeles, Calif., Oct. 29, 1954. Title No. 53-4 is a part of copyrighted JOURNAL OF THE AMERICAN CONCRETE INSTITUTE, V. 28, No. 1, July 1956, *Proceedings* V. 53. Separate prints are available at 50 cents each. **Discussion** (copies in **triplicate**) should reach the Institute not later than Nov. 1, 1956. Address 18263 W. McNichols Rd., Detroit 19, Mich.

†Professor of Civil Engineering, California Institute of Technology, Pasadena, Calif.

of a future earthquake cannot be known at the time a structure is designed, it is necessary to rely on the instrumental recordings of past earthquakes. However, studies[1] have shown that the ground motions of past earthquakes fall into a definite pattern and there seems to be no reason why future earthquakes should differ radically.

When analyzing a proposed structure one could compute the stresses and deformations induced if the structure were subjected to the ground motion recorded during past earthquakes. For most structures, at least those that have several modes of vibration, such an analysis would be time consuming and does not seem feasible for normal design procedure unless the proposed structure was very special. What is desirable is a method of design that takes into account all of the pertinent facts but which, even at the sacrifice of some accuracy, is sufficiently simple and straightforward for normal design procedures. Such a method must give approximately the same factor of safety for different structures and the same factor of safety for different parts of the same structure. In the case of the concrete chimney this requires that a 300-ft high chimney have the same factor of safety as one only 50 ft high; that a 30-ft diameter chimney have the same factor of safety as one of 10-ft diameter; that a chimney of 24-in. wall thickness have the same factor of safety as one of 10-in. wall thickness; and that the factor of safety at midheight be the same as that at the base.

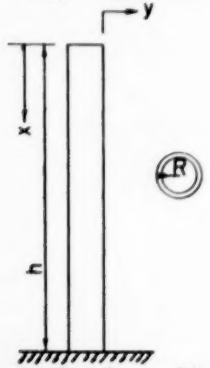

Fig. 1—Cantilever chimney

The proposed method of design achieves this; however, because of the simplifications introduced there is some loss of accuracy.

CANTILEVER CHIMNEY, RIGIDLY FIXED AT BASE

If a cantilever chimney of uniform cross section, as shown in Fig. 1, has its base subjected to horizontal ground motion, it is well known[2] that the displacement at any point can be computed from the expression

$$y = \sum_n \frac{1}{p_n} F_n \int_0^T a e^{-c_n(T-t)} \sin p_n(T-t)dt \quad \ldots\ldots (1)$$

where

y = lateral displacement at time T

$F_n = F_n\left(\frac{\alpha_n x}{h}\right)$ = function giving shape of nth mode

x = coordinate measured along the axis
α_n = dimensionless number, $\alpha_1 = 1.88$; $\alpha_2 = 4.69$; $\alpha_3 = 7.85$

$p_n = \alpha_n^2 \sqrt{\frac{EI}{\rho h^4}}$, for small damping

E = Young's modulus
I = moment of inertia
h = height of chimney
ρ = mass per unit length
a = ground acceleration
c_n = damping factor (viscous damping)

If the ground acceleration a is that recorded during an earthquake, Eq. (1) can be used to compute the motion of the chimney, and the shear and bending moment can be computed by taking the appropriate derivatives:

$$M = EI \frac{\partial^2 y}{\partial x^2} = \sqrt{\rho EI} \sum_n F_n'' \int_0^T a e^{-c_n(T-t)} \sin p_n(T-t) dt \quad (2)$$

$$V = EI \frac{\partial^3 y}{\partial x^3} = \frac{\sqrt{\rho EI}}{h} \sum_n \alpha_n F_n''' \int_0^T a e^{-c_n(T-t)} \sin p_n(T-t) dt \quad (3)$$

Numerical computations using the preceding equations would be lengthy so that the following simplifications are introduced. It will be noted that each term of each of the equations contains the expression

$$\int_0^T a e^{-c_n(T-t)} \sin p_n(T-t) dt \quad (4)$$

Anaylsis of strong-motion earthquake records[1] shows that the maximum value of this integral, for moderate damping can be approximated by the following expression

$$A_n(1 - e^{-2T_n}) \quad (5)$$

where

T_n = period of vibration = $\frac{2\pi}{p_n}$
A_n = coefficient depending on intensity of ground motion and damping

Fig. 2 and 3 show a comparison of Eq. (5) with values computed from recorded ground motion.

If Eq. (5) is used in Eq. (2) and (3) instead of Eq. (4) it is equivalent to adding the maximum values of the modes of vibration. The effect of using Eq. (5) is thus to overestimate somewhat the probable stresses and displacements and properly a factor should be introduced to allow for this. However, an arbitrary factor must be chosen anyway to establish the intensity of ground motion to be used in the design and this can be adjusted to take care of the overestimation. The important point to note is that the use of Eq. (5) affects all chimneys

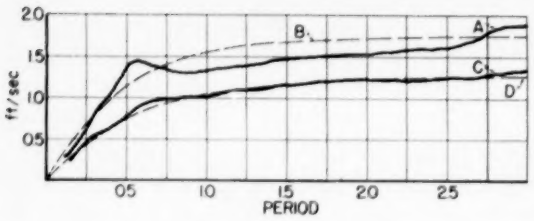

Fig. 2—Maximum value of Eq. (4) evaluated for the N-S component of ground motion of the El Centro earthquake of May 18, 1940. Curve A is for 20 percent of critical damping, curve C is for 40 percent of critical damping, B and D are Eq. (5) fitted to the curves

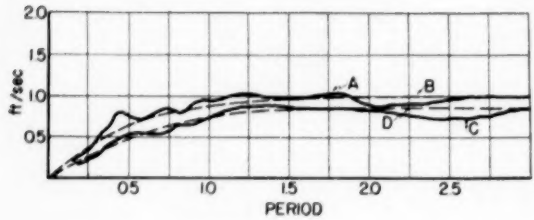

Fig. 3—Maximum value of Eq. (4) evaluated for the S69E component of the July 21, 1952, Tehachapi earthquake. Curve A is for 10 percent and curve C is for 20 percent of critical damping, B and D are Eq. (5) fitted to the curves

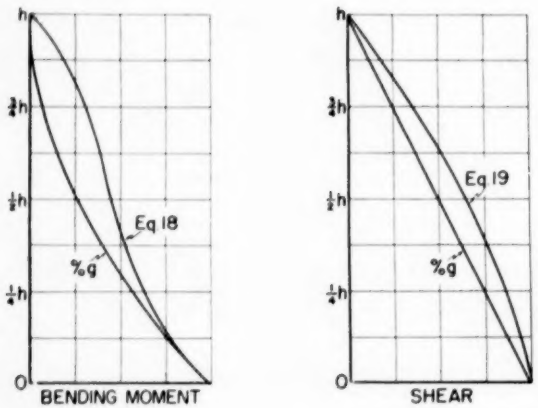

Fig. 4—Comparison of shapes of bending moment and shear diagrams given by Eq. (18) and (19) and those given by the percent g method

in a similar fashion and does not affect the relative factors of safety. The bending moment and shear may thus be written

$$M = \sqrt{\rho EI} \sum_n F_n''[A_n(1 - e^{-\pi T_n})] \quad (6)$$

$$V = \frac{\sqrt{\rho EI}}{h} \sum_n \alpha_n F_n'''[A_n(1 - e^{-\pi T_n})] \quad (7)$$

Tests on a concrete building [3] indicate that the fraction of critcal damping is dependent on the internal damping of the concrete and is essentially independent of the frequency of vibration. The A_n may thus be taken the same for each mode of vibration. The period T_n is larger for the higher modes and therefore if T_n is set equal to T_1 the effect of the higher modes is somewhat overestimated. Keeping this in mind, the approximate expressions for the bending moment and shear are:

$$M = [A(1 - e^{-2T_1})] \sqrt{\rho EI} \sum_n F_n'' \quad (8)$$

$$V = [A(1 - e^{-2T_1})] \frac{\sqrt{\rho EI}}{h} \sum_n \alpha_n F_n''' \quad (9)$$

It will be noted that each of these expressions is composed of three factors, the first giving the influence of the ground motion, the second giving the influence of the physical properties of the chimney, and the last giving the shape of the bending and shear diagrams. When these last factors are evaluated for the first three modes of vibration* and allowance is made for the overestimation of the higher modes, the results can be represented by the following expressions:

$$\sum_n F_n'' = B_1 \left[0.6 \left(\frac{x}{h} \right)^3 + 0.4 \left(\frac{x}{h} \right)^4 \right] \quad (10)$$

$$\sum_n \alpha_n F_n''' = B_2 \left[\frac{5}{3} \frac{x}{h} - \frac{2}{3} \left(\frac{x}{h} \right)^3 \right] \quad (11)$$

These shapes are only approximate and tend to overestimate the influence of the higher modes for the more rigid chimneys.

APPLICATION TO DESIGN

The expressions for shear and bending moment can be written

$$M = D_1(1 - e^{-2T_1}) \sqrt{\rho EI} \left[0.6 \left(\frac{x}{h} \right)^3 + 0.4 \left(\frac{x}{h} \right)^4 \right] \quad (12)$$

$$V = D_2(1 - e^{-2T_1}) \frac{\sqrt{\rho EI}}{h} \left[\frac{5}{3} \frac{x}{h} - \frac{2}{3} \left(\frac{x}{h} \right)^3 \right] \quad (13)$$

where the factors D_1 and D_2 contain the effect of the damping and the intensity of the ground motion. For a circular chimney of centerline radius R it may be verified that for $E = 3 \times 10^6$ psi

$$2T_1 = \frac{4\pi}{p_n} = \frac{5}{9500} \frac{h^2}{R}$$

*The details of this calculation are given in the appendix.

which for convenience may be approximated by

$$2T_1 = \left(\frac{h}{h_o}\right)^2 \frac{R_o}{R} \qquad (14)$$

$h_o = 100$ ft
$R_o = 5$ ft

Also

$$\sqrt{\rho EI} = \sqrt{\left(\frac{\gamma}{g} 2\pi Rt\right) E(\pi R^3 t)}$$

where t is the wall thickness and γ is the weight per cu ft of concrete.* This may be written

$$\sqrt{\rho EI} = 2\frac{w}{g} \pi R^2 t \sqrt{\frac{gE}{2\gamma}} = \rho R \sqrt{\frac{gE}{2\gamma}} \qquad (15)$$

Since E, g, γ are essentially the same for all chimneys the factor

$$\frac{\sqrt{gE}}{2\gamma}$$

may be lumped with the factors D_1 and D_2 to obtain

$$M = C_1 wR\left(1 - e^{-\left(\frac{h}{h_o}\right)^2 \left(\frac{R_o}{R}\right)}\right)\left(0.6\left(\frac{x}{h}\right)^4 + 0.4\left(\frac{x}{h}\right)^6\right) \qquad (16)$$

$$V = C_2 \frac{wR}{h}\left(1 - e^{-\left(\frac{h}{h_o}\right)^2 \left(\frac{R_o}{R}\right)}\right)\left(\frac{5}{3}\frac{x}{h} - \frac{2}{3}\left(\frac{x}{h}\right)^3\right) \qquad (17)$$

where w is the weight per ft.

If the coefficients C_1 and C_2 are evaluated from the preceding analysis for 10 percent of critical damping, for the two components of recorded ground motion of the El Centro, Calif., December, 1934; El Centro, May, 1940; Olympia, Wash., April, 1949; and Arvin-Tehachapi, Calif., July, 1952, earthquakes, which are the strongest recorded ground motions, one obtains values for the coefficients as follows:

$$600 < C_1 < 1200$$
$$1400 < C_2 < 2800$$

However, these values apply to rigidly built-in cantilevers and in actual practice the base of a chimney is not absolutely rigid and the precise value of damping that a chimney may have during an earthquake is not known either. If the coefficients are evaluated so that the moment and shear at the base are equal to those produced by the above earthquakes in the first mode of vibration only, one obtains

$$200 < C_1 < 400$$
$$400 < C_2 < 800$$

*If the chimney has a lining, γ should be taken to be the total weight per sq ft. of concrete plus lining, divided by the thickness of concrete.

Properly, the values of C_1 and C_2 to be used should be established on the basis of tests and observations of existing structures. Unfortunately, there is little of such information available. It appears that the next best procedure is to utilize the fact that structures similar to short rigid chimneys designed for 20 percent g load have withstood strong earthquake motion satisfactorily, and to determine the C_1 and C_2 so as to give the same factor of safety as is obtained by designing short, rigid chimneys for 20 percent g.

Values of C_1 and C_2 can be deduced by noting that for short, rigid chimneys (h/r_0) the preceding equations give for the moment and shear at the base

$$M = C_1 w \frac{h^2}{h_0^2} R_0 = k \frac{wh^2}{2} \qquad (k = 2C_1 R_0/h_0^2)$$

$$V = C_2 w \frac{h}{h_0^2} R_0 = kwh \qquad (k = C_2 R_0/h_0^2)$$

The terms k $(wh^2/2)$ and kwh are the moment and shear at the base of a rigid chimney where k is the fraction of g of horizontal acceleration. Corresponding to $k = 0.2$ the factors C_1 and C_2 are: $C_1 = 200$ and $C_2 = 400$. With these values Eq. (16) and (17) can be written in the form

$$M = (0.2A)\frac{wh^2}{2}\left[0.6\left(\frac{x}{h}\right)^4 + 0.4\left(\frac{x}{h}\right)^4\right] \qquad (18)$$

$$V = (0.2A)wh\left[\frac{5}{3}\left(\frac{x}{h}\right) - \frac{2}{3}\left(\frac{x}{h}\right)^3\right] \qquad (19)$$

where

$$A = \frac{1 - e^{-b}}{b}$$

$$b = \left(\frac{h}{h_0}\right)^2\left(\frac{R}{R_0}\right)$$

$h_0 = 100$ ft
$R_0 = 5$ ft
h = height of chimney
R = centerline radius
x = distance from top of chimney

These equations may be interpreted as follows. The term $0.2A$ represents the lateral load factor; for an extremely rigid chimney $A = 1$, and the factor corresponds to a lateral force produced by an acceleration of $0.2g$. The factor A represents the influence of the physical characteristics of the chimney upon its response to the ground motion; the magnitude of A decreases for more flexible structures. The factors $wh^2/2$ and wh are the bending moment and the shear at the base and the expressions within the brackets give the shapes of the bending moment and shear diagrams.

These equations give design bending moments and shears which take into account the characteristics of recorded strong-motion earthquakes, and also take into account the effect of the physical properties of the chimney on its response to the ground motion. The shapes of the bending and shear diagrams given by Eq. (18) and (19) are the approximate envelopes of maximum shear and bending during an earthquake. To show how these equations compare with the moments and shears given by a uniform, static, lateral load, Fig. 4 to 8 have been prepared. Fig. 4 compares the bending and shear diagrams and to make the comparison of shapes clear the moment and shear at the base are taken to be the same for both methods. It is seen that Eq. (18) and (19) give larger bending moments and shears at the midheight than are given by the percent g method of design. It can thus be concluded that the percent g method will under-design the middle region of the chimney as compared to the base and it can be expected that chimneys designed by that method will have a tendency to fail in the middle portion. Such failures were observed following the Tokyo earthquake of 1923. Mononobe[4] reported the locations of the points of failure of 115 concrete and brick chimneys. His findings are given in Table 1 where it is seen that 60 percent of the failures were above the third-point.

TABLE 1—LOCATION OF POINTS OF FAILURE OF 115 CHIMNEYS

Location	No.
h-0.9h	5
0.9h-0.8h	10
0.8h-0.7h	13
0.7h-0.6h	12
0.6h-0.5h	11
0.5h-0.4h	11
0.4h-0.3h	11
0.3h-0.2h	8
0.2h-0.1h	14
0.1h- 0	20

Fig. 5 and 6 compare the bending moment and shear at the base of a 20-ft diameter chimney as computed by Eq. (18) and (19) and by the percent g method. It is seen that for a short rigid chimney, Eq. (18) gives bending moments that agree with the percent g method, but for taller, more flexible structures the bending moment appreciably is below that given by the percent g method, and for heights greater than 300 ft the bending moment remains constant. This limiting value of the bending moment is a consequence of the dynamic properties of cantilever beams. It does not mean that the motion excited by the earthquake is the same for all chimneys above 300 ft high, for if Eq. (1) is adjusted in the same fashion as Eq. (18), that is, to give the same maximum displacement at the top for a short

rigid chimney as produced by a 20 percent g load, the maximum displacement at the top is given by

$$y_{max} = \frac{2}{10}\frac{wh^4}{8EI}\frac{(1-e^{-b})}{b} \quad (20)$$

A plot of this equation for $R = 10$ ft is shown in Fig. 7 where it is seen that the displacement increases rapidly with the height and for $h > 300$ ft the displacement increases as h^2. Thus a 600 ft high chimney would experience displacements four times as great as a 300-ft chimney. However, a 600-ft chimney is more flexible than one 300 ft high, in fact the flexibility is just four times as great so that the bending moments associated with the displacements of the 600-ft chimney are the same as those associated with the smaller displacements of the 300-ft chimney. The dropping off of the shear, as shown in Fig. 6, occurs for the same reason, namely, that the flexibility of the chimney increases rapidly with height. One can obtain an intuitive feeling for the validity of Eq. (18) and (19) by imagining a 20-ft diameter concrete pipe supported horizontally in such a way that it is free to vibrate back and forth. If one end is clamped and shaken with a motion corresponding to an earthquake, the behavior of the pipe will be the same as that of a chimney. It is clear that if the pipe is 1 mile long the bending moments produced will not be the same as the bending produced by a percent g load and, in fact, the maximum moments produced in a 2 mile long pipe will be essentially the same as in the 1 mile long pipe. As can be seen from Eq. (18) and (19), as the height of the chimney is increased a point will be reached where the design for wind load will govern rather than the design for earthquakes.

Fig. 8 shows the bending at the base as computed from Eq. (18), for chimneys 200 ft high with a range of radii, and the same quantities computed for a 20 percent g load. It is seen that the moments and shears are reduced by the flexibility of small radii chimneys.

Eq. (18) and (19) are based on the supposition that chimneys of all proportions are comparable and should all have the same factor of safety; therefore, they should not be used for chimneys that are unusual in some way so that they are not similar to the ordinary type of chimney. It may also be that larger factors of safety are desirable for tall chimneys than for short chimneys.

TAPERED AND BATTERED CHIMNEYS

The foregoing analysis was for chimneys of uniform cross section whereas most chimneys have a wall thickness which diminishes toward the top and may have a variable radius which also diminishes toward the top. Properly, an analysis similar to the foregoing should be made for such structures, however, so many combinations of batter and taper are possible that this approach would be awkward for ordinary design. For special chimneys such an analysis should be made but for ordinary chimneys with nominal batter and taper the following method is proposed.

The influence of the batter and taper may be taken into account in the following approximate fashion. Compute the bending moment and shear at any section by

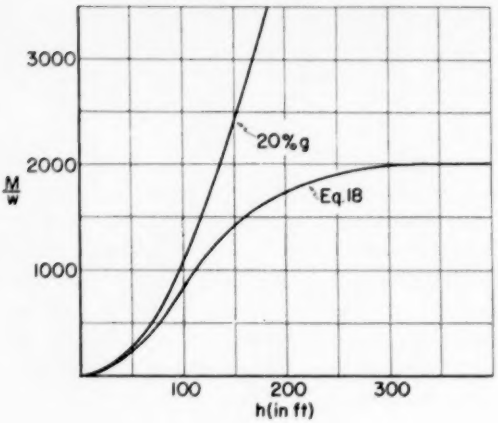

Fig. 5—Variation of maximum bending moment at the base with height of chimney. Eq. (18) compared with moment given by 20 percent g load for chimney of 10-ft radius

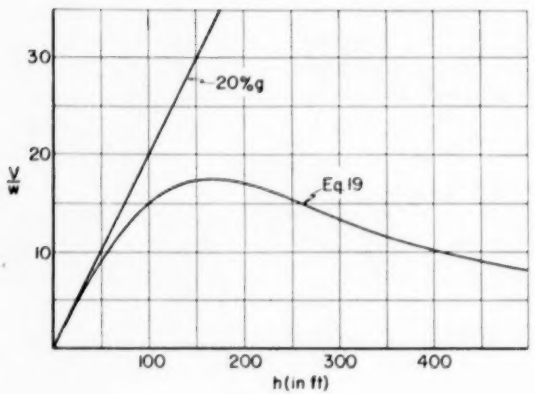

Fig. 6—Variation of maximum shear at base with height of chimney. Eq. (19) compared with shear given by 20 percent g load for 10-ft radius chimney

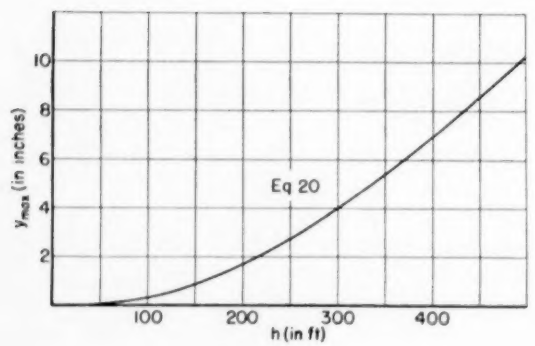

Fig. 7—Maximum displacement at top of chimney for 10-ft radius and various heights

$$M = M_s\left(\frac{W\bar{x}}{W_s\bar{x}_s}\right) \quad (21)$$

$$V = V_s\left(\frac{W}{W_s}\right) \quad (22)$$

M = moment at section
V = shear at section
M_s = moment given by Eq. (18) for chimney of same height and same base radius
V_s = shear given by Eq. (19) for chimney of same height and same base radius
W = weight of chimney above section
W_s = weight of uniform chimney (Eq. (18) above section
$\bar{x}$ = distance from section to center of gravity of portion of chimney above the section
$\bar{x}_s$ = distance from section to center of gravity of portion of uniform cross section chimney above section

This procedure will give a moment at the base of short rigid chimneys the same as that obtained by a 20 percent g design. For tall chimneys the procedure will give good results if the fundamental period of vibration of the battered or tapered chimney does not differ too much from the period of the uniform cross section chimney used in Eq. (18) and (19). If the batter or taper is sufficiently large to indicate a significant difference in periods, the radius of the equivalent uniform chimney should be determined so as to give the same period as the tapered chimney. In this connection, it may be noted that battering the wall decreases the period of vibration and tapering the radius increases the period of vibration, and to underestimate the period is to be conservative.

Example

Let the chimney to be investigated have the following properties:

h = 250 ft
R = 10-ft centerline radius at base
R = 5-ft centerline radius at top
t = 2 ft wall thickness at base
t = 6 in. wall thickness at top

The taper and batter are considered to vary linearly along the length of the chimney. The proportions are sufficiently far from those of a uniform chimney so that the fundamental period of vibration should be checked. This can be done by the energy method as follows. If the chimney is vibrating freely in a steady state in the first mode, the displacement is given by $y \sin p_1 t$. The strain energy of bending and the kinetic energy of vibration are given by

$$S.E. = \left[\frac{1}{2}\int_0^h \frac{M^2}{EI}\,dx\right] \sin^2 p_1 t$$

$$K.E. = \left[\frac{1}{2}\int_0^h \rho y^2 p_1^2 dx\right] \cos^2 p_1 t$$

Equating the maximum strain energy to the maximum kinetic energy gives the

period of vibration T_1 as

$$T_1 = \frac{2\pi}{p_1} = 2\pi \left(\frac{\int_0^h \rho y^2 dx}{\int_0^h \frac{M^2}{EI} dx} \right)^{\frac{1}{2}} \quad \text{(20)}$$

A satisfactory approximation is obtained by taking the bending moment, M, and displacement, y, to be those produced by the weight of the chimney if it were a horizontal cantilever beam. The integrals in Eq. (20) can be calculated by one of the usual numerical methods. In the present example the chimney has no lining but in case that it does the weight of the lining should be included in the calculations.

Eq. (20) for the present example gives a period of 2.1 sec. For a uniform chimney having $h = 250$, $R = 10$, $t = 2$, Eq. (14) gives a period of 1.65 sec so that the tapered chimney has a somewhat longer period. Writing

$$\frac{1}{2}\left(\frac{h}{h_o}\right)^3 \left(\frac{R_o}{R}\right) = 2.1$$

and solving for R gives the following equivalent uniform chimney having the same period as the tapered one:

$R = 8$ ft
$h = 250$ ft
$t = 2$ ft (arbitrary)

Table 2 gives the results of the calculations of the moments and shears.

TABLE 2—MOMENTS AND SHEARS (X 10^{-5})

	(1)	(2)	(3)	(4)	(5)	(6)	(7)	(8)	(1)×(7)	(2)×(8)
x, ft	M_{ou}	V_{ou}	Wx	$W_o\bar{x}_o$	W	W_o	(3)÷(4)	(5)÷(6)	M	V
50	64	0.58	42	189	1.7	7.5	0.22	0.23	14	0.13
100	95	1.05	200	750	4.7	15	0.27	0.31	26	0.33
150	120	1.40	550	1700	9.1	22	0.33	0.40	41	0.56
200	160	1.70	1160	3000	15	30	0.39	0.51	67	0.87
250	230	1.90	2100	4700	24	38	0.45	0.63	105	1.20

M_{ou} = moments for 8-ft radius chimney [Eq. (18)], ft-lb x 10^{-5}
V_{ou} = shears for 8-ft radius chimney [Eq. (19)], lb x 10^{-5}
M = moments for tapered chimney, ft-lb x 10^{-5}
V = shears for tapered chimney, ft-lb x 10^{-5}

From Table 2 it is seen that the moment and shear at the base of the tapered chimney are equal respectively to those given by a percent g design where the fractions of g are

$$\text{For moment: } \frac{105}{2100} = (0.05)g$$

$$\text{For shear: } \frac{1.2}{38} = (0.032)g$$

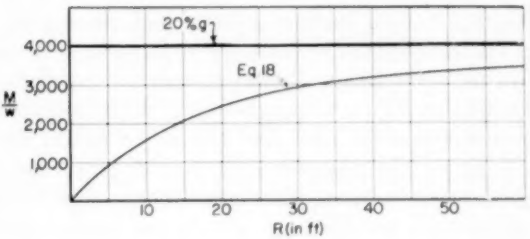

Fig. 8—Variation of maximum bending moment at base with radius of chimney. Eq. (18) compared with moment given by 20 percent g load for 200 ft high chimney. Variation of shear with radius is directly proportional to the variation in moment

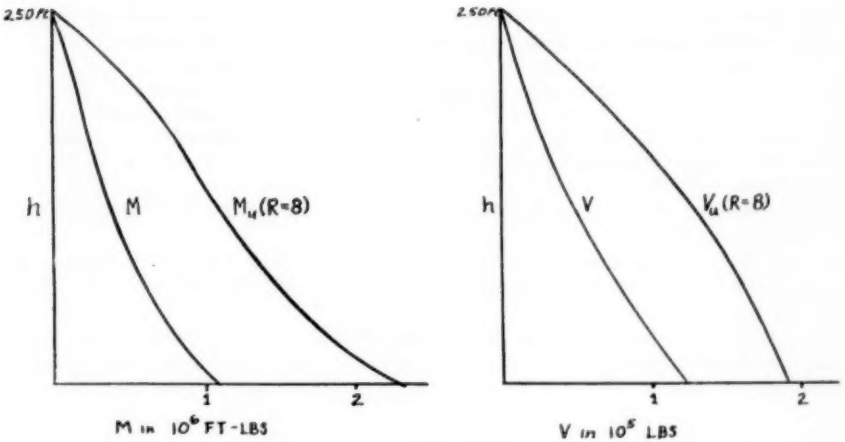

Fig. 9—Moments and shears for tapered chimney

The bending moment at the base is equal to that given by a wind load of 10 psf of projected area. Had the calculations been made on the basis of a uniform chimney of 10-ft radius instead of 8-ft radius the moments and shears would have been found to be 15 percent larger. The moments and shears listed in Table 2 are shown in Fig. 9.

SUMMARY

Eq. (18) and (19) embody a number of approximations, and to make these clear they are listed below.

1. A "standard" earthquake is used which has the characteristics of the average of the strong ground motions recorded in the past.

2. Mathematical expressions for bending moments and shear have been simplified and this results in an overestimation of the higher modes in the case of short, rigid chimneys. For the very rigid chimney the bending moment and shear should be more nearly like those given by the percent *g* method.

3. Formulas have been adjusted to give maximum moment and shear at the base

which, for rigid chimneys, agrees with those given by a 20 percent g load. This, in effect, establishes the earthquake intensity to be used in the design. It is assumed that the same factor of safety is desirable for chimneys of all heights and it is assumed that the dynamical behavior of all chimneys is similar, that is, the percent of damping is the same, and restraint at base is the same.

4. Shapes of the bending and shear diagrams given by application of the method are only approximate. This is due to the simplifications introduced and to the fact that it is not possible to predict the precise character of future earthquake ground motion.

The proposed method of calculating design values of bending moments and shears gives values that take into account the dynamic influence of the mass, height, radius, wall thickness, and variation of radius and thickness over the height.

REFERENCES

1. Housner, G. W., Martel, R. R. and Alford, J. L., "Spectrum Analysis of Strong-Motion Earthquakes," *Bulletin,* Seismological Society of America, V. 43, No. 2, Apr. 1953.

2. Timoshenko, S. P., *Vibration Problems in Engineering,* D. Van Nostrand Co., Inc., New York, 1937.

3. Alford, J. L., and Housner, G. W., "Dynamic Test of a Four-Story Reinforced Concrete Building," *Bulletin,* Seismological Society of America, V. 43, No. 1, Jan. 1953.

4. Mononobe, N., "Investigation of Damage to Chimneys and Tower-Shaped Constructions During Earthquakes," *Report of the Committee for Investigation of Prevention of Earthquake Damage,* Excerpt from No. 100D, Tokyo, Japan, Jan. 1925.

APPENDIX

For a uniform cantilever beam the expressions in Eq. (8) and (9) have the following forms:

$$\sum F_n'' = \sum_n \left\{ \frac{8\left(\frac{\cosh \alpha_n \frac{x}{h} + \cos \alpha_n \frac{x}{h}}{\cosh \alpha_n + \cos \alpha_n} - \frac{\sinh \alpha_n \frac{x}{h} + \sin \alpha_n \frac{x}{h}}{\sinh \alpha_n + \sin \alpha_n}\right)}{\alpha_n(\sinh \alpha_n + \sin \alpha_n)\left(\frac{\cosh \alpha_n - \cos \alpha_n}{\cosh \alpha_n + \cos \alpha_n} - \frac{\sinh \alpha_n - \sin \alpha_n}{\sinh \alpha_n + \sin \alpha_n}\right)} \right\}$$

$$\sum \alpha_n F_n''' = \sum_n \left\{ \frac{8\left(\frac{\sinh \alpha_n \frac{x}{h} - \sin \alpha_n \frac{x}{h}}{\cosh \alpha_n + \cos \alpha_n} - \frac{\cosh \alpha_n \frac{x}{h} + \cos \alpha_n \frac{x}{h}}{\sinh \alpha_n + \sin \alpha_n}\right)}{(\sinh \alpha_n + \sin \alpha_n)\left(\frac{\cosh \alpha_n - \cos \alpha_n}{\cosh \alpha_n + \cos \alpha_n} - \frac{\sinh \alpha_n - \sin \alpha_n}{\sinh \alpha_n + \sin \alpha_n}\right)^2} \right\}$$

When these expressions are evaluated for n summed from 1 to 3 and allowance is made for the aforementioned overestimation of the higher modes, the results can be expressed by Eq. (10) and (11).

For such discussion of this paper as may develop please see Part 2, December 1957 *Journal*. In *Proceedings* V. 53 discussion immediately follows the June 1957 *Journal* pages.

Title No. 53-5

Structural Analysis by Dynamic Load Parameters*

By JAMES A. CHENEY†

SYNOPSIS

Summarizes the method of normal modes which may be used in the analysis of structures under blast and earthquake excitation. Solutions are simplified to give equations involving several basic nondimensional parameters. The equation which applies to all structural problems solved by the method of normal modes is:

$$\text{Deflection} = C \sum_{i=1}^{N} \frac{\left[\begin{matrix}\text{Characteristic}\\ \text{Function}\end{matrix}\right]\left[\begin{matrix}\text{Participation}\\ \text{Factor}\end{matrix}\right]\left[\begin{matrix}\text{Dynamic}\\ \text{Load Factor}\end{matrix}\right]}{\left[\begin{matrix}\text{Characteristic}\\ \text{Number}\end{matrix}\right]}$$

The bracketed terms are nondimensional factors, the C-term carrying the required dimensions. Application is made to a reinforced concrete building under earthquake and blast loading.

INTRODUCTION

Use of orthogonal functions in solving dynamic problems in structures is not new. Engineering literature is well populated with articles and books giving detailed discussions and examples of the method. However, as yet, civil engineers have not adopted the procedure in the analysis of buildings under earthquake and blast loading. In the case of earthquake loading, the most common procedure is to design for an assumed horizontally applied load equal to some percentage of the weight of the structure. This percentage of the gravity force has been chosen on the basis of experience and judgment of practicing engineers. Blast design, being of general interest only recently due to its application in civil defense, has been treated more fully from the theoretical standpoint than has aseismic design.

However, as will be pointed out, the theory and solutions obtained from blast problems are equally applicable to earthquake problems. Conversely, methods used in the analysis of the response of structures to ground motion may readily be used to analyze the response of structures to blast. A great deal may be gained by comparing progress made in both fields.

---

*Presented at the ACI Seventh Regional Meeting, Los Angeles, Calif., Oct. 29, 1954. Title No. 53-5 is a part of copyrighted JOURNAL OF THE AMERICAN CONCRETE INSTITUTE, V. 28, No. 1, July 1956, *Proceedings* V. 53. Separate prints are available at 50 cents each. **Discussion** (copies in **triplicate**) should reach the Institute not later than Nov. 1, 1956. Address 18263 W. McNichols Rd., Detroit 19, Mich.

†Structures Engineer, Missile Systems Division, Lockheed Aircraft Corp. Los Angeles, Calif.

The purpose of this paper is to present the normal mode method of analysis in a simplified form. It is hoped that the simplified equations involving parameters having some physical significance will clarify the approach and make it more amenable to use in general design.

NOMENCLATURE

Certain basic quantities used in the derivation to follow are shown in Fig. 1. Other symbols will be defined as they are first used.

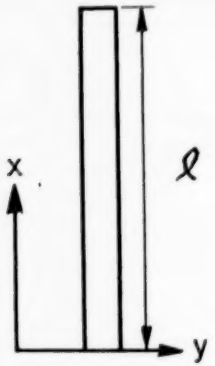

Fig. 1—Basic relationships

E = modulus of elasticity
EI = flexural rigidity about the z axis
e = base of natural logarithms (2.73)
g = acceleration due to gravity
I = moment of inertia about the z axis
l = length of beam
m = mass per unit length
M = bending moment about the z axis
P = force in the y direction
Q = generalized force in the y direction
q = generalized coordinate
t = time
T = kinetic energy
U = potential energy
V = shear in the y direction
x = distance along the beam
$y,\dot{y},\ddot{y}$ = transverse displacement, velocity, acceleration
z = axis of rotation normal to xy plane

THEORY

For the purpose of presentation, examples will be limited to cases involving structures which may be approximated by uniform beams. The differential equation of motion of a beam, neglecting shear deformation and rotatory inertia, has been derived many times. Two of the more convenient references are Timoshenko[1] and Karman and Biot.[2] This differential equation may be solved by any one of the classical methods. It is known that these methods lead to a unique solution in terms of an infinite series of characteristic functions (normal modes) which are orthogonal. Much labor can hence be saved by adopting the common procedure of assuming the form of the solution and evaluating the coefficients of each term (method of normal coordinates).

The case of a beam subjected to motion at the supports will be treated here, and similarities between this and other types of loading will be pointed out. No restrictions will be made as to end conditions for the beam; however it will be postulated that all supports will undergo the same displacements. Expanding the de-

flection of the beam relative to its supports in terms of generalized or normal coordinates, we obtain

$$y(x,t) = y_o(x,t) + \sum_{i=1}^{\infty} \phi_i(x) q_i(t) \quad \ldots\ldots (1)$$

where $y_o\ (x,t)$ = motion of the supports; $\phi_i\ (x)$ = characteristic function; $q_i\ (t)$ = generalized coordinate.

The equations of motion of a beam in terms of its generalized coordinates are Lagrange's equations.[2]

$$\frac{d}{dt}\left(\frac{\partial T}{\partial \dot{q}_i}\right) - \frac{\partial T}{\partial q_i} + \frac{\partial U}{\partial q_i} = Q_i\ (i = 1, 2, 3 \cdots \infty) \quad \ldots\ldots (2a)$$

$$\frac{d}{dt}\left(\frac{\partial T}{\partial \dot{y}_o}\right) - \frac{\partial T}{\partial y_o} + \frac{\partial U}{\partial y_o} = Q_o \quad \ldots\ldots (2b)$$

where

$$U = \frac{EI}{2}\int_0^l \left(\frac{d^2y}{dx^2}\right)^2 dx \cdots \text{(potential energy)} \quad \ldots\ldots (3)$$

$$T = \frac{m}{2}\int_0^l \dot{y}^2 dx \cdots \text{(kinetic energy)} \quad \ldots\ldots (4)$$

$$\left.\begin{aligned} Q_i &= \int_0^l P(x,t)\,\frac{\partial y}{\partial q_i}\,dx \cdots \\ Q_o &= \int_0^l P(x,t)\,\frac{\partial y}{\partial y_o}\,dx \cdots \end{aligned}\right\} \text{(generalized force)} \quad \ldots\ldots (5)$$

Substituting Eq. (1) in Eq. (3) and (4) results in

$$U = \frac{EI}{2}\sum_{i=1}^{\infty} q_i^2 \int_0^l \left(\frac{d^2\phi_i(x)}{dx^2}\right)^2 dx \quad \ldots\ldots (6)$$

$$T = \frac{m\dot{y}_o^2 l}{2} + m\dot{y}_o \sum_{i=1}^{\infty} \dot{q}_i \int_0^l \phi_i(x)dx + \frac{ml}{2}\sum_{i=1}^{\infty} \dot{q}_i^2 \quad \ldots\ldots (7)$$

In the case being considered the only force applied to the beam is applied to the supports. However, the motion of the supports is not a function of q_i. Therefore

$$Q_i = \int_0^l P(x,t)\,\frac{\partial y_o}{\partial q_i}\,dx = 0 \quad \ldots\ldots (8)$$

Substituting Eq. (6), (7), and (8) into Lagrangian equations the following equation is obtained:

$$m\ddot{y}_o \int_0^l \phi_i(x)dx + ml\ddot{q}_i + EIq_i \int_0^l \left(\frac{d^2\phi(x)}{dx^2}\right)^2 dx = 0 \quad \ldots\ldots (9)$$

The characteristic function represents the shape of the harmonically vibrating beam in the absence of external excitation. This function has been established as

$$\phi_i(x) = A \sin \beta x + B \cos \beta x + C \sinh \beta x + D \cosh \beta x \quad \ldots\ldots (10)$$

where $\beta^4 = m\omega^2/EI$. This may be verified by study of reference 1. The arbitrary constants are determined by the boundary conditions imposed on the beam and the condition of orthogonality, namely

$$\int_0^l m\phi_i^2(x)dx = \begin{cases}\text{Zero for } i \neq j \\ \text{Arbitrary for } i = j\end{cases} \quad (11)$$

For the case $i = j$, it is convenient to normalize the equation by letting the arbitrary value of the integral be equal to ml. It follows then that

$$\int_0^l m\phi_i^2(x)dx = ml \quad (12)$$

Defining ϕ'' as $\frac{1}{\beta^2}\frac{d^2\phi_i(x)}{dx^2}$ it follows from Eq. (10) and (12) that Eq. (9) becomes

$$m\ddot{y}_o\int_0^l \phi_i(x)dx + ml\ddot{q}_i + EIl\beta_i^4 q_i = 0 \quad (13)$$

Rearranging and defining $\frac{EI}{m}\beta_i^4 = \omega_i^2$

$$\ddot{q}_i(t) + \omega_i^2 q_i(t) = -\ddot{y}_o\frac{1}{l}\int_0^l \phi_i(x)dx \quad (14)$$

It can be shown[1] that ω_i are natural undamped frequencies of free vibration and that for conditions of zero velocity and acceleration at time equal zero, Eq. (14) has the following general solution:

$$q_i(t) = -\frac{1}{\omega_i}\int_0^t \ddot{y}_o(\nu)\frac{1}{l}\int_0^l \phi_i(x)dx \cdot \sin\,\omega_i(t-\nu)d\nu \quad (15)$$

$$q_i(t) = -\frac{1}{\omega_i^2}\frac{1}{l}\int_0^l \phi_i(x)dx \cdot \omega_i\int_0^t \ddot{y}_o(\nu)\sin\,\omega_i(t-\nu)d\nu \quad (16)$$

The above equations solve for the unknown function q_i, and theoretically the problem is solved. If the same procedure were followed for the case of an arbitrary impulsive load on a beam, the following solution for q_i would be derived:

$$q_i(t) = \frac{P_o}{\omega_i^2 l}\cdot\frac{1}{l}\int_0^l \phi_i(x)\overline{W}(x)dx \cdot \omega_i\int_0^t f(\nu)\sin\,\omega_i(t-\nu)d\nu \quad (17)$$

where the applied load

$$w(x,t) = \frac{P_o}{l}\overline{W}(x)f(t) \quad (18)$$

P_o ... maximum total blast force
$\overline{W}(x)$ ... space distribution of force
$f(t)$ ... time variation in the force

In the above solution for blast loading it has been assumed that the load may be broken down in the manner indicated. If for any reason the space distribution of force is a function of time or the time variation of force is a function of distance, the above solution is invalid. However, many times blast loadings may be approximated closely by the above assumption.

SIMPLIFIED EQUATIONS

In fairly recent years studies have been made which simplify the numerical work involved in using the normal mode approach. One of the most important publications has been the tabulation of characteristic numbers, characteristic functions, and the successive derivatives of the characteristic functions. These tables are due to Young and Felgar and have been published by the University of Texas.[3] Other investigators, such as G. W. Housner and W. T. Thomson have applied electronic computers in solving the time varying part of the solution.[4,5]

To see how these various investigations fit together, it is convenient to express Eq. (16) and (17) in the following form:

$$q(t) = \frac{Ck_iD_i}{(\beta l)^4} \qquad (19)$$

Where

For blast	For earthquake
$C = \frac{P_o l^3}{EI}$	$C = \frac{mgl^4}{EI}$
$k_i = \frac{1}{l}\int_0^l \phi_i(x)\overline{W}(x)dx$	$k_i = \frac{1}{l}\int_0^l \phi_i(x)dx$
$D_i = \omega_i \int_0^t f(\nu) \sin \omega(t-\nu)d\nu$	$D_i = \omega_i \int_0^t \frac{\ddot{y}_o}{g} \sin \omega_i(t-\nu)d\nu$
$(\beta l)^4 = \frac{\omega_i^2 m l^4}{EI}$	$(\beta l)^4 = \frac{\omega_i^2 m l^4}{EI}$

With the exception of the factor C, all of the above coefficients are nondimensional. By comparison between the two columns it is possible to see the similarities as well as the essential differences between earthquake and blast response.

Participation factor

The coefficient k_i determines to what extent various modes participate in the statical deflection for the blast case. It is therefore called the participation factor. The value this factor takes is a weighted average of the characteristic function $\phi_i(x)$. When the exciting force is uniformly distributed over the length of the beam, $\overline{W}(x) = 1$, and the participation factor for blast becomes a straight average of $\phi_i(x)$.

As may be seen from the coefficient C, the weight of the structure is analogous to an exciting force, in the earthquake case. Inasmuch as a uniform beam is under consideration, it is consistent that k_i for the earthquake case is shown as a straight average of $\phi_i(x)$. If the beam had a distribution of weight $\overline{W}(x)$, the k_i for earthquake would be the same as for blast.

Dynamic load factor

A dynamic load factor is so termed because it tells how much the static response is magnified to obtain the dynamic response. This is precisely what the factor D_i does. For the blast case the integral involves the time variation of load $f(t)$ while

in the earthquake case the time variation in acceleration (expressed as percentage of gravity) is substituted. It should be noted that the dynamic load factor must be applied to the response of each mode separately, since in general D_i will be different for different modes.

For design purposes it is the maximum D_i that is of interest. Although there is no certainty that the maximum values of D_i will occur at the same time for various modes, the times are not greatly different and one must always consider the worst probable condition in design. Determination of the dynamic load factor for all but the most simple load histories becomes a difficult numerical task. It is here that analog computers have come to the aid of the engineer.

G. W. Housner observed that the quantity D_i represented the acceleration in percent of gravity of a one-degree-of-freedom structure of frequency ω_i. Substituting real earthquake accelerograms for the term $\ddot{y}_o$ and determining the maximum value of the integral for all reasonable values of frequency, a distribution of acceleration versus period could be drawn which is similar to a distribution of light intensity versus wave length. For this reason the curves of maximum D_i versus period which have been obtained by means of electronic computers have been referred to as earthquake spectra.[4]

Damping may be included in the differential equation of motion of a beam by including a force term which is proportional to velocity and in phase with the deflection. This results in the addition of an exponential term in the dynamic load factor, namely

$$D_i = \omega_i \int_0^t f(\nu) e^{n\omega_i(t-\nu)} \sin \omega_i(t-\nu) d\nu \quad \ldots\ldots\ldots\ldots\ldots\ldots\ldots\ldots\ldots\ldots (20)$$

where n is the percent of critical damping. Housner has shown the effect of the inclusion of damping on the earthquake spectra.

Most of the published work giving actual values of maximum dynamic load factors has been for earthquake excitation. However, analog computer techniques are equally applicable to blast excitation. W. T. Thomson has been carrying on research at the University of California along these lines.[5]

Characteristic values

There are two characteristic values that enter in the solution which are properties of the freely vibrating beam. One of these values is the characteristic function $\phi_i(x)$ which describes the shape of the ith mode. The other value is the characteristic number $\beta_i l$. For uniform beams the characteristic values are determined by end conditions and Eq. (11) and (12).

Young and Felgar[3] have tabulated values of $\phi_i(x)$, $\phi_i'(x)$, $\phi_i''(x)$, $\phi_i'''(x)$ and $\beta_i l$ for all combinations of clamped, pinned, and free end conditions with the exception of the pinned-pinned case which results in a simple sine function. The primed values are the successive derivatives of $\phi_i(x)$ divided by successive powers of β_i to retain nondimensionality.

Moment and shear

Substituting factors described above in Eq. (1):

$$y(x,t) = y_o(t) + \frac{mgl^4}{EI}\sum_{i=1}^{\infty}\frac{\phi_i(x)k_i(x)}{(\beta l)_i^4}D_i(t) \quad \ldots\ldots(21)$$

For the blast solution

$$y(x,t) = \frac{P_o l}{EI}\sum_{i=1}^{\infty}\frac{\phi_i(x)\ k_i(x)}{(\beta l)_i^4}D_i(t) \quad \ldots\ldots(22)$$

The designing engineer is usually more interested in moments and shear than in deflection. Since $\phi_i(x)$ is the only variable quantity in the equation above that is a function of x, it is the only value that changes.
For earthquake:

$$M(x,t) = mgl^2\sum_{i=1}^{\infty}\frac{\phi_i''(x)k_i(x)}{(\beta_i l)^2}D_i(t) \quad \ldots\ldots(23)$$

For blast:

$$M(x,t) = P_o l\sum_{i=1}^{\infty}\frac{\phi_i''(x)k_i(x)}{(\beta_i l)^2}D_i(t) \quad \ldots\ldots(24)$$

For earthquake:

$$V(x,t) = mgl\sum_{i=0}^{\infty}\frac{\phi_i'''(x)k_i(x)}{\beta_i l}D_i(t) \quad \ldots\ldots(25)$$

For blast:

$$V(x,t) = P_o\sum_{i=0}^{\infty}\frac{\phi_i'''(x)k_i(x)}{\beta_i l}D_i(t) \quad \ldots\ldots(26)$$

It should be noted that these solutions have neglected shear deformation and rotatory inertia. However, for most engineering purposes these effects are negligible.[6]

APPLICATION

Earthquake

An example of the use of the equations derived above will be made in the analysis of the Arvin High School, Arvin, Calif., for the earthquake of July 21, 1952. The west end wall of the administration building which fractured during the shock will be studied.

The epicenter of the main shock was in the vicinity of Wheeler Ridge, approximately 20 miles from Arvin. The seismograph closest to the epicenter was at Taft, Calif., about 25 miles from the epicenter. After study of the earthquake spectra and the opinions of qualified investigators such as G. Housner, the conclusion was reached that the earthquake intensity at Arvin corresponded roughly to that represented by the El Centro earthquake of May 18, 1940. The earthquake spectra for the El Centro earthquake and the Arvin earthquake are shown in Fig. 2.

The Arvin High School administration building is a two-story reinforced concrete building with brick veneer except the second-story wall at the west end which was 8½-in. reinforced grouted brick masonry. This is the wall that was most severely fractured. The south second-story walls had minor spalls at their bases indicating rocking had occurred. Details of the west second-story wall and roof are shown in Fig. 3 and 4.[7]

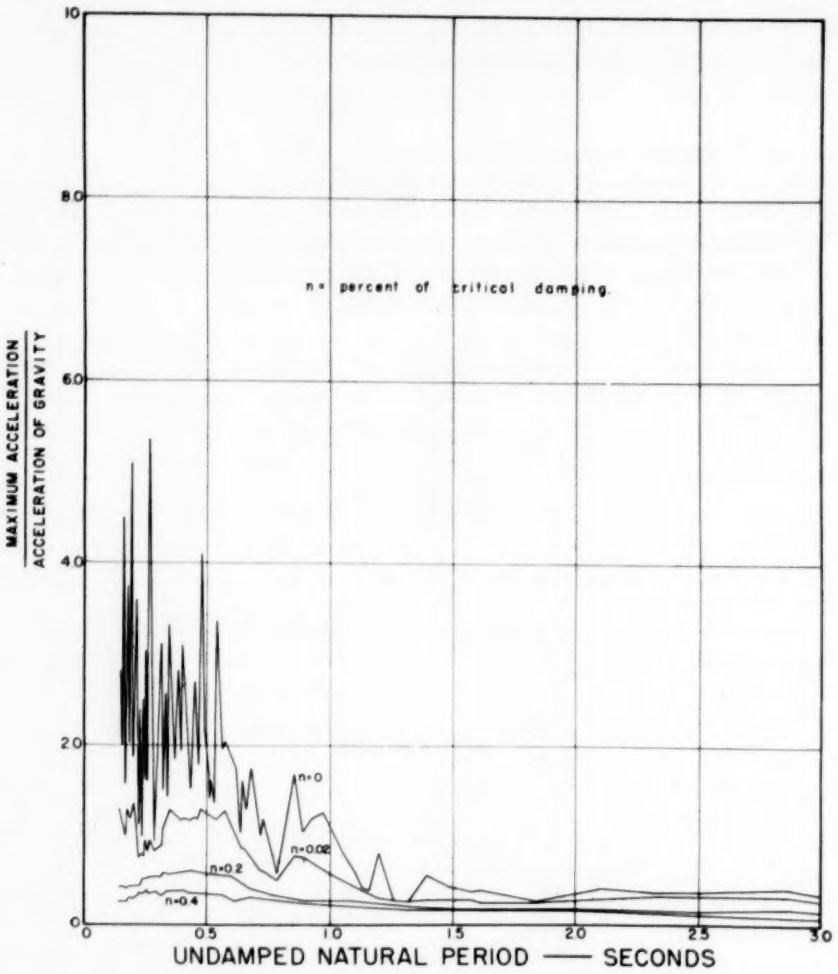

Fig. 2—Acceleration spectra for El Centro, Calif., earthquake of May 18, 1940

The shear strength of the west upper story wall was reduced because of an unsatisfactory bond between the mortar and the brick. Contrary to specifications metal lath had been placed in some of the bed joints to facilitate grouting. Nevertheless, it has been estimated that the wall should have been good for 40 psi on the gross area.

The loads entering the walls are due to the inertia of the roof slab. For the purpose of analysis, the roof slab may be approximated by a simply supported beam undergoing lateral motion. It may be assumed that the interior columns and parti-

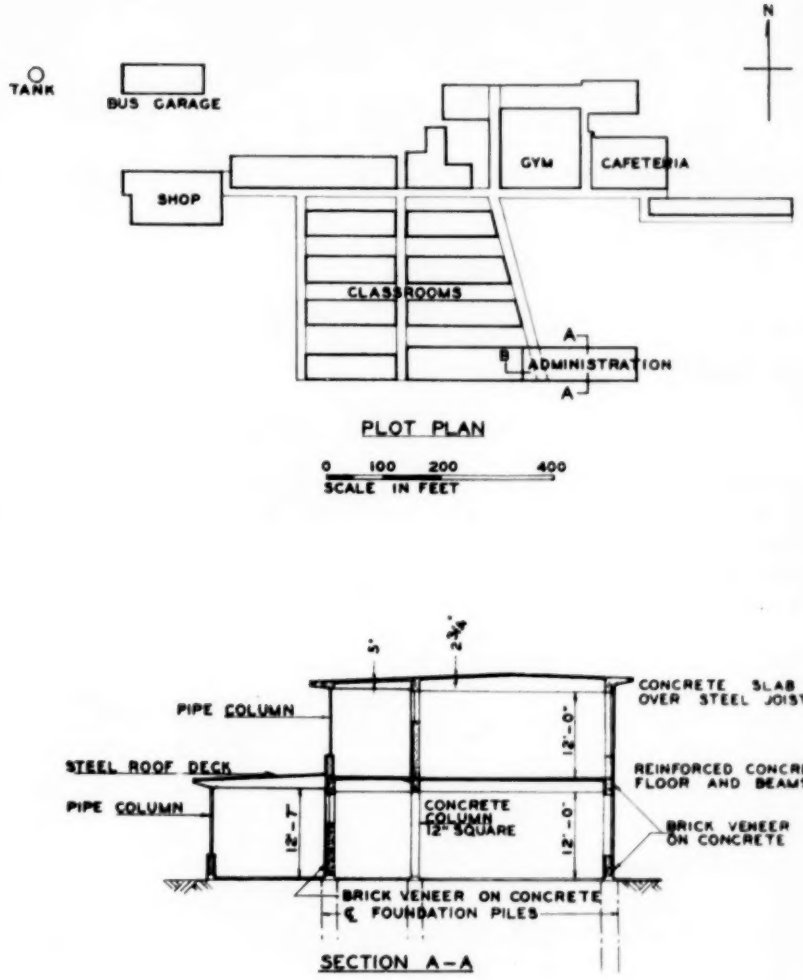

Fig. 3—Arvin High School

tions give vertical support but do not offer lateral resistance to motion. The parameters for the simply supported beam condition are tabulated below:

$$\phi_i(x) = \sqrt{2} \sin \frac{i\pi x}{l} \text{ where } i = 1, 2, 3, \text{ etc.}$$

$$\phi_i'(x) = \sqrt{2} \cos \frac{i\pi x}{l}$$

$$\phi_i''(x) = -\sqrt{2} \sin \frac{i\pi x}{l}$$

$$\phi_i'''(x) = -\sqrt{2} \cos \frac{i\pi x}{l}$$

$$\beta_i l = i\pi$$

$$k_i = \frac{1}{l}\int_0^l \sqrt{2}\sin\frac{i\pi x}{l}\,dx = \frac{2\sqrt{2}}{i\pi}$$

$$\text{Period } T_i = \frac{2\pi}{\omega} = \frac{2}{(i)^2\pi}\sqrt{\frac{ml^4}{EI}}$$

If the roof slab remains in the elastic range during its vibratory motion, the following material properties may be used:

$$E = 2.5 \times 10^6 \text{ psi}$$
$$I = 90 \times 10^6 \text{ psi}$$
$$m = \frac{304 \text{ lb per in.}}{386 \text{ in. per sec}^2} = 0.79\frac{\text{lb-sec}^2}{\text{in.}^2}$$

The fundamental period of vibration is

$$T = \frac{2}{\pi}\sqrt{\frac{0.79(2400)^4}{2.5 \times 90 \times 10^{12}}} = 0.218 \text{ sec}$$

Assuming a representative damping factor for masonry of 0.10, a value of 0.8 may be picked for the dynamic load factor. Since the higher modes will have shorter periods than the fundamental, the dynamic load factor, D_i, for higher modes will not vary noticeably from 0.8.

It remains now to evaluate the necessary parameters to solve the shear equation:

$$V = mgl\sum_{i=1}^{\infty}\frac{\phi_i'''k_iD_i}{\beta_i l}$$

$$= 0.79(386)(2400)\left\{\frac{\sqrt{2}\left(\frac{2\sqrt{2}}{\pi}\right)0.8}{\pi} + \frac{\sqrt{2}\left(\frac{2\sqrt{2}}{3\pi}\right)0.8}{3\pi}\right\}$$

$$= 365{,}000 \text{ lb } (0.8) = 294{,}000 \text{ lb}$$

For a gross cross-sectional area of the end wall of 3000 sq in. the average shearing stress would be 97 psi.

This theoretical load was never realized in the structure since the wall failed at a much lower stress. However, had the wall been properly constructed it is doubtful that it could have withstood the above loads. This is not entirely surprising since structures of this type have reserve strength represented by the interior walls and columns.

The largest factor in reducing the stresses induced by the earthquake is the fact that small failures occurring within the structure prior to a major fracture can increase the apparent damping coefficient to the point where the resultant dynamic load factor is within reasonable limits. In addition, other vibratory motions such as rocking of the building on its foundation could also reduce the dynamic load factor by way of increasing the natural period of vibration.

An important point has been demonstrated in this problem. In the above example, the solution could have been obtained as readily by multiplying the static shear at the wall under a one g loading by the dynamic load factor D_i. This follows

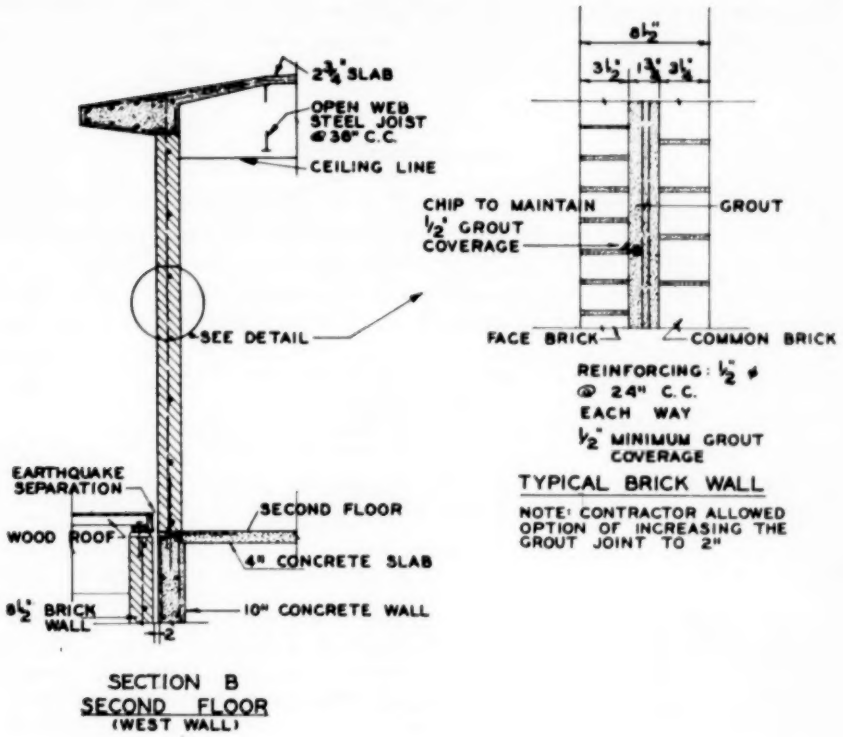

Fig. 4—Arvin High School

from the definition of the dynamic load factor, namely the factor by which the static response is multiplied to obtain the dynamic response. Moment and deflection for stiff structures such as the Arvin administration building may be obtained in a similar manner. Structures having long periods of vibration take advantage of the reduction in the value of D_i as shown in the spectra.

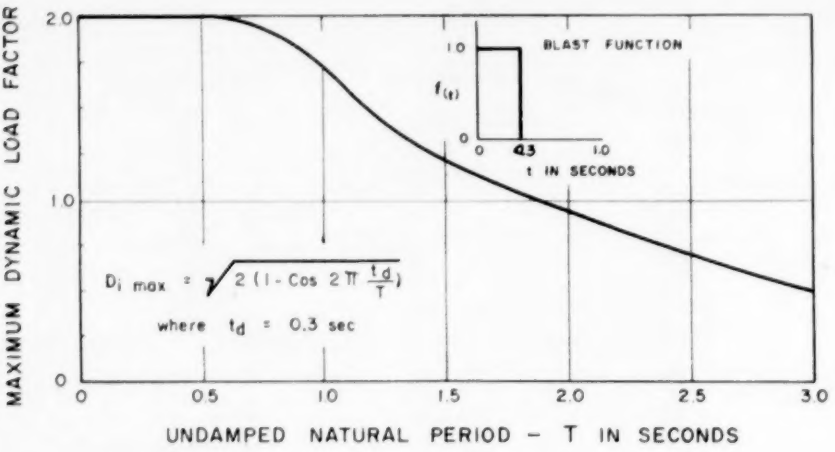

Fig. 5—Maximum dynamic load factor for step function shock of 0.3-sec duration versus undamped natural period, T

Blast

A somewhat more hypothetical example for blast type loading could be obtained by analyzing the above structural element under an impulsive loading. If we assume a pulse type load of 0.3 sec duration time, the maximum D_i plotted against period takes the appearance shown in Fig. 5. This curve might reasonably be called the blast spectrum.

Since the period of the roof slab is 0.218 sec, the dynamic load factor for all modes is roughly 2.0. In other words, the dynamic response is twice the static response under the maximum blast load.

CONCLUSION

It was shown how the response of beams under dynamic loads may be expressed as a series expansion involving four nondimensional parameters and one dimensional constant. The equation takes the following form:

$$y = C \sum_{i=1}^{\infty} \frac{\phi_i(x) k_i D_i(t)}{(\beta_i l)^4} \qquad (29)$$

This form of solution is not limited to beams. In fact, all structures subjected to dynamic excitation, where the principle of superposition is valid and loads may be broken up into a time variation times a space distribution, may be analyzed using the above form of solution.

Prototype structures must be approximated by simplified models to satisfy the above conditions. Structures having uniform distributions of mass such as stacks, silos, or individual structural elements may be approximated by beam theory. Buildings where weight is concentrated at floor levels may be approximated by the so-

called shear building. Structures having large shearing deflections in comparison with their bending deflections may be approximated by the so-called shear beam. All of these simplified structures may be analyzed using the simplified form shown above.

ACKNOWLEDGMENTS

The writer is highly indebted to D. F. Moran, chief structural engineer, Quinton Engineers, for his review and helpful advice on numerical aspects of the paper and to Karl V. Steinbrugge, structural engineer, Pacific Fire Rating Bureau, for the aid given in preparing figures. The methods presented in this paper were developed under the guidance of Prof. W. T. Thomson at the University of California at Los Angeles.

REFERENCES

1. Timoshenko, S., *Vibration Problems in Engineering*, D. Van Nostrand Co., Inc., New York, 1938.

2. Karman, Th., and Biot, M. A., *Mathematical Methods in Engineering*, McGraw-Hill Book Co., Inc., New York, 1940.

3. Young, D., and Felgar, R. P., Jr., "Tables of Characteristic Functions Representing Normal Modes of Vibration of a Beam," *Engineering Research Series* No. 44, Bureau of Research, University of Texas.

4. Housner, G. W., Martel, R. R., and Alford, J. L., "Spectrum Analysis of Strong-Motion Earthquakes," *Bulletin*, Seismological Society of America, V. 43, No. 2, April 1953.

5. Thomson, W. T., "Impulsive Response of Beams in the Elastic and Plastic Range," *Journal of Applied Mechanics*, Sept. 1954.

6. Jacobsen, L. S., "Natural Periods of Uniform Cantilever Beams," *Transactions*, ASCE, 1939, p. 402.

7. Steinbrugge, K. V., and Moran, D. F., "An Engineering Study of the Southern California Earthquake of July 21, 1952," *Bulletin*, Seismological Society of America, V. 44, No. 2B, Apr. 1954.

For such discussion of this paper as may develop please see Part 2, December 1957 *Journal*. In *Proceedings* V. 53 discussion immediately follows the June 1957 *Journal* pages.

Spacing of Reinforcement in Beams*

By S. J. CHAMBERLIN†

SYNOPSIS

The effect of spacing of parallel bars was studied in modified beams. Simulated variations in spacing were obtained by varying the width of the concrete at the steel in different specimens. Two-point symmetrical loading was used on one- and two-bar specimens made with two different concretes. Steel consisted of # 4 bars—plain, old-style deformed, and modern deformed, and one modern # 6 bar. Embedded length-diameter ratios varied from 6 to 21.33. Bar slippages at the load points and at the free ends, deflections, and steel strains were measured.

Ultimate loads increased with wider spacing until tensile failures developed. Measured bar slippages were greater for the narrowest spacing than for the others. All plain-bar beams failed by excessive slippage of the steel. Deformed-bar beams which did not fail in tension failed either by rupture of the concrete along a horizontal plane at the centerline of the steel or in combination with diagonal tension. Results indicate that an effective clear spacing of three bar diameters may be required.

INTRODUCTION

The three-way specification of the ACI Code‡ governing the spacing of parallel bars in beams ostensibly provides for sufficient concrete to develop safe transfer of stress both between steel and concrete and between concrete and concrete. In an earlier paper§ which dealt wholly with pull-out splices where the pull in opposite directions was transferred from one bar to another through intervening concrete, the specimens were designed to furnish information on the effect of spacing of bars on bond. Results indicated that bond was not affected significantly for clear spacings of one diameter and three diameters and that tied splices for deformed bars actually developed greater resistance to load than spaced splices.

If one assumes that the high quality concrete necessary for precast members can be so placed around the bars that the bond itself is not adversely affected by close spacing, the question still remains of how much concrete is needed to carry the stress from the bars up and into the beams.

*Received by the Institute Feb. 7, 1955. Title No. 53-6 is a part of copyrighted JOURNAL OF THE AMERICAN CONCRETE INSTITUTE, V. 28, No. 1, July 1956, *Proceedings* V. 53. Separate prints are available at 50 cents each. **Discussion** (copies in **triplicate**) should reach the Institute not later than Nov. 1, 1956. Address 18263 W. McNichols Rd., Detroit 19, Mich.

†Member American Concrete Institute, Professor of Theoretical and Applied Mechanics, Iowa State College, Ames, Iowa.

‡"Building Code Requirements for Reinforced Concrete (ACI 318-51)."

§Chamberlin, S. J., "Spacing of Spliced Bars in Tension Pull-Out Specimens," ACI JOURNAL, Dec. 1952, *Proc.* V. 49, pp. 261-274.

The shearing stress on a horizontal plane through the concrete at the center of a single layer of bars should equal the amount of stress transmitted by bond from the underside of the bars. The critical area has a width equal to the clear distance between bars. Working stresses of $0.10f_c'$ and $0.03f_c'$ for bond and shear respectively give a required clear spacing between bars of 5.2 bar diameters.

Since this is absurd as compared with practice, it has been suggested that the horizontal shear is of no consequence. Actually the $0.03f_c'$ value is based on diagonal tension requirements rather than those for pure shear. After a careful study of shearing tests, Hognestad* concludes that shearing strength of concrete is about two-thirds the compressive strength. A working stress of $0.30f_c'$ in pure shear would provide for a factor of safety of slightly more than two (based on the two-thirds figure) and would require a minimum clear spacing of one-half bar diameter.

Combined with the shearing stresses are the tensile stresses in the concrete from the bond action. Some minimum width of concrete between bars is necessary to avoid splitting.

Considering our lack of understanding of the stress phenomena in beams, the code requirement of one bar diameter does not seem unreasonable. In beams in which web reinforcement, either vertical or inclined, is welded to the longitudinal steel, as in some types of precast floor beams, the shear would probably be taken largely by the web steel. The action of vertical stirrups, wired rather than welded to the main steel, is not as clear.

This report presents the results of one phase of a general project on lapped splices and the spacing of reinforcing bars. The object has been to investigate the effect of the spacing of unspliced, parallel bars on the load-carrying capacity of beams.

OUTLINE OF INVESTIGATION

A modified beam specimen was used as offering a simple first approach to discovering the minimum width of concrete which will suffice to provide the required amount of interaction between steel and concrete. The cross section of the central portion of all of the beams, that between the two-point symmetrical loading, was kept constant (Fig. 1) to duplicate beam conditions in the region of constant moment and zero shear. Exposure of the steel between load points also simplified the measurement of strains and slippages of the bars. The exposed portion of the bar corresponds to the projecting length to which the load is applied in a pull-out specimen. Slippage measured at the section under the load is the equivalent of loaded-end pull-out slippage. End portions of the beams, from load point to reaction, had a narrowed bead of different width in different specimens on the tension side in an attempt to accomplish a variable bar-spacing effect. The cross sections shown in Fig. 2 illustrate the idea. The solid lines indicate the end sections as cast, and the dotted lines indicate the conditions they attempt to simulate. Most of the beams had the narrowed bead of concrete beneath only the horizontal diameter of the bars as shown. One group had the bead extending up into the beam above the steel. Most of the beams were 6 x 6 in.

*Hognestad, Elvind, "What Do We Know About Diagonal Tension and Web Reinforcement in Concrete?" *Circular Series* No. 64, University of Illinois Engineering Experiment Station.

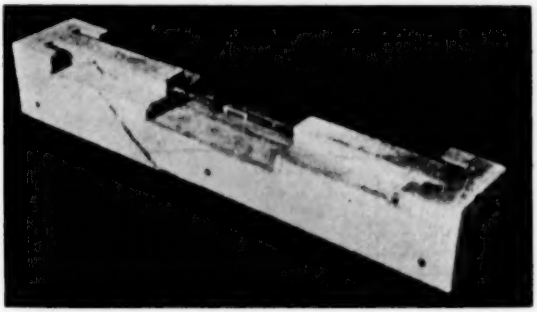

Fig. 1—Modified beam for simulated spacing. Combination of fracture at base of bead and diagonal tension

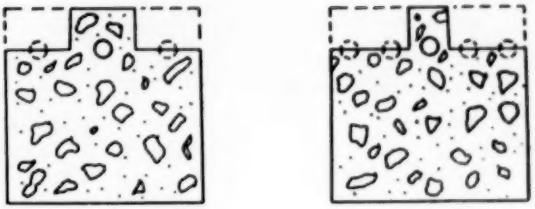

Fig. 2—Solid lines indicate cross sections as cast; dotted lines indicate the spacing of bars attempted to simulate

in over-all cross section, 36 in. long with a span of 32 in. (Fig. 3), although one group of 9 x 9 x 54-in. beams was included.

Beam specimens are summarized in Table 1. Series I was an exploratory series with only one specimen of a kind. Specimens varied from the extreme case of no concrete beneath the lower half of the bar, simulating no clear space, to full 6-in. section of the end portions. Triplicate specimens were cast for the four different simulated spacings of the plain and deformed bars of series II. Series III was the main series and consisted of three specimens of a kind with two concrete strengths for the smaller beams. The 6 x 6-in. beams of 6- and 3-in. embedment only had vertical web reinforcement consisting of two No. 11 gage wires spaced at 1 in. in the two end portions well away from the steel and beads. The larger beams with the # 6 bars (Fig. 4) were geometrically similar to the smaller specimens but had only one length of embedment and one concrete strength.

Two # 4 bars were used in the beams of series IV (Fig. 5). One group of beams had the variable-width bead up to the centerline of the steel as in the other series, while another group had the concrete extending upward twice as far. The specimens had web reinforcement away from the bead, of four vertical wires of No. 14 gage spaced at 1 in. in the end portions. Two additional beams had similar vertical reinforcement brought down under the reinforcement in the bead and back up into the compression zone of the concrete. Only one specimen of a kind was cast for series IV.

MATERIALS, FABRICATION, AND TEST METHODS

Materials

The cement was "Northwestern States" brand, type I, purchased locally. That used in series I and II was from dealer stock. For the other series of tests, the cement purchased on two separate occasions was from a newly opened car at the dealer's plant.

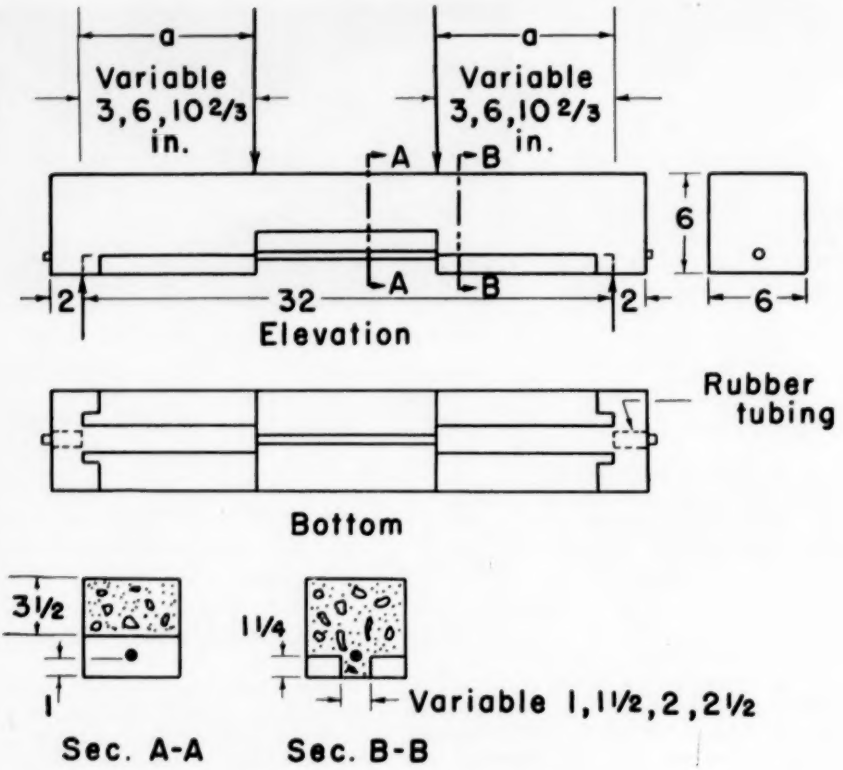

Fig. 3—Beams with one # 4 bar

The gravel for series I and II was ¾-in. maximum size from the Skunk River at Ames, Iowa, and was cleanly separated in the laboratory into two sizes, No. 4 to ⅜ in. and ⅜ to ¾ in., before proportioning. It was recombined, using 40 percent of the finer gravel and 60 percent of the coarser. For series III and IV, the gravel was from the Des Moines River at Boone, Iowa. It was separated into two sizes, No. 4 to ⅜ in. and ⅜ to ¾ in., at the aggregate plant. The Skunk River sand used in all of the concrete was poorly graded, lacking both in fines and in coarse material.

Concrete mixtures, other than for exploratory series I, were designed to have 28-day cylinder strengths of about 3500 and 5000 psi. The two lots of cement for series III and IV, however, gave about 20 percent higher strengths than for series II. The mixtures are listed in Table 2. Concrete was mixed in a one-half sack tilting drum mixer. When the total batch required exceeded the capacity of the mixer, two batches were mixed within a few minutes of one another and then remixed together by hand. The mixtures were all plastic and workable with an average slump of 3 in.

Reinforcing steel for exploratory series I was from laboratory stock of # 4 old-type deformed bars, bar A in Fig. 6. The # 4 plain bars, bar B, and the two sizes, # 4 (C)

TABLE 1—SUMMARY OF BEAM SPECIMENS

Series	Reinforcement (Concrete strength, psi)	Bead width (depth), in.	Clear spacing,* in.	Embedment,† in.	No. of tests
		6 x 6 x 36-in. beams			
I	One # 4, old def. p = 0.0069 (3700, 14-day)	0,1,1½,2,6 (1¼)	0,½,1,1½,5½	10 2/3	5
II	One # 4, plain p = 0.0069 (3680)	1,1½,2,2½ (1¼)	½,1,1½,2	10 2/3	12
II	One # 4, mod. def. p = 0.0069 (3680)	1,1½,2,2½ (1¼)	½,1,1½,2	10 2/3	12
III	One # 4 mod.def. p = 0.0069 (4470)	1,1½,2,2½ (1¼)	½,1,1½,2	6	12
		1,1½,2,2½ (1¼)	½,1,1½,2	3	12
III	One # 4 mod.def. p = 0.0069 (5870)	1,1½,2,2½ (1¼)	½,1,1½,2	10 2/3	12
		1,1½,2,2½ (1¼)	½,1,1½,2	6	12
		1,1½,2,2½ (1¼)	½,1,1½,2	3	12
		9 x 9 x 54-in. beams			
III	One # 6, mod.def. p = 0.0064 (4470)	1½,2¼,3,3¾ (1 3/8)	¾,1½,2¼,3	16	12
		6 x 6 x 36-in. beams—2-bar			
IV	Two # 4, mod.def. p = 0.0138 (4540)	2,2½,3 (1¼)	0,½,1 (Between bars)	12	3
		2,2½,3 (1¼)	0,½,1	6	3
		2,2½,3 (2½)	0,½,1	12	3
		2,2½,3 (2½)	0,½,1	6	3
		Full section	1	12	1
		Full section	1	6	1
	(Plus stirrups in bead)	2½ (1¼)	½	12	1
	(Plus stirrups in bead)	2½ (1¼)	½	6	1
				Total	117

*Simulated clear spacing.
†Distance from load points to reaction.

and # 6 (D) were sent directly from the mill in three separate shipments corresponding to the three series. Bars C and D were of a type representative of modern deformed bars meeting the requirements of ASTM A 305-50T. Dimensions and physical properties of the four bars are listed in Table 3 of the earlier referenced paper by Chamberlin.

The reinforcing rods extended ½ in. beyond the ends of the beams and were covered with soft rubber tubing ⅛ in. thick for a length of 2½ in. from the ends, destroying the bond from the ends of the beam to the reaction points. The deformations of the modern type deformed bar used are oriented in opposite directions on the two sides of the bar. For uniformity, the single-bar specimens of both bar sizes were all cast with the two opposite longitudinal ribs of the bar on a vertical diameter. The

TABLE 2—CONCRETE MIXTURES

Series	W/C, weight	Proportions,* weight	Compressive strength, psi
I	0.57	1:2.36:2.66	3700 (14 days)
II	0.62	1:2.72:3.13	3680
III	0.62	1:2.64:2.95	4470
	0.47	1:1.88:2.17	5879
IV	0.62	1:2.64:2.95	4540

*Saturated surface-dry.

two-bar specimens were cast with the two ribs on a horizontal diameter (rib to rib for the adjacent bars).

Web reinforcement for the 3- and 6-in. embedded lengths of series III consisted of a cage made from 4 x 2—11/11 welded wire mesh. The cage was in the shape of an inverted U with the legs standing on the shoulders of the cross section of the end portions of the beam. All the horizontal wires were clipped off close to the verticals except for two, one on each side located at approximately the neutral surface. Two cages were telescoped to give horizontal spacings of 1 in. for the vertical wires. The beads contained no vertical steel.

All of the beams of series IV were vertically reinforced with a cage of 2 x 1—14/14 galvanized wire mesh, bent into an inverted U shape. All the horizontal wires were clipped except for one on each side near the neutral surface of the beam. The wires forming the vertical legs of the cage were doubled back resulting in four wires, two on each side, at horizontal spacings of 1 in. The web steel did not extend into the beads, except for two supplementary beams of embedded lengths of 6 and 12 in. and shallow beads of 2¼ in. width, where the web steel went down around the reinforcement and back up.

Beams were cast in horizontal layers with longitudinal reinforcement at the bottom. Concrete was rodded and spaded by hand until adequate placement was assured. Top surfaces were covered with moist burlap, and beams were left in the molds for two days or more. The smaller beams were moist cured by immersion until 1 day before testing, then were kept under damp burlap until tested at 28 days (14 days for series I). The larger beams were kept covered with damp burlap in a moist room without sprays.

Test method

Beams were tested upside down as cast in a 20,000-lb hand-operated testing machine. The load passed through a spherical bearing block to a steel loading beam and then through rollers, corresponding to reactions. Load points under the beam were adjusted to correspond to the different lengths of embedment of the bars. One of the rollers at the load points rested on a spherical bearing block. Steel plates, 2 x ½ in., with ⅜-in. leather pads were used at each point of contact. At the outer ends of the beams the inner half (1 in.) of the leather pads had bearing widths on the concrete of 4½ in. for all of the smaller specimens, since the clearance between the bead and "feet" was kept constant. The outer halves of the pads rested on the full 6 in. width of concrete. Bond was destroyed and the pressure reduced on the steel by the soft rubber tubing that covered the bars from the center of the reaction to the end of the beam. Slips at the loaded end of the bar were measured with two dials at each point. Measured slip was corrected by subtracting the strain in the steel between the dials and the concrete face. Slips were measured with a single dial at each outer end.

Steel strains in the longitudinal steel were measured with two electric resistance SR-4 type A-1 gages on each bar (Fig. 1). Lugs were ground off the deformed bars for a length of about 2 in., but tensile tests indicated that the yield point was not discernibly affected by removal of the lugs. Strain gages were applied to opposite sides of the bar in the single-bar beams and on the top and bottom of each bar in the double-bar beams.

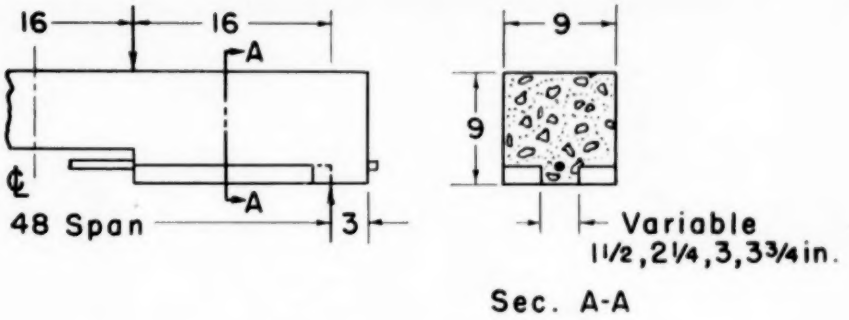

Fig. 4—Beams with one # 6 bar

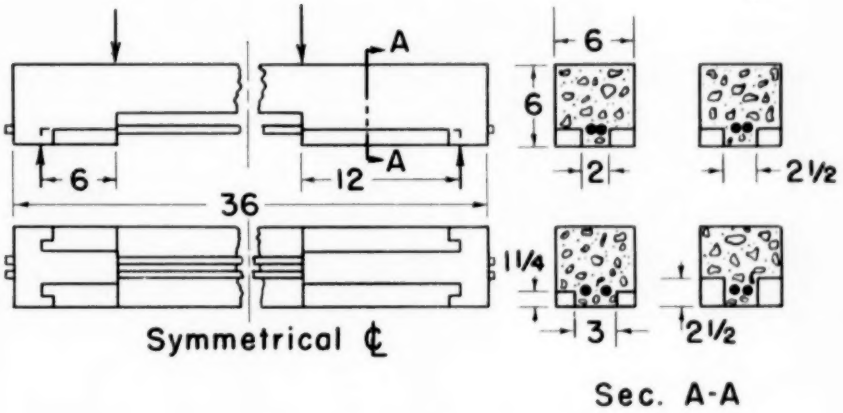

Fig. 5—Beams with two # 4 bars

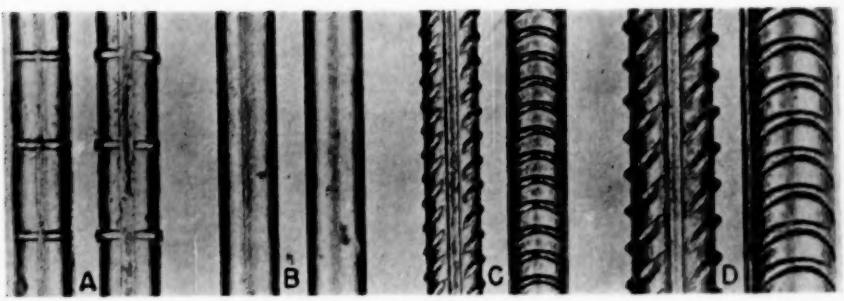

Fig. 6—Front and side view of bars. A, # 4 old-style deformed; B, # 4 plain; C, # 4 modern deformed; D, # 6 modern deformed

TABLE 3—AVERAGE VALUES AT ULTIMATE LOAD

	1*	2*	3*	4*	5*	6*	7*	8*	9*	10*
Series (Steel)	a, in.	Clear space, in.	P, load, lb	Failure	T M/jd, lb	T, lb	s_s $T/2A_s$, psi	u T/A_c, psi	u $V/\Sigma ojd$, psi	v V/bjd, psi
3700-psi concrete—14-day										
I	10 2/3	0	2600	Bond	3240	2560	—	(305)	(387)	51
(1 ♯4)		½	2960	Bd	3690	3460	324	206	220	58
(Old def.)		1	4600	Bd	5740	5230	245	312	342	90
		1½	8000	Bd	9970	9100	284	542	595	156
		5½	7800	T	9720	9240	—	550	581	152
3680-psi concrete										
II	10 2/3	½	2800	Bond	3490	3210	—	191	208	55
(1 ♯4		1	3960	Bond	4940	4490	—	268	295	77
plain)		1½	3995	Bond	4980	4260	—	254	297	78
		2	4300	Bond	5360	4930	—	294	320	84
(Def.)	10 2/3	½	5400	Bd	6730	6030	565	359	402	105
		1	6580	Bd	8200	7200	338	429	490	129
		1½	7270	Bd-DT	9070	8330	260	496	540	142
		2	8110	Bd-DT-T	10,110	9610	225	573	604	158
4470-psi concrete										
III	6	½	7270	Bd	5030	4560	760	486	533	139
(1 ♯4)		1	9870	Bd	6820	6350	529	674	723	188
		1½	10,900	Bd	7540	7070	393	751	789	208
		2	12,510	Bd-DT	8650	8010	334	850	916	239
	3	½	9000	Bd	3110	2160	720	458	659	172
		1	10,930	Bd	3780	3200	534	679	800	209
		1½	15,280	Bd	5276	4590	510	975	1118	292
		2	15,870	Bd-DT	5480	5070	422	1077	1160	302
(1 ♯6)	16	¾	15,080	Bd	17,230	15,700	653	415	456	120
		1½	15,830	Bd	18,110	17,800	370	471	479	126
		2¼	16,960	Bd-DT	19,400	21,000	292	556	513	135
		3	16,330	Bd-DT	18,700	20,200	210	534	494	130
5870-psi concrete										
III	10 2/3	½	6690	Bd	8140	7390	692	440	486	127
(1 ♯4)		1	7500	T(Bd)	9110	8250	387	492	545	143
		1½	7970	T	9700	8810	276	525	579	152
		2	7970	T	9700	8810	206	525	579	152
	6	½	9570	Bd	6550	5960	993	633	696	182
		1	11,410	Bd	7810	6880	573	730	830	217
		1½	13,350	Bd	9140	8270	459	878	970	254
		2	13,950	T	9550	8670	361	921	1013	266
	3	½	10,240	Bd	3510	2670	890	566	745	195
		1	12,710	Bd	4350	4020	671	854	925	242
		1½	15,530	Bd	5320	4720	525	1002	1130	296
		2	18,170	Bd-DT	6220	5900	491	1252	1320	346
4540-psi concrete										
IV	6	½	13,800	Bd	9860	9360	780	496	522	274
(2 ♯4)		¾	15,600	Bd-DT	11,130	10,070	559	534	590	310
Shallow		¾†	15,660	Bd-DT	11,180	10,230	569	543	592	311
bead		1	17,200	Bd-DT	12,280	11,080	461	587	650	342
	12	½	9020	Bd-DT	12,890	10,560	440	280	341	179
		¾	10,960	Bd-DT	15,650	14,100	392	374	414	218
		¾†	13,600	T	19,430	17,480	486	463	514	270
		1	12,000	Bd-DT	17,150	15,320	319	416	454	238
Deep	6	½	8000	Bd-DT	5710	4060	338‡ 338§	215	302	198
bead		¾	9000	Bd-DT	6430	5280	293 352	280	340	216
		1	12,500	Bd-DT	8930	7760	323 431	411	473	292

TABLE 3 (Contd.)—AVERAGE VALUES AT ULTIMATE LOAD

Series (Steel)	1* a, in.	2* Clear space, in.	3* P, load, lb	4* Failure	5* T M/jd lb	6* T, lb	7* s_t $T/2A_s$, psi	8* u T/A_o, psi	9* u $V/\Sigma ojd$, psi	10* v V/bjd, psi
	12	½	7200	Bd-DT	10,280	8940	372 372	237	272	178
		¾	8560	Bd-DT	12,230	11,390	316 380	302	324	206
		1	9500	Bd-DT	13,570	11,690	244 325	310	359	222
	6	Full sec	20,500	DT	14,650	13,670	—	725	775	407
	12	Full sec	13,000	T	18,580	17,500	—	464	491	258

*Columns are identified by number, as follows:
1. Distance from nearer load to support.
2. Simulated clear space.
3. Total ultimate load on beam.
4. Type of failure: Bd—Bead rupture, DT—Diagonal tension, T—Yield point stress in steel.
5. Total tension in bar (or bars) computed from moment at ultimate.
6. Total tension in bar (or bars) determined from strain observations.
7. Horizontal shearing unit stress at center line of bar, $T_o/(2$ shear area).
8. Bond stress at ultimate, $T_o/($bond area).
9. Bond stress at ultimate, usual assumptions.
10. Shearing unit stress at ultimate, usual assumptions.

†Stirrup in bead.
‡At centerline of bars, $T_o/(2$ shear area).
§At base of bead, $T_o/($shear area).

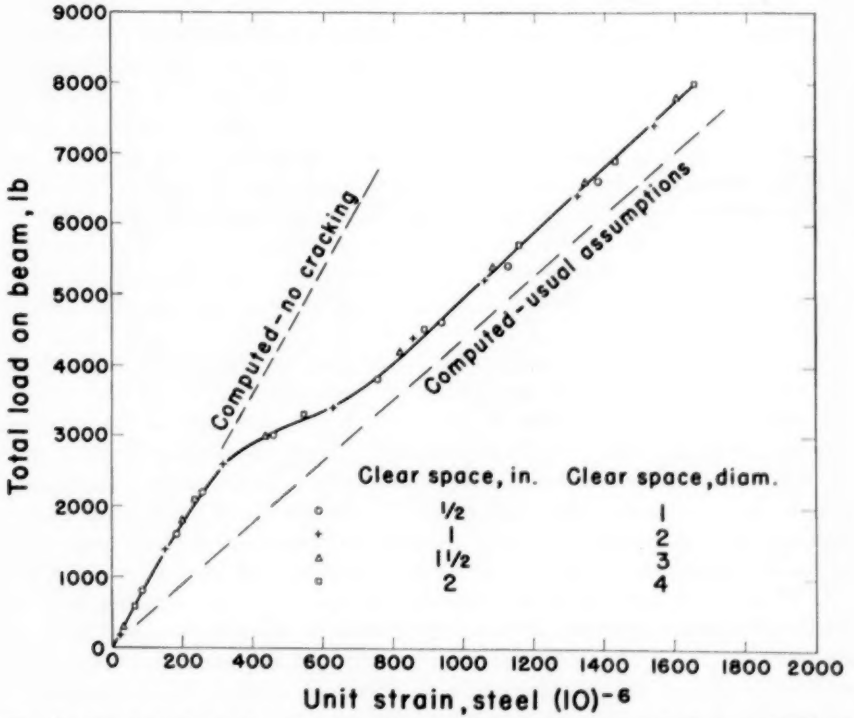

Fig. 7—Load-strain, series III, # 4 deformed bar, 10 2/3-in. embedment, 5870-psi concrete

Loads were applied in increments of a few hundred pounds, depending upon the estimated load-carrying capacity of the beam, and the tests were carried to the ultimate load. Loading was halted at each increment to read the dials and strains, and readings were obtained in general on the increment before the ultimate. In some cases, the fracture occurred while the readings were being taken. Slow continuous loading would have been preferred, but no practical scheme for taking readings "on the run" was devised.

RESULTS

General

Average values at ultimate load are listed in Table 3. For series II and III, the results are averages of three specimens of a kind. Column 1 lists the distance (*a* in Fig. 3) from the nearer load to the reaction for the two-point symmetrical loading. The ultimate load *P* of column 3 is the total load on the machine. The type of failure is given in column 4. Computed values for the total tension in the steel are given in column 5 to compare with the tension values determined from observations of strain, column 6. The average horizontal shearing unit stress (column 7) in the concrete at the centerline of steel was computed as one-half of the total tension in the steel, as determined from strain measurement, divided by the net area of the concrete. This assumes that half of the load is transmitted by bond from the underside of the bars. For values of the horizontal shear at the base of the deep beads (series IV) the total tension was divided by the product of the length and the width of the bead. The average unit bond stress of column 8 was obtained by dividing the total tension in the steel (column 6) by the product of the perimeter of the bar, or bars, and the embedded length. For comparison, bond stresses were computed in the usual way for column 9. Vertical shearing unit stresses, column 10, were determined in the usual manner, where the total shear was one-half the ultimate load. The stresses in the table are average values at the ultimate load and are not in most cases ultimate strength values.

Curves to indicate the variation of measured strain in the steel to the load on the beam were prepared for each group of specimens. Fig. 7, for example, is the load-strain curve for beams of 10 2/3-in. embedment and of the stronger concrete, series III. Each point is the average of three specimens of a kind, and the four different symbols indicate the four different bead widths. The change from an initial constant slope at about 2000 lb corresponds to the beginning of a tensile crack in the central portion of the beams. Computed values for steel strain for an uncracked beam, using the entire area of the concrete plus the transformed area of the steel, agree with the observed strains up to the cracking load as shown. The S-curve between 2000 and about 4000 lb indicates the opening up of the crack or cracks. Computed steel strains based on the usual assumptions for reinforced concrete are in accord with the observed strains after the period of adjustment. Since the central cutaway portion was the same for all the beams of the group, and since the reduced section was essentially a large initial tensile

crack, the agreement of the steel strains of the four sets of specimens is only natural and was to be expected. Other load-strain curves are not shown but were used to evaluate the unit strain in the steel at ultimate load except where the steel was stressed to the yield point.

Similarly, average load-deflection curves were plotted for all groups of specimens. The start and opening up of a tensile crack was again evident in the 2000- to 4000-lb range. Load-deflection curves did not indicate any significant difference in action between beams of different simulated spacings except for loads approaching the ultimate.

Load-slip curves were prepared for each set of specimens and are presented (Fig. 9—12) for some of the beams having specimens in triplicate, series II and III. Data for the load-slip curves are from the average of six observations of slips, since slips were measured at both ends of the beams. Average curves for slips at the fractured ends as compared with those for the undamaged ends showed no discernible difference for the small beams except for loads near the ultimate. Localized failures and opening up of cracks did affect the measured slips at the loaded ends of the #6 bar of the larger beams, and for the wider spacings, the curves are separated (Fig. 11) for the failed and unfailed ends.

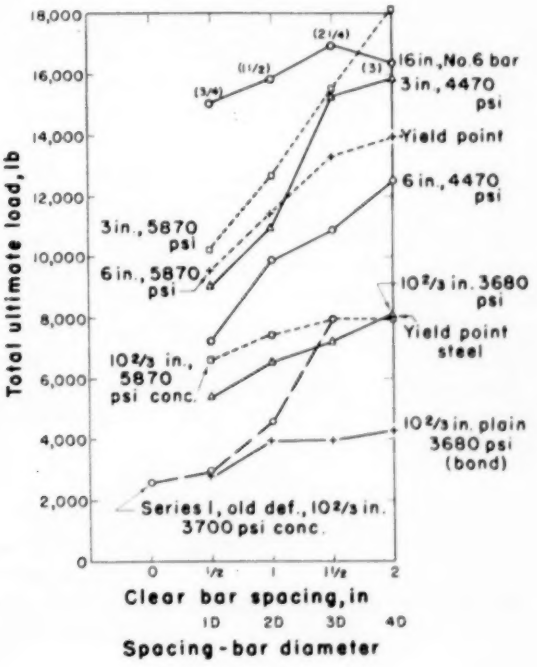

Fig. 8—Ultimate load, series I, II, III

Series I

Ultimate loads of beams with old-style deformed bars increased with increase of the simulated spacing (Fig. 8) until the yield point load was developed in the steel. The beam with the zero simulated spacing, no concrete beneath the horizontal diameter of the bar, failed by the bar coming loose from the concrete. The bond of the bar half-embedded in the concrete appeared to be intact before test but could easily have been disturbed in stripping, handling, and attaching of dials. The zero simulated spacing is not considered practical and was attempted only for the exploratory series. Beams with the ½-, 1-, and 1½-in. clear spacings failed by rupture of the concrete at the base of the bead with no other visible damage to the beams. Concrete at the fractured sections appeared to be of good quality with no evidence of voids or inadequate placement. The specimen of full width failed by reaching yield point stress in the steel, while the beam with 1½-in. spacing failed at a slightly greater load without an indication of yield point stress.

Load-slip curves (not shown) for both the free and loaded ends of the beam having the ½-in. spacing indicated only slightly better bond action than for the beam with zero spacing. Curves for the specimen with 1½-in. spacing and for the full width beam were comparable. At a loaded-end slip of 0.030 in., spacings of zero, ½, and 1 in. developed loads of 57, 64, and 74 percent, respectively, of the average of the 1½-in. and full width spacings.

Results indicate that for the condition of series I, a clear spacing of three bar diameters was required to develop the full strength of the beams.

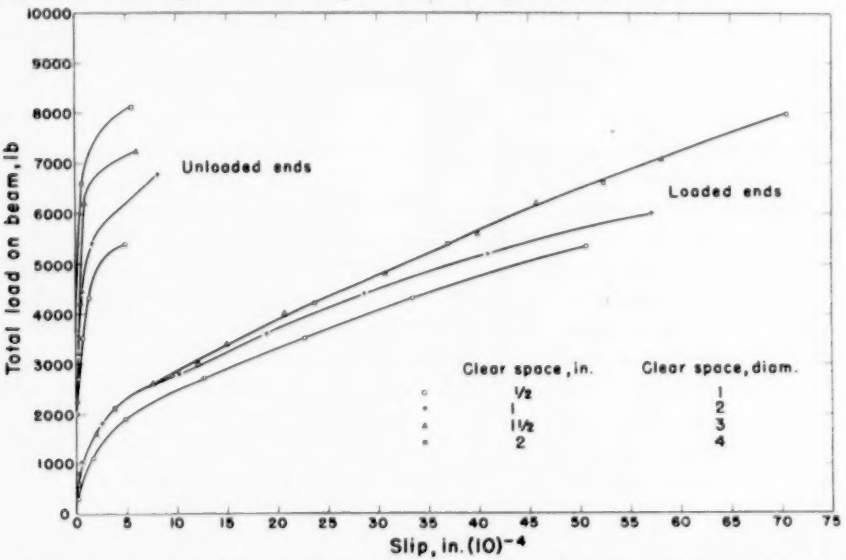

Fig. 9—Load-slip, series II, # 4 deformed bar, 10 2/3-in. embedment, 3700-psi concrete

Series II

All of the plain-bar specimens failed in bond by slippage in the concrete with all of the beads intact at the ultimate loads. Load-carrying capacity was not affected by the different spacings (Fig. 8) except for the narrowest of ½ in. Load-slip curves showed a similarity of bond action for all four spacings until cracking loads of about 2000 lb were developed. After a tensile crack or cracks had formed in the central portion, beams with the ½-in. spacing developed greater slips than those with the three wider spacings. The average ultimate bond stress for the three wider spacings was 272 psi, calculated from strain measurements, as compared with an average at 191 psi for the narrowest spacing.

Ultimate loads for beams with modern deformed bars increased directly with increase in spacing (Fig. 8). Loading arrangement and concrete quality were the same as those for the plain bars. All specimens with ½- and 1-in. spacings failed by one of the beads of each rupturing at the base for the full length but remaining fixed to the bar. One of the beams with 1½-in. spacing fractured in a similar manner, but the other two specimens of the group had the bead fracture between the outer end of the beam and a diagonal crack as shown in Fig. 1. The ruptured section at the base of the bead was more jagged than that for the narrower spacings. Two of the beams with widest spacing, 2 in., fractured in a manner similar to that shown in Fig. 1, while the third specimen of the set failed by reaching yield point stress in the steel with no visible distress in the beads. Load-slip curves of Fig. 9 for the unloaded ends indicate progressively poorer bond action as the spacing for the bar decreased. At the loaded ends, slippage for the bar with narrowest spacing was relatively greater than that for the other three spacings from the beginning of loading. Loaded-end slippage for the bars spaced at 1, 1½, and 2 in. were the same up to loadings of 2500 lb; beyond that the two wider spaced bars had identical slips.

The ultimate load curves of Fig. 8 for the three types of bars, old-style deformed (series I), plain and modern deformed, are comparable because the main variable is type of bar. Type of failure, however, was different and there was only one specimen of a kind for the old-style bars. Concrete strengths were the same, although specimens of series I were tested at 14 days. Average bond stress and shearing unit stress at the ultimate load plotted against the bar spacing would give curves of the same shape and relative magnitude of those of Fig. 8, since nominal bar sizes, beam cross sections, and lengths of embedment (10 2/3 in.) were the same for the three types of bars.

Series III

Ultimate load curves for beams of 6- and 3-in. length of embedment with 4470-psi concrete, and of 10 2/3-, 6- and 3-in. embedment with the 5870-psi concrete are shown in Fig. 8.

Six-inch length of embedment specimens of the lower strength concrete with the three narrower spacings of bars, ½, 1, and 1½ in., all failed by one of the

beads of each fracturing at the base and usually remaining attached to the rod. Beams with the widest spacing (2 in.) developed tension cracks in the beads that were visible at a few increments of load below the ultimate. At the ultimate load, the beads fractured at their bases between tensile cracks. The beads were broken up and a diagonal tension crack opened up in the body of the beam. The load-slip curves of Fig. 10 indicate essentially similar bond action for the bars of the three widest spacings, with the narrowest spaced bar again exhibiting greater slippage.

Similar specimens of the lower strength with only 3 in. of embedment were more erratic than those of longer embedments, as might be expected. The beams all failed by one of the beads fracturing off at the base. Specimens with the two narrower beads broke off cleanly with the beads intact. The two wider spaced specimens had the bead broken up with the concrete tearing out between stirrups. Load-slip curves indicated that the bond action was similar for the two wider spaced bars with the two narrower spacings producing greater slips.

Ultimate loads for the 9 x 9-in. beams containing the #6 bar are shown in Fig. 8 with the clear spacing of ¾, 1½, 2¼, and 3 in. plotted in terms of 1, 2, 3, and 4 bar diameters to compare with those of the smaller beams. Load-carrying capacity increased with an increase in spacing up to 2¼ in. (3D), although the percentage increase was not as great as that for the smaller beams.

Two of the specimens of narrowest spacings, ¾ in., failed at approximately the same load by one of the beads of each fracturing off cleanly at the base. At an ultimate 15 percent greater than that of the two companion beams, one of the beads broke off accompanied by a diagonal tension crack in the body of the beam at about midlength of the bead. Tension cracks were observed in the beads of the 1½-in. space specimens as the load approached the ultimate, with cracks at the base of the beads extending from the tension cracks out toward the ends of the beams. Two of the beams had a bead of each fracture at the base at the ultimate, while the third had a bead break off between a diagonal tension crack and the end of the beam. Two of the specimens with 2¼-in. spacing failed at about the same load in a combination of diagonal tension and bead fracture back of the diagonal crack. The third specimen of the set had an ultimate 13 percent greater than the other two and failed by developing yield point stress in the steel with no visible evidence of distress by diagonal tension. Single tension cracks were visible in each bead before the ultimate. At the ultimate load one bead split longitudinally down the center, and the bead broke loose between the end of the beam and the tensile crack. Beams with the widest spacing, 3 in., failed by diagonal tension, with one bead of each breaking off between the diagonal crack and the end of the beam.

Load-slip curves (Fig. 11) reflect the formation of the tensile cracks and local failures in the beads between the load points and the ends of the beams of the three wider spaced specimens. Slips at the load points were measured as the relative movement of the bar with respect to the vertical face of the concrete where the bar emerged. Loaded-end slips for the beams of narrowest spacing in-

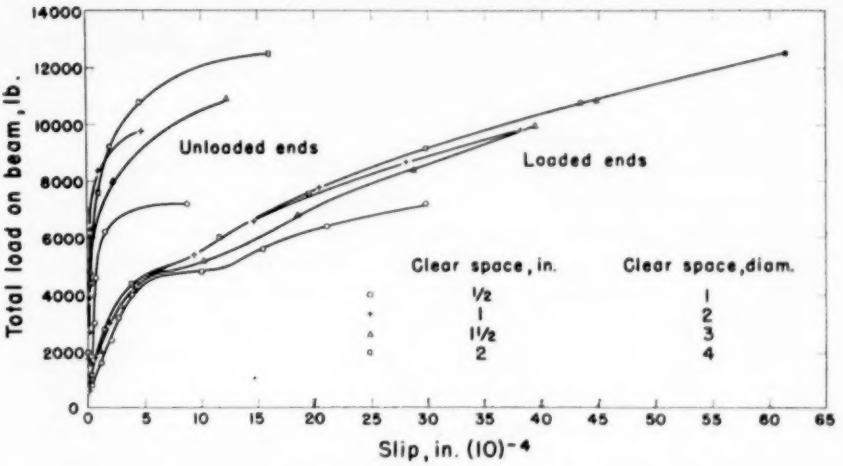

Fig. 10—Load-slip, series III, # 4 deformed bar, 6-in. embedment, 4470-psi concrete

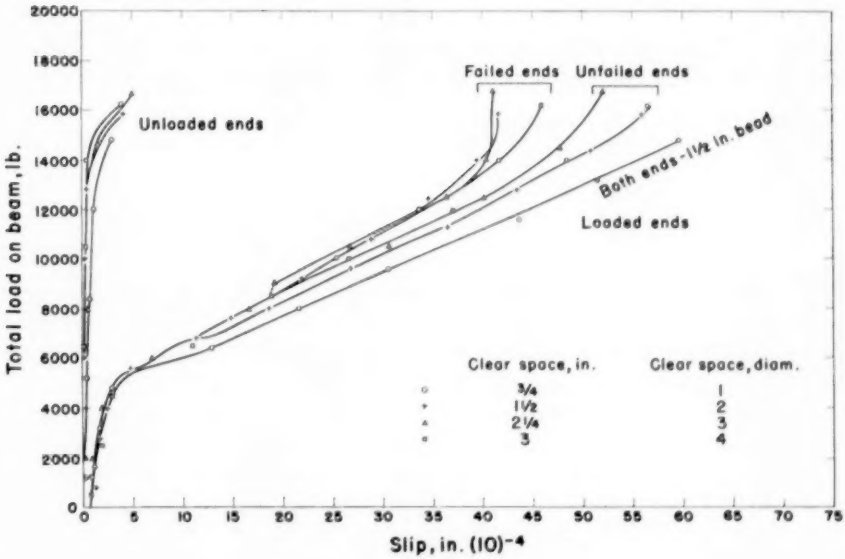

Fig. 11—Load-slip, series III, #6 deformed bar, 16-in. embedment, 4470-psi concrete

creased with load in a manner similar to that of the smaller beams with the #4 bars. Curves for the other three spacings are separated out into slips at the loaded end of the bead that ruptured and those for the bead that remained attached to the beam. Slip at the failed end practically halted as tension cracks in the beads opened up before the ultimate.

Ultimate loads for the beams of the stronger concrete and #4 bars increased with wider spacings (Fig. 8) until yield point in the steel was reached in the 2-in. spacings for both the 6- and 10 2/3-in. lengths of embedment. The approach of the two curves of different concrete strength for the 3-in. embedment at 1½-in. spacing is due, in part at least, to the variation in ultimate loads of each group. Results for the other three spacings were in better agreement.

Load-slip curves for the loaded ends of the beams with 10 2/3-in. embedment and the stronger concrete indicated somewhat less slippage, after a tensile crack had developed in the central portion of the beam, as the spacing increased. There was not enough slippage at the free ends to be significant. Specimens with the narrowest spacing failed by one of the beads of each breaking off cleanly at the base. One of the beams of 1-in. spacing failed by the bead rupturing off along its base at an ultimate load of only 180 lb less than the average of the other two of the set which failed by reaching yield point in the steel. All of the specimens with the two wider spacings failed by tension in the steel with the beads intact.

There seems to be little difference in the load-slip curves (Fig. 12) for the three wider spaced bars with the 6-in. length of embedment and the stronger concrete. The curves for the loaded and unloaded ends indicate less effective bond for the narrowest spaced specimens. The widest spaced specimens (2 in.)

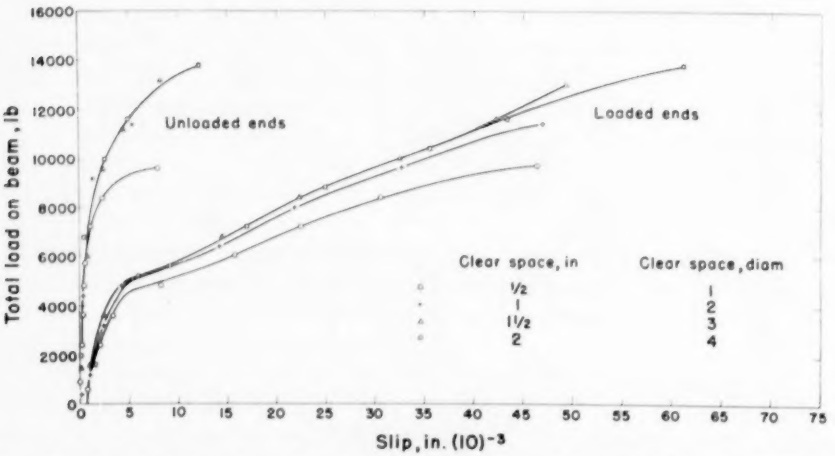

Fig. 12—Load-slip, series III, #4 deformed bar, 6-in. embedment, 5870-psi concrete

all failed by developing yield point stress in the steel; but all of the other beams failed by one of the beads breaking off at the base, though one specimen of 1-in. spacing had a diagonal tension failure accompany that of the bead failure.

Load-slip curves indicated progressively poorer bond action as the spacing was reduced in the 3-in. length of embedment specimens of the higher strength. Beams with the narrowest spacing failed by one of the beads breaking off cleanly at the base. One of the beads of all of the 1-in. spaced bar specimens broke off at the base with concrete tearing out on the side of the bar toward the neutral surface of the beam. Two of the 1½-in. specimens ruptured at about the same load with one of the beads of each breaking off and tearing up the concrete at its base. The other beam of the set carried 25 percent greater load and ruptured with a combination of diagonal tension and bead failure. All of the beams with 2-in. spacing carried about the same ultimate load with two of the specimens having a combination of diagonal tension and bead rupture and the third specimen failing by a tearing off of one bead without any observed diagonal tension cracks.

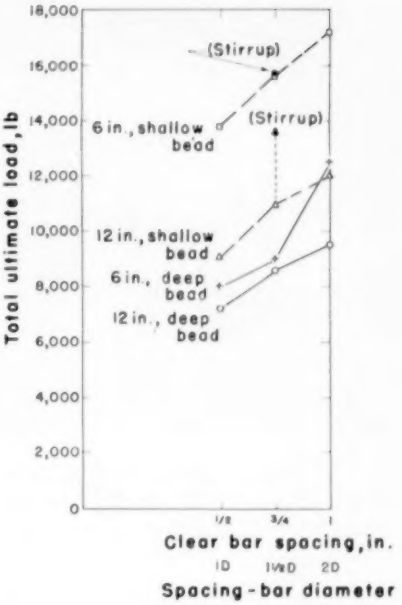

Fig. 13—Ultimate load, series IV, double bar

Series IV

Ultimate loads for the beams with two #4 bars are plotted in Fig. 13. Ultimate loads increased with wider spacings in a manner similar to that of the single-bar specimens. The shallow bead specimen of 12-in. embedment with the stirrups around the ¾-in. spaced bars in the bead carried considerably more load, 13,600 as compared with 10,960 lb, than its companion that had stirrups only above the bead. Stirrups in the 6-in. bead of the same bar spacing showed no appreciable increase in load-carrying capacity. The 6-in. embedment specimen with narrowest spacing and with the shallow bead (depth to centerline of steel as in the single-bar beams) failed with rupture along a horizontal plane at the base of one of the beads. All of the other shallow-bead specimens of both lengths of embedment failed in a combination of diagonal tension and horizontal fracture at the base of one of the beads. Fig. 14 shows a typical failure of one of the

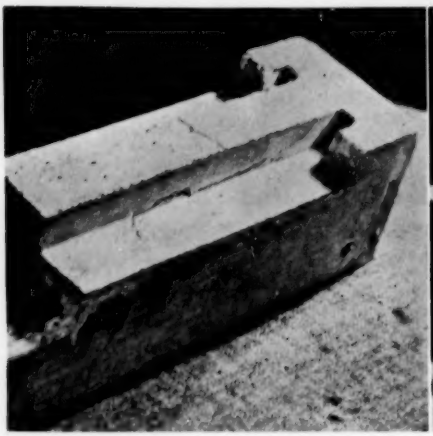

Fig. 14—Fracture of two-bar specimen, 12-in. embedment, bead to centerline of steel

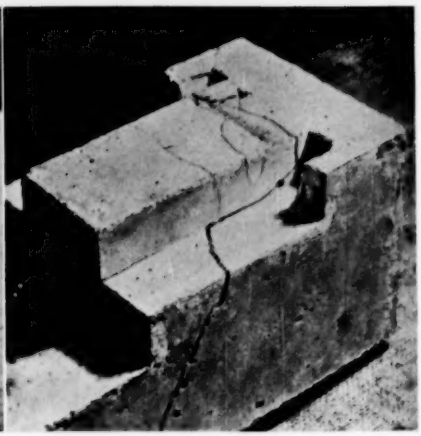

Fig. 15—Typical failure of two-bar beam, with 6-in. embedment, shallow bead

12-in. length of embedment beams. One of the beads has fractured along a horizontal plane for a length of about 9 in. from the line of the reaction to the diagonal crack. Load-slip curves (not shown) for the loaded end have an up-turn near the end, as did the ¾-in. specimens (Fig. 11), indicating greatly reduced slip at the exposed face as loads approached the ultimate. A typical failure for the 6-in. length of embedment bar is shown in Fig. 15.

Beams with the 2½-in. deep bead carried considerably less load than their shallow-bead companions. Average ultimate loads were 63 and 79 percent of those with 6- and 12-in. long shallow beads, respectively. The narrowest bead specimen of 12-in. length ruptured along a horizontal plane at the centerline of the bars for part of the length of the bead with the fracture extending into a diagonal crack, as shown in Fig. 16. For the other two beams of the group, the rupture was along a horizontal plane at the centerline of the steel near the outer ends of the beam, extended along a diagonal into a horizontal plane along the base of the bead and then continued as a diagonal crack in the body of the beam. The two narrow spaced bars of 6-in. length of embedment failed by fracture along a horizontal plane at the base of one of the beads accompanied by a diagonal tension crack. The widest-spaced specimen failed primarily in diagonal tension with the diagonal crack in the bead and in the body of the beam separated by a horizontal crack about 1 in. long at the base of the bead.

The 12-in. length of embedment beam of full section failed by tension in the steel at a load of about 8 percent greater than the 3-in. wide, shallow-bead beam. The full-section beam of 6-in. embedment failed in diagonal tension at 19 percent greater load than its 3-in. wide, shallow-bead companion.

Load-slip curves for series IV (not shown) were similar to those of series II and III, but there was not the tendency of the curve for the narrowest spacing to be separated out below the others.

SUMMARY AND CONCLUSIONS

The ultimate load curves of Fig. 8 and 13 indicate that the load-carrying capacity of the beams increased with wider simulated spacing until yield point stress was developed in the steel. One-bar specimens with narrower simulated spacings of the deformed bar failed by rupture along a horizontal plane at the centerline of the steel (base of the bead). The widest simulated spacing usually resulted in a combination of diagonal tension and bead fracture or tension failure in the steel.

Splitting action of the deformed bars must have contributed to the bead failures, although the plot of average bond stress at the ultmate load (Fig. 17) shows that action is not entirely a simple function of unit bond stress, since the values vary with the length-diameter ratio of the embedded bar. Bond stresses of Fig. 17 were evaluated by dividing the tension in the steel, as determined from strain measurements, by the embedded area. Calculated bond values of column 9, Table 3, are higher. Allowable bond stress for the concretes of this investigation permitted by the ACI Building Code is 350 psi. A factor of safety of 2½ would require a bond stress of 875 psi. This value is shown as the horizontal line on Fig. 17. Variation of unit bond stress at the ultimate with effective bar spacing as determined by Ferguson, Turpin, and Thompson* and shown in their Fig. 6 is indicated by the dotted line in the lower portion of Fig. 17. Their results were based mainly on tests of eccentric pull-out specimens, although there were some spot checks with beam tests. Most of their tests were with an embedded length-diameter ratio of 12, which would correspond to an embedded length of 6 in. for the # 4 bars of this investigation. Loading, concrete mixtures, bar sizes and type, all were different. It is not believed that the higher bond values obtained in these tests were because of the compressive forces at the beam reactions, since the ends of the bar were covered with rubber tubing and the load was distributed over the ends of the beam, as described earlier.

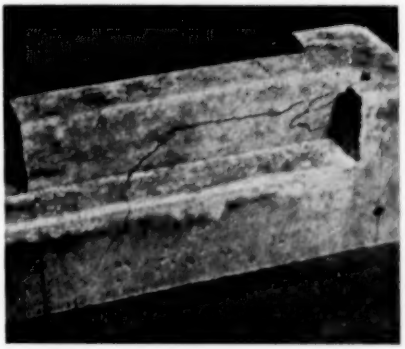

Fig. 16—Two-bar specimen with ½-in. simulated spacing, 12-in. embedment, deep bead

*Ferguson, Phil M., Turpin, Robert D., and Thompson, J. Neils, "Minimum Bar Spacing as a Function of Bond and Shear Strength," ACI JOURNAL, June 1954, *Proc.* V. 50, pp. 869-887.

Nor is the splitting of the beads directly a function of the total tension in the steel. Fig. 18 is a plot of the measured total tension in lb at the ultimate against the simulated spacing. Values of horizontal unit shearing stress at the ultimate load (column 7, Table 3) for the different bar spacings are shown in Fig. 19.

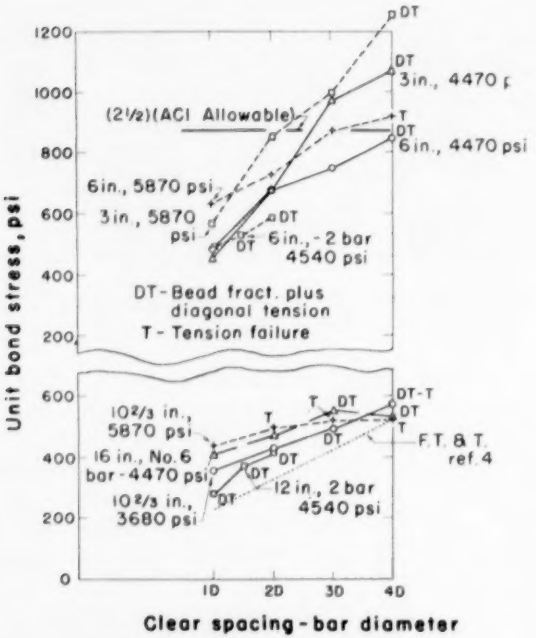

Fig. 17—Unit bond stress at ultimate load, series II, III, IV, deformed bar

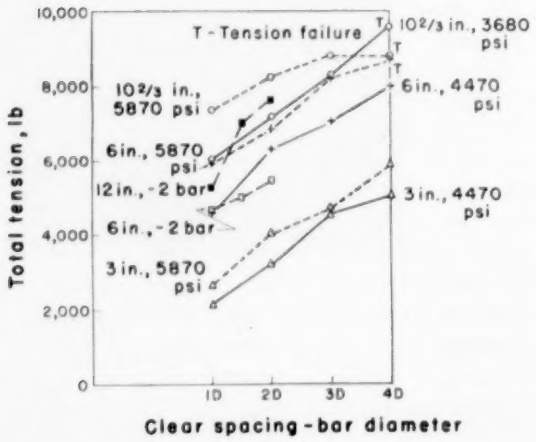

Fig. 18—Total tension each bar at ultimate load

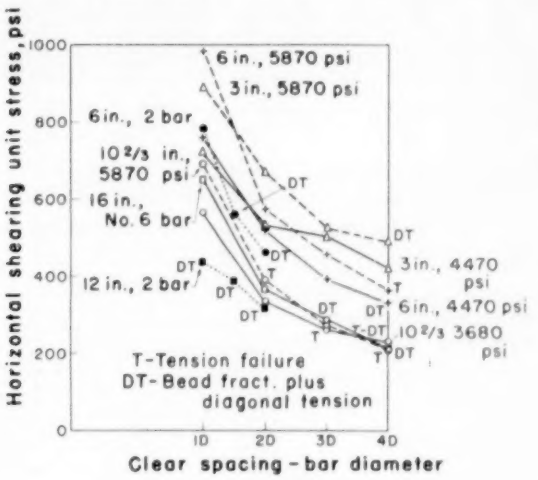

Fig. 19—Average horizontal shearing unit stress at centerline of bars at ultimate load

The horizontal shearing stresses vary both with spacing and embedded length of bar.

Computed vertical unit shearing stresses at maximum load, column 10, Table 3, are low even for those specimens that failed ultimately in combination with diagonal tension. The ultimate load curve of Fig. 8 also serves essentially as a vertical shear curve; since the total shear was one-half of the total load, the width of the small beams was constant and the *jd* value varied but little. It has long been recognized that horizontal reinforcement is of assistance in resisting diagonal tension and that the effectiveness depends upon anchorage of the bars. It follows, as these tests show, that the vertical shear is also dependent upon an adequate width of concrete provided by bar spacing. That fracture along a horizontal plane at the centerline of bars is due to shear as well as splitting action of the deformed bars is evidenced by the horizontal fractures at the base of the deep beads of series IV well away from the bars. Clark* and others have shown that the distance from the reaction to the load is an important factor in shear (diagonal tension) strength which is further verified in these tests.

Results from the two-bar specimens, in general, agreed with those from the single-bar beams. The load-slip curves for the 12- and 6-in. length of embedment (bead depth to centerline of the two bars) showed about the same variation in bond action with simulated spacing as the 10 2/3- and 6-in. embedments, respectively, of the single-bar specimens of the same strength except that the curves for the narrowest spacing were not separated out from the others as clearly. Bond stresses developed at the ultimate load were comparable, as is indicated in Fig. 17, although the two-bar specimens failed more definitely in diagonal tension. There was only one specimen of a kind for the beams containing two bars.

*Clark, A. P., "Diagonal Tension in Reinforced Concrete Beams," ACI JOURNAL, Oct. 1951, *Proc.* V. 48, pp. 145-156.

Conclusions are necessarily limited to the results of this investigation. It seems axiomatic to state that considerably more investigation is required with respect to larger beams, greater number of bars, additional layer of bars, continuity, stirrups welded to the bars, and other variables before definite recommendations can be made. However, results from these tests should apply directly to the width of concrete required at the steel in the legs of channel sections and at the stems of thin T-beams, if these are without welded web steel.

1. Load-carrying capacity of the beams increased with wider spacing until failure was in the steel.
2. Load-slip curves indicated greater slippages at both ends of the bar for the simulated spacing of one bar diameter than for the wider spacings, even for plain bars. For spacings other than the narrowest, slippage was usually, but not significantly, reduced as spacing increased.
3. Results from the one group of tests using beams with the larger #6 bar showed the same trend with simulated bar spacing as that of the #4 bar specimens, but the effects were not as pronounced. Failures in the larger-bar specimens were complicated by tensile cracks in the beads, diagonal tension, and possibly inadequate cover below the bar.
4. Increasing the concrete strength 31 percent, from 4470 to 5870 psi, increased the load-carrying capacity of companion beams that did not fail in tension by an average of 22 percent for lengths of embedment of 6 in., and 11 percent for embedded lengths of 3 in.
5. Fracture along a horizontal plane at the centerline of the rods is not due to the splitting action of the deformed bars alone but also to the action combined with horizontal shear.
6. The amount of vertical shear developed is a function of the effective width of the concrete at the centerline of bars as well as other factors.
7. Specimens of the type used in this investigation require an effective clear spacing of reinforcement of three bar diameters to develop their load-carrying capacity with an adequate factor of safety.

ACKNOWLEDGMENTS

The project was sponsored by the Committee on Reinforced Concrete Research of the American Iron and Steel Institute. The author appreciates the counsel and interest of C. A. Willson, research engineer for the committee. The study was conducted as one phase of IEES Project 269-S of the Iowa Engineering Experiment Station.

In an advisory capacity, Prof. H. J. Gilkey exercised general over-all supervision of the project. Appreciation is also expressed to A. R. Livingston (deceased), assistant professor, and E. L. Munger, instructor of theoretical and applied mechanics; and to R. R. Fleming, former member of the staff.

For such discussion of this paper as may develop please see Part 2, December 1957 *Journal*. In *Proceedings* V. 53 discussion immediately follows the June 1957 *Journal* pages.

CURRENT REVIEWS

of Significant Contributions in Foreign and Domestic Publications

Bridges

Built-up concrete channels form bridge deck

R. C. DORLAND, *Engineering News-Record*, V. 156, No. 14, Apr. 5, 1956, pp. 46-48

Built-up concrete channels combining prestressed flanges and a cast-in-place top were used on a six-span bridge in San Diego, Calif. These sections served as both deck and stringers for the superstructure. The spans were 28 ft 6 in.; the ribs were prestressed with $\frac{3}{8}$-in. pre-tensioned strand. Special mild steel clip anchors were crimped on the prestressing strands for anchorage in the concrete.

Dams

Steenbras Dam strengthened by post-tensioning cables

S. S. MORRIS, *Civil Engineering*, V. 26, No. 2, Feb. 1956, pp. 33-37

To strengthen and raise dam in Union of South Africa, the existing dam was prestressed with post-tensioning cables. Straight sections were raised and post-tensioned; curved portion of dam was raised but not post-tensioned as arch action made strengthening unnecessary. Cantilever wall constructed on, and anchored to, top of dam provided freeboard for addition which raised storage level 6 ft 6 in. Each post-tensioning cable was 1.4-in. diameter and made up of 37 wires of 0.2-in. diameter. Cables were designed on a semi-endless system, whereby each ran over precast concrete cable heads at top with each end grouted in foundation rock. Tension was introduced into cable by raising cable head with hydraulic jack and holding head in raised position by inserting precast packing blocks. Calculation of cable stress, method of distributing high compressive stress under cable head to dam, and anchorage grouting are detailed.

Design

Applied structural design of buildings

THOMAS H. MCKAIG, Dodge Books, New York, 2nd Edition, 1956, 442 pp., $12.50

The book is intended primarily for the use of practicing designers, architects, structural engineers, plant engineers, and draftsmen. Primarily a structural handbook, the material includes examples of practical applications in the three materials: structural steel, reinforced concrete, and structural timber. In addition to the ordinary problems of design of elements, one chapter includes a treatment on complex structures with practical examples applicable to most industrial construction. The final chapter on office practice includes practical material such as cost data, instructions for checking shop drawings, use of soil tests, and structural check lists. No attempt is made in this book to develop theory of structural analysis.

A part of copyrighted JOURNAL OF THE AMERICAN CONCRETE INSTITUTE, V. 28, No. 1, July 1956, *Proceedings* V. 53. Address 18263 W. McNichols Rd., Detroit 19, Mich. Where the English title only is given in a review, the book or article reviewed is in English. If it is followed by a foreign title the work reviewed is in that language. In those cases where the foreign title cannot conveniently be set in type or is not available, the language of the original article is indicated in parentheses following the English title. Copies of articles or books reviewed are **not** available through ACI. Available addresses of publishers are listed in the June "Current Reviews" each year. In most cases ACI can furnish addresses of publications added later.

For those members that cut apart this section for pasting on cards for card indexes, a limited number of complimentary reprints of the "Current Reviews" section are available from ACI headquarters on request.

Direct application to the principle of virtual work (El principio del trabajo virtual con una aplicación immediata)

M. R. Caballero, *Ingeniería Civil* (Mexico City), V. 7, No. 73, Nov. 1955, pp. 9-18
Reviewed by Manuel Renasco, Jr.

Deals with certain particular applications to the principle of virtual work, both by theory and experiments, and attempts to draw an approach to the proof of the general case. The proof given applies mainly to rigid bodies and to certain elastic bodies with external restrictions. From the above proofs, a direct application is shown when the principle is used on a plain bar by applying additional deductions drawn from Bresse equations.

Substructure analysis and design

Paul Andersen, The Ronald Press Co., New York, 2nd Edition, 1956, 336 pp., $7

Intended for two purposes: as a text to explain the subject and as a reference book for a practicing structural engineer. The material in the first edition has been brought up to date with the inclusion of new design information. The book will be of little interest to soil technicians since this phase of the problem has been developed only as it concerns the designer of foundations. The design principles throughout are illustrated with applications as practicable examples and includes illustrative problems. The book should be appreciated by structural engineers as well as student engineers.

Influence lines for continuous beams. Part 2—Three-span continuous beams, constant moment of inertia

Walter C. Boyer and Joel I. Abrams, *Technical Report* No. 4, Civil Engineering Department, Johns Hopkins University, Nov. 1955, 210 pp.

Tables containing influence line data—reactions, moment over support, and various maximum interior span moment combinations—are presented in dimensionless form. Contains data for 45 selected cases giving close coverage in the range of span ratios from 1.6 to 0.6.

Mechanics of ultimate loads, slopes, and deflections for continuous beams and rigid frames

G. Ernst, G. Swihart, and A. Riveland, *Bulletin* No. 6, University of Nebraska, Nov. 1954, 18 pp.

This paper adds to the analytic methods developed for predicting conditions of a structure at failure. It develops a relationship between load and deflection for ultimate load similar to that common for elastic analysis methods of design loads. This relationship is developed by methods which parallel the load, slope, deflection relationships in use under the elastic theory. The possibility of a local failure prior to full development of all critical sections is considered, so that ultimate load methods may be applied simply to continuous beams and rigid frames.

Materials

Significance of free lime in portland cement with regard to the resistance of concrete to aggressive influences (Uber die Bedeutung des freien Kalkes im Portlandzement für die Widerstandsfähigkeit des Betons gegen aggressive Einwirkungen)

F. W. Meier-Grolman, *Zement-Kalk-Gips* (Wiesbaden), V. 9; No. 1, Jan. 1956, pp. 15-28; No. 2, Feb. 1956, pp. 58-71
Reviewed by Henry H. Werner

Presents new theories about the action of free lime in cement and a new definition of the conception of "free hydrate of lime" in set cement. The critical limit of free CaO is established as 0.5 percent for concrete up to 300 kg of cement per cu m. The influence of C_3A in cement is also explained and a permissible value not exceeding 6 percent is established.

The best estimation of resistance of concrete is based on the determination of the modulus of elasticity by the acoustic method instead of measurement of linear expansion. By evaluation and interpretation of test results new theoretical notions were established regarding the action and effects of sulfates in the mortar bed.

On the basis of theoretical considerations and the results of the evaluation the "aggressiveness modulus A" was formulated as a quotient of those constituents of cement reacting topochemically and in the liquid phase. With this, the resistance of concrete can be determined with certainty at an early stage. The aggressive action will be proportionally less as the A-modulus and density increase. An optimum composition was indicated. The demonstration of the decisive effect of the free CaO content in portland cement led to a straightforward explanation of the behavior under sulfate attack of pozzolanic, blast furnace, Ferrari, and high-alumina cements and of concrete treated with steam under pressure or by the Ocrat process.

In cases where concrete is exposed to strong attack, the beneficial effect of air-entraining agents is slight in comparison with other factors determining the aggression. The possibility was pointed out of binding the free lime by chemical means during cement production.

Electronographic study of the morphology and crystallization properties of calcium silicate hydrates

A. GRUDEMO, *Proceedings* No. 26, Swedish Cement and Concrete Research Institute at the Royal Institute of Technology, Stockholm, 1955, 103 pp., 15 Kr. AUTHOR'S SUMMARY

After a brief review of the available data concerning the phase diagram and the crystallization properties of the calcium silicate hydrates formed at low temperatures, the experimental methods used in the present studies are described, and particularly, the techniques used for obtaining reliable crystallographic data with the electron diffraction microscope are elaborated in some detail. The methods of preparation of various calcium silicate hydrate materials are described, and their crystallization properties are illustrated by means of electron micrographs and diffraction diagrams. Electron and x-ray diffraction data are compared.

The calcium silicate hydrates show great variations with regard to their morphological properties. The most frequently appearing compound, CSH(B), may under certain conditions develop comparatively large, foil-like crystals, but in saturated and supersaturated lime solutions a fibrous or needle-like growth of the calcium silicate hydrate crystals seems to be promoted. The crystallization properties of the calcium silicate hydrates are compared with those of a few other silicate minerals with layer lattices. The possibilities of drawing conclusions from the various observations concerning the structure and mechanical properties of cement gels are discussed briefly.

Pavements

Experimental concrete pavements

Report on pavement research project in Indiana

W. T. SPENCER, H. ALLEN, and P. C. SMITH, *Bulletin* No. 116, Highway Research Board, Apr. 1956, pp. 1-56

Describes the location, design, materials, construction, traffic, and early performance of an experimental concrete pavement built in Indiana to study the effectiveness of subbases in the control of pumping.

The pavement sections, having plain concrete, 15-ft joint spacing, and no subbase, have shown distress due to the pumping. There has been no pumping or extrusion of material in the sections having an open-graded subbase. Further observations will be necessary to determine the relative effectiveness of the various types and thicknesses of subbases in the control of pumping. In addition to the continuation of the performance study, a program to measure the deflections of the concrete pavements under both static and moving loads was initiated late in 1953.

Report on pavement research project in Ohio

CHARLES W. ALLEN and L. D. CHILDS, *Bulletin* No. 116, Highway Research Board, Apr. 1956, pp. 57-72

The project was built in the summer and fall of 1952 in an attempt to determine the performance of various thicknesses of subbase on a main truck route. It is divided into four sections,

two with contraction joints on 100-ft centers and two with contraction joints on 20-ft centers. Various subbase conditions are included, ranging from no subbase, open-graded subbase, dense-graded subbase, and soil-cement subbases. This progress report is concerned mainly with the construction of the test road. Although performance observations made to date are included, it is much too early to attempt to draw any conclusions from them except that all subbase treatments used performed better than untreated sub-grade, especially under the 100-ft slabs where several failures have occurred.

Design of concrete roads

A. R. COLLINS, *The Structural Engineer* (London), V. 34, No. 2, Feb. 1956, pp. 62-66

Reviewed by C. P. SIESS

An excellent brief review. Considers stresses due to traffic and temperature variations and methods of computing them but points out that use of stress analyses in design is limited by uncertainties in the assumed conditions on which they are based. Concludes that in practice design must be based on the results of carefully collected and evaluated experience. Presents table issued by Road Research Laboratory for selection of slab and base thickness and reinforcement as a function of traffic intensity and subgrade characteristics. Discusses types and spacing of joints.

Structural aspects of road design: Soil mechanics

P. L. CAPPER, *The Structural Engineer* (London), V. 34, No. 2, Feb. 1956, pp. 56-61

AUTHOR'S SUMMARY

A short account of the application of soil mechanics to road design. The principles by which wheel loads are transmitted to and resisted by the subgrade are discussed. Several methods of pavement design are reviewed, in which the necessary pavement thickness is related to the soil properties. Some experimental results are given to show the correlation of certain soil properties and their variation with moisture content. Finally a brief reference is made to cement stabilization.

Load-transmission test for flexible paving and base courses—Part IV

R. C. HERNER, *Technical Development Report* No. 269, Civil Aeronautics Administration Technical Development and Evaluation Center, Aug. 1955, 11 pp. (available from Office of Technical Services, Washington, D. C., $0.50)

Presents test data from load transmission measurements to illustrate the relative effectiveness of typical base and subbase materials. Test apparatus consists of a pneumatic tire load applied on the surface of a sample pavement mounted upon a "mechanical subgrade." The mechanical subgrade consists of small steel plates mounted on plungers and calibrated springs. Micrometers below the mechanical subgrade measure the deflection at various points, thus permitting the stress distributed to the subgrade to be calculated. The test is particularly interesting in that the apparatus might be modified to make similar measurements to check structural designs of concrete pavements. The most apparent modification required, of course, would be to enlarge the area of the "mechanical subgrade" since the rigid pavement will distribute a stress over a much larger area and perhaps provision for measurement of negative deflection would be necessary.

Precast concrete

Precast floor systems (Decken aus Fertigbauteilen)

Bulletin No. 119, Deutscher Ausschuss für Stahlbeton, Berlin, 1955, 36 pp., 10. 4 D. M.

Presents the results of research by Otto Graf and Gustav Weil. The first paper deals with the bond developed in composite construction consisting of precast concrete beams and cast-in-place slab floors. Four variations of beam types were tested which ranged from bond on horizontal surface only to complete embedment of the T-stem in the cast-in-place slab. The conclusions indicate that bond strengths up to approximately 60 psi may be developed without the use of keys or special shear reinforcement. Much higher bond values were developed against vertical surfaces than horizontal surfaces of the precast

beams. The second investigation deals with composite construction in which various patented (German) light beam and truss systems are used to carry precast block and later to act as reinforcement for the cast-in-place topping.

Properties of concrete

Mathematical-statistical evaluation of quality testing of mass concrete (Mathematisch-statistische Auswertung der Guetepruefungen von Massenbeton)

E. Tremmel and A. Wogrin, *Der Bauingenieur* (Berlin), V. 30, No. 1, Jan. 1955, pp. 28-32

Reviewed by Aron L. Mirsky

Basic mathematical theory of statistics applied to study of strength and factors of safety of plain (mass) concrete. Purpose: better utilization of this construction material.

Comments on an indirect tensile test on concrete cylinders

P. J. F. Wright, *Magazine of Concrete Research* (London), V. 7, No. 20, July 1955, pp. 87-96

Author's Summary

A test which originated in Brazil for determining the tensile strength of concrete involves applying a compressive load to opposite generators of a cylindrical specimen. The specimen fails in tension along the diametral plane containing the load. Experiments with this test have shown that:

(1) Packing strips of relatively soft material are necessary between the specimen and the platens of the testing machine. Plywood strips ½ in. wide and ⅛ in. thick are satisfactory for the purpose, but the material and dimensions of the strips have little effect, provided they can conform to small irregularities in the surface of the specimen.

(2) Cylinders 6 in. in diameter by 6 in. long may be used for concrete containing aggregate up to ¾-in. maximum size. Longer specimens may tend to give more uniform results, while smaller specimens may give higher average values.

(3) The new test gives results higher than those given by a direct tensile test, but lower than the modulus of rupture of beams. It tends to give more uniform results than the direct tension or transverse test, but less uniform results than a compression test on cubes.

Measurement of elastic constants by means of vibrations in beams (in Swedish)

Hans Weibull, *Meddelande* No. 118, Statens Provningsanstalt, Stockholm, 1955, 8 pp.

Author's Summary

Three different methods to determine the elastic constants by means of vibrations in beams are described. Some experiments on concrete are shown. These give the change of Youngs' modulus with the age of the concrete during a drying period. The acoustical spectrum of a beam is calculated and results compared with experiments.

Practical aspects of concrete volume shrinkage

H. S. Woodard, *Consulting Engineer*, V. 7, No. 3, Mar. 1956, pp. 42-45

Reviewed by Aron L. Mirsky

Nine factors affecting shrinkage and cracking of concrete are listed and discussed. Both novice and expert will find this article of interest and value—as a primer for the one, as a review for the other.

Note on the intrinsic curve of concrete (Note sur la courbe intrinseque des betons)

R. Peltier, *Annales des Ponts et Chaussees* (Paris), V. 125, No. 6, Nov.-Dec. 1955, pp. 779-789

Reviewed by Aron L. Mirsky

First part of note reports briefly results of experiments on concrete specimens in compression. Providing special frictionless bearing details at the ends of the specimens resulted in purely vertical fissures and no barreling; rupture was coarse, as in tension, and the specimen was broken into small vertical prisms.

Second part discusses extension of the intrinsic curve theory (see also *Annales des Ponts et Chaussees*, V. 123, No. 6,

Nov.-Dec. 1953; "Current Reviews," ACI JOURNAL, Dec. 1954, *Proc.* V. 51, p. 390), first to a mortar containing a large number of spherical voids, then to a large number of spherical balls in contact, and finally to concrete. Conclusion is that theory is applicable to concrete.

Investigation of the suitability of Prepakt concrete for mass and reinforced concrete structures—Appendix A and B

Technical Memorandum No. 6-330, Waterways Experiment Station, Aug. 1954, 50 pp., $0.75

Describes materials used in the Prepakt concrete process. Results of tests on permeability and natural weathering resistance of the material are given. Observations on the use of prepacked concrete in field operations are included for two projects, covering construction procedures and the temperature rise encountered, as well as core test strengths.

Alignment chart for the evaluation of the dynamic modulus of elasticity and Poisson's ratio for concrete

W. H. KING and I. D. G. LEE, *Magazine of Concrete Research* (London), V. 7, No. 21, Nov. 1955, pp. 165-168

AUTHORS' SUMMARY

Describes the method of construction and use of an alignment chart for the solution of the dynamic modulus of elasticity and Poisson's ratio from observations obtained in the electrodynamic test for longitudinal resonant frequency and the test for ultrasonic pulse velocity of concrete specimens.

Variation of concrete strength due to delay in placing

K. RAY, J. K. KARMAKAR, and S. K. DATTA, *The Indian Concrete Journal* (Bombay), V. 30, No. 2, Feb. 1956, p. 42

Reports data from a series of tests conducted to determine the variation of concrete strength resulting from delays between the mixing of a concrete and preparing the standard test cylinders. Optimum strength resulted after a 2- to 3-hr delay. The authors attribute the increase of approximately 20 percent in the strength to a decrease in the water-cement ratio due to evaporation losses and absorption of water by the aggregates. After 3 hr serious losses of strength began.

Concrete in sea water (Beton im Seewasser)

A. HUMMEL and K. WESCHE, *Bulletin* No. 124, Deutscher Ausschuss für Stahlbeton, Berlin, 1956, 21 pp., 5 D. M.

Continues the report begun in *Bulletin* No. 102 (Jan. 1954). Reports on continuing investigations after longer periods of exposure. Performance of the various concretes is rated by the compressive strength (on cubes) and loss in weight. Includes some 30 enlarged photographs of sawed cross sections cut through the center of the various cubes.

Structural research

Tensile crack exposure tests

Technical Memorandum No. 6-412, Waterways Experiment Station, July 1955, 30 pp., $0.75

Reinforced concrete beams using different types of reinforcement and air-entrained and normal concrete were stressed and exposed to severe natural weathering in salt water. Control specimens were exposed but not loaded. Results indicated the superiority of air-entrained concrete and also indicated an increasing deterioration with increasing stress. Reinforcement tested included new and old-style deformations, rail steel and billet steel bars.

Effect of moment-shear ratio on diagonal tension cracking and strength in shear of reinforced concrete beams

A. FELDMAN and C. P. SIESS, *Structural Research Series* No. 107, Civil Engineering Studies, University of Illinois, June 30, 1955

HIGHWAY RESEARCH ABSTRACTS Feb. 1956

Concepts regarding the effect of the moment-shear ratio on diagonal tension cracking and strength in shear of reinforced concrete beams were verified by tests of two-point loaded beams. However, the hypothesis advanced to predict the behavior and strength of uniformly loaded beams was not verified by tests

conducted. It is evident from the studies carried out in this program that some other and probably more complicated explanation of the behavior of uniformly loaded beams will have to be developed.

Experimental study on model grillage beam bridge with slab clamp connection (in Japanese)

M. Naruoka, H. Omura, and K. Ito, *Journal of Japan Society of Civil Engineers* (Tokyo), V. 40, No. 12, Dec. 1955, pp. 658-664

Authors' Summary

The stress and deflection of the model grillage beam bridge with slab clamp connection were measured. Model bridge consisted of five main beams, one load distributing cross beam and slab which was connected to steel girder by slab clamp usually used. The result of experimental study shows that the measured stress and deflection differ considerably from the theoretical values calculated by assuming that the beam is either perfectly composite or noncomposite. The measured values, however, coincide with the theoretical values calculated by the theory of imperfect composite beam. Applying the load to the second and fourth beam simultaneously, the ultimate load was 70 percent of that of model composite beam bridge and 125 percent of that of model noncomposite beam bridge.

Load distribution in multi-webbed bridge structures from tests on plastic models

G. Little and R. E. Rowe, *Magazine of Concrete Research* (London), V. 7, No. 21, Nov. 1955, pp. 133-142 Authors' Summary

A multi-webbed bridge structure is one which is intermediate between the two extreme cases, *i.e.*, a no-torsion grillage and a full-torsion slab, considered in the load distribution analyses.

The theoretical interpolation formula which gives the distribution factors for this type of construction makes use of a torsion parameter, α. Tests have been made on Perspex bridge models to determine the correct value of this parameter consistent with assumptions of analysis.

The manner in which the parameter is determined for a beam and slab bridge and a box-section bridge is illustrated, and the theoretical and experimental distribution factors are compared for each type of bridge.

Ultimate strength and deformation of plastic hinges in reinforced concrete frameworks

W. W. L. Chan, *Magazine of Concrete Research* (London), V. 7, No. 21, Nov. 1955, pp. 121-132

Authors' Summary

By comparing the idealized assumption of plastic hinges concentrated at points and the actual spread of plasticity, the validity of the plastic hinge theory of reinforced concrete frameworks is verified and the expressions for calculating the available plastic rotations are derived. Tests show that lateral binding considerably increases the stress-strain capacity of reinforced concrete sections, and this can be employed to increase the rotation of critical plastic hinge zones. Further tests on struts provide information on the curvature distribution along plastic zones.

Investigation of continuous concrete beams at far-advanced compressive strains in concrete (in Swedish)

H. Nylander and S. Sahlin, *Bulletin* No. 18, Division of Building Statics and Structural Engineering, Royal Institute of Technology, Stockholm, 1955, 38 pp.; *Betong* (Stockholm), V. 40, No. 3, 1955, pp. 241-275

The method of limit design can be applied to reinforced concrete structures if their dimensions and areas of reinforcement are such that failure begins when the yield point stresses are reached in the tension reinforcement under bending. For high ratios of reinforcement, it is necessary to take account of the fact that the moment in the cross section most heavily stressed at the load causing complete failure of the structure in its entirety is smaller than the maximum moment which this cross section is able to withstand. Furthermore, failure in shear and failure due to excessive bond

stresses are more liable to occur as the ration of reinforcement becomes higher. The authors report the results obtained from investigations on 26 continuous reinforced concrete beams. The beams were considerably different in design from those designed in accordance with the theory of elasticity.

Transverse strength of masonry walls

C. B. MONK, JR., "Symposium on Methods of Testing Building Construction," *Special Technical Publication* No. 166, ASTM, 30 pp.

Presents the results of tests on small brick buildings with the walls loaded by lateral pressure to failure. Purpose of the test program was to develop rational design data for unreinforced masonry underlateral load to justify or modify arbitrary thickness to height ratios and lateral support requirements by rule of thumb in most building codes.

General

Treatise on reinforced concrete (Traité de béton armé)

A. GUERRIN, Dunod, Paris, 1952, V. I, II and III, 314, 300 and 315 pp.

Reviewed by J. J. POLIVKA

Three-volume textbook—(1) general information, properties of materials, experimental mechanics of reinforced concrete; (2) design of reinforced concrete structures; and (3) foundations—is a thorough and concise presentation of most important knowledge on concrete.

V. I, Part 1, contains chapters on history; properties of materials and various mixes; effects of temperature and fire; impermeability and resistance to corrosion; members in tension, flexure and compression; corresponding arrangement of reinforcement, especially under consideration of isostatics. Part 2: experimental and theoretical mechanics referring to three-dimensional stress distribution and phenomena during failure (von Karman, Ros, Eischinger, Richart, Caquot, Goguel, Mesnager, Considére, Baes, Paris); shear and torsion; ductility; tests by Spitzer, Morsch, Gehler, von Emperger, Klokner, Baes, Santarella; shrinkage and plastic flow; effects of repeated loading. Other subjects include straight and bent reinforcement; stirrups and ties; anchorage; spiral reinforcement and results of tests (Considére, Bach, Feret, Talbot, Morsch, von Emperger, Saliger, L'Hermite); wire mesh and expanded metal; principles of prestressed concrete (Freyssinet, Dischinger); elimination of shrinkage effect by expansive cements (Lossier).

V. II contains assumptions, theories, and details of design and chapters on combined bending and compression, localized compression, buckling, variation of modulus of elasticity, design of members with various shapes and cross sections and of composite structural types, wall beams. Statically indeterminate structures (continuous beams and frames with constant and variable moments of inertia) are covered, as well as slabs supported along periphery with comparison of various methods (Mesnager, Resal, Pigeau, Chaudy, Navier, Marcus, Dubas, Lowe, Timoshenko), with a number of examples (rectangular, circular, triangular slabs under uniform and concentrated loads); continuous slabs and mushroom slabs (Marcus, Caquot).

Of special interest is V. III which treats all kinds of concrete foundations in unprecedented thoroughness. Part 1 contains important data on soil mechanics, such as soil tests and testing equipment, properties of various soils, distribution of soil pressure, possible improvements of soils. Part 2 contains material on different types of foundations: continuous slabs under bearing walls and pilasters; spread footings under columns; foundation slabs carrying various numbers of concentrated loads; analysis of various shapes of foundation slabs; conic hollow slabs; full-slab foundations, plain and strengthened by network of beams; convex and concave full-slabs, with and without ties and stiffening members; slabs with inverted capitals; foundation wells, their arrangement and execution;

top structures of foundation wells. Sections are included on various types of piles cast in soil (Compressol, Franki, Simplex, Vibro, Zenth, Standard, Express, Rodio, Frotte-Forum, Grimaud, Mega, Takechi, de Waal); precast piles (Grimaud, Lacombe, hollow and twisted piles); effect of various shapes of piles on their bearing capacity; methods of driving piles; structural consideration for lifting and impact; determination of bearing capacity of piles, empirical and theoretical formulas (Rankine, Vierendeel, Benabencq, Dorr, Caquot-Kerisel); bearing of piles under consideration of dynamic forces, with various methods of design (Engineering News-Record, Crandell-Sprenger, Hiley, Benabencq, Vierendeel, Buisson, Pigeau, Redtenbacher, Brix); loading tests of piles; batter and anchor piles and their resistance; resistance of piles under inclined loading; design and details of top slabs on one and greater number of piles (triangular, square, rectangular, hexagonal, circular, and irregular top slabs). Cofferdams and caissons in reinforced concrete, cast-in-place and precast, are covered. Part 3 includes special foundations; box foundations, types and methods of construction; waterproofing (admixtures, protective coatings and layers, hollow slabs and walls); waterproofing of existing box foundations (interior facing under high pressure); foundations in yielding and sliding soils, on fills, and wet soils; foundations of buildings and machines exposed to shocks and vibration; and strengthening of existing foundations. All subjects are amply illustrated and clarified by many practical examples and calculations.

Notes on coloring concrete block

WILLIAM GRANT, *Concrete*, V. 64, No. 4, Apr. 1956, pp. 39-41

Describes the various pigments available for coloring concrete and concrete block. Advantages and disadvantages are discussed. Includes brief directions for use of pigments and simple tests for their suitability which require "neither great skill nor elaborate apparatus."

Proportioning concrete (Betong-proporsjonering)

SVEN THAULOW, Norsk Cementforening, Oslo, 1955, 142 pp.

Presents a simple, rapid, and sufficiently accurate proportioning method based on all the usual tests of concrete aggregates which allows all mix calculations to be carried out on the job site. The book includes the three common methods of specifying concrete mix proportions: by weight, by absolute volume, and by loose volume. Proportioning instructions are based on a measurement of consistency developed by the Norwegian Portland Cement Assn. using a field apparatus called "concrete tester." Consistency is measured as the number of blows of a hinged handle of given size and weight under gravity force required to compact the concrete. Proportioning methods based on maximum unit weight, based on individual grading curves of aggregate, and based on the fineness modulus are described. It is recommended that proportioning be based on a fineness modulus method. Advice is included on selecting materials and proportioning for (a) concrete with high compressive strength; (b) concrete with high tensile strength; (c) low permeability; (d) resistance to freezing and thawing; (e) resistance to abrasion; (f) resistance to high temperature and fire, and (g) with air entrainment. One chapter deals with field adjustments required by changes in materials or changes in qualities of the concrete desired.

Recent slip-formed structures (Neuere Gleitschalungsbauten)

G. MERKLE, *Der Bauingenieur* (Berlin), V. 30, No. 2, Feb. 1955, pp. 41-46

Reviewed by ARON L. MIRSKY

Descriptions of several recent German structures (silos, coal-blending bunkers, and multistory apartment houses) built by slip-form methods.

Foundation engineering

R. HAMMOND, Philosophical Library, New York, 1956, 192 pp., $10

Deals with practical foundation problems and their solution, covering a wide range of foundation types. Includes a

short introduction to soil mechanics to provide a background for the explanation of practical designs. Photographs are used to show actual construction and the problems presented. Special line drawings illustrate and amplify the explanations and descriptions. Each chapter is followed by an adequate list of references to recent papers and books from which further and more detailed information can be obtained, if required. Although the book is of most value as background study for the young civil engineer and student, it does offer the result of a wide range of experience to the practicing engineer. The latter, for instance, will find of particular interest a chapter on "vibration control foundations," which illustrates practical design methods for machine foundations.

Portable ultrasonic concrete testing apparatus

R. H. Elvery and D. W. Vale, *Magazine of Concrete Research* (London), V. 7, No. 21, Nov. 1955, pp. 161-164

Authors' Summary

The new apparatus described is basically similar to the Road Research Laboratory (England) ultrasonic equipment but has been designed to be more convenient for field testing work. It has been built in two separate units for easy portability and the weight has been reduced to approximately half that of the original apparatus. It is still necessary to provide an a-c main supply for the equipment. A number of new features have been incorporated, providing greater convenience in use and servicing.

Fire protection equipment list

Underwriters' Laboratories, Inc., Jan. 1956, 282 pp.

The section on building materials (pp. 15-75) includes three groups: fire hazard, fire retardant; and miscellaneous or unclassified. The retardant group (pp. 35-74) includes approved detail drawings for various degrees of protection for columns, floors, roofs, ceiling, and wall construction and should be of considerable value to structural engineers for planning purposes.

Modern chemical processes

Editors of *Industrial and Engineering Chemistry*, Reinhold Publishing Corp., New York, V. 4, 1956, 202 pp., $5

Nineteen contemporary industrial chemical processes are described including the historical background, plant installation, process in operation of plants; economics of the process; and future prospects. This volume is intended to supplement Volumes 1 to 3 as a "perpetual inventory of American chemical technology." The section on portland cement production (pp. 47-59) is a well-written summary of the historical background, chemical process, and an excellent description of the operation of the Permanente Cement Co. plant.

Special varieties of concrete (Betony specjalne)

W. Muzynski, *Materialy Budowlane* (Warsaw), No. 7, 1954, pp. 175-182

Polish Technical Abstracts No. 3 (9), 1955

Discusses recent scientific achievements as affecting watertight, frost resistant, acidproof, and fire resistant concrete. Includes suggestions for further development.

Concrete and reinforced concrete (Beton i zelbet)

E. S. Suwalski, *Budown. i Archit.* (Warsaw), 2nd Edition, 1954, 292 pp.

Polish Technical Abstracts No. 3(19), 1955

Basic information on the technology of concrete and methods of planning, calculating, and constructing reinforced concrete structures. Includes chapters on materials, calculation of members, reinforced concrete structures, construction, examples, and tables.

Insulation of large underground chambers (Die Isolierung grosser Raeume unter Tage)

Siegfried W. Markl, *Der Bauingenieur* (Berlin), V. 30, No. 2, Feb. 1955, pp. 55-58

Reviewed by Aron L. Mirsky

Comparison of four methods of insulating large underground chambers for power plants and similar uses. A cost comparison is included.